Phoenix Telecommunications

Jim Taylor, Stan Butman, Chad Edwards, Peter Ilott, Richard Kornfeld, Dennis Lee, Scott Shaffer, and Gina Signori

August 2010

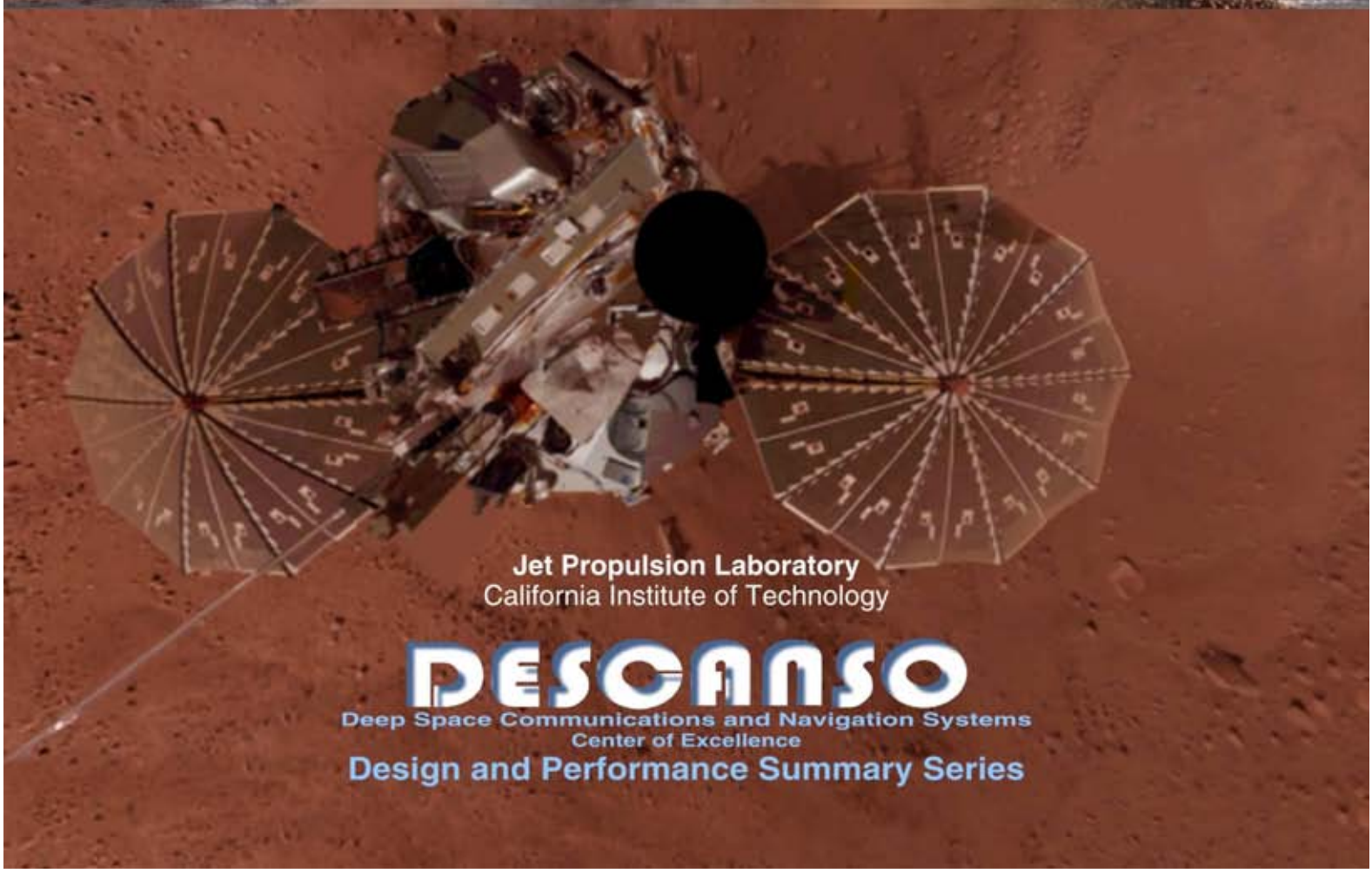

Jet Propulsion Laboratory
California Institute of Technology

DESCANSO
Deep Space Communications and Navigation Systems
Center of Excellence
Design and Performance Summary Series

The Cover

The upper cover image is an artist’s concept of the Phoenix Lander with legs deployed and thrusters on just before landing on the surface of Mars. This rendition was created by Corby Waste of JPL in 2003. As the Mars program artist, he has created artwork for several Mars missions [1].

During lander surface operations, the Phoenix project generated many exotic images from Mars. One of these, the lower cover image [2], is a vertical projection that combines hundreds of exposures taken by the lander’s Surface Stereo Imager camera and projects them as if looking down from above. The black circle is where the camera itself is mounted on the lander, out of view in images taken by the camera. North is toward the top of the image. This view comprises more than 100 different Stereo Surface Imager pointings, with images taken through three different filters at each pointing. The images were taken in the period from the 13th Martian day, or sol, after landing to the 47th sol (June 5 through July 12, 2008). The lander's Robotic Arm appears cut off in this mosaic view because component images were taken when the arm was out of the frame.

DESCANSO Design and Performance Summary Series

Article 15

Phoenix Telecommunications

Jim Taylor
Stan Butman
Chad Edwards
Peter Ilott
Richard Kornfeld
Dennis Lee
Scott Shaffer
Gina Signori

Jet Propulsion Laboratory
California Institute of Technology
Pasadena, California

National Aeronautics and
Space Administration
Jet Propulsion Laboratory
California Institute of Technology
Pasadena, California

August 2010

This research was carried out at the Jet Propulsion Laboratory, California Institute of Technology, under a contract with the National Aeronautics and Space Administration.

Reference herein to any specific commercial product, process, or service by trade name, trademark, manufacturer, or otherwise, does not constitute or imply endorsement by the United States Government or the Jet Propulsion Laboratory, California Institute of Technology.

Copyright 2010 California Institute of Technology. Government sponsorship acknowledged.

DESCANSO DESIGN AND PERFORMANCE SUMMARY SERIES

Issued by the Deep Space Communications and Navigation Systems
Center of Excellence
Jet Propulsion Laboratory
California Institute of Technology

Joseph H. Yuen, Editor-in-Chief

Articles in This Series

Article 1—"Mars Global Surveyor Telecommunications"
Jim Taylor, Kar-Ming Cheung, and Chao-Jen Wong

Article 2—"Deep Space 1 Telecommunications"
Jim Taylor, Michela Muñoz Fernández, Ana I. Bolea Alamañac, and Kar-Ming Cheung

Article 3—"Cassini Orbiter/Huygens Probe Telecommunications"
Jim Taylor, Laura Sakamoto, and Chao-Jen Wong

Article 4—"Voyager Telecommunications"
Roger Ludwig and Jim Taylor

Article 5—"Galileo Telecommunications"
Jim Taylor, Kar-Ming Cheung, and Dongae Seo

Article 6—"Odyssey Telecommunications"
Andre Makovsky, Andrea Barbieri, and Ramona Tung

Article 7—"Deep Space 1 Navigation: Extended Missions"
Brian Kennedy, Shyam Bhaskaran, J. Edmund Riedel, and Mike Wang

Article 8—"Deep Space 1 Navigation: Primary Mission"
Brian Kennedy, J. Edmund Riedel, Shyam Bhaskaran, Shailen Desai, Don Han,
Tim McElrath, George Null, Mark Ryne, Steve Synnott, Mike Wang, and Robert Werner

Article 9—"Deep Impact Flyby and Impactor Telecommunications"
Jim Taylor and David Hansen

Article 10—"Mars Exploration Rover Telecommunications"
Jim Taylor, Andre Makovsky, Andrea Barbieri, Ramona Tung,
Polly Estabrook, and A. Gail Thomas

Article 11—" Mars Exploration Rover Navigation"
Louis A. D'Amario
Article 12 —"Mars Reconnaissance Orbiter Telecommunications"
Jim Taylor, Dennis K. Lee, and Shervin Shambayati

Article 13 —"Dawn Telecommunications"
Jim Taylor

Article 14 —"Mars Science Laboratory Telecommunications Systems Design"
Andre Makovsky, Peter Ilott, and Jim Taylor

Article 15 —"Phoenix Telecommunications"
Jim Taylor, Stan Butman, Chad Edwards, Peter Ilott, Richard Kornfeld, Dennis Lee, Scott Shaffer, and Gina Signori

Table of Contents

THE COVER ..... **II**

TABLE OF CONTENTS ..... **V**

LIST OF FIGURES ..... **VII**

LIST OF TABLES ..... **IX**

Blank x

Foreword ..... **xi**

Acknowledgements ..... **xiii**

PREFACE ..... **XV**

1 MISSION AND SPACECRAFT SUMMARY **1**

1.1 Mission Description **1**
1.1.1 Objectives 1

1.2 Launch/Arrival Period Selection **2**
1.2.1 Phoenix Landing Site 2

1.3 LAUNCH PHASE AND INITIAL ACQUISITION **5**
1.3.1 Launch Vehicle 5
1.3.2 Launch Sequence 6

1.4 Cruise Phase **9**

1.5 Entry, Descent, and Landing (EDL) Phase **11**

1.6 Flight System Description **17**
1.6.1 Engineering Subsystems and Functions 18
1.6.2 Payload (Science Instruments) 20

2 TELECOM SUBSYSTEM OVERVIEW **27**

2.1 Telecom for Launch and Cruise **27**
2.1.1 Initial Acquisition 27
2.1.2 Cruise 29

2.2 Entry, Descent, and Landing **34**

2.3 Surface Operations **38**

2.4 X-Band Flight Subsystem Description **40**
2.4.1 Small Deep Space Transponder (SDST) 42
2.4.2 X-Band Solid State Power Amplifier (SSPA) 47
2.4.3 Antennas 48
2.4.4 X-band Microwave Components 52

2.5 UHF Flight Subsystem Description **54**

2.5.1 UHF Transceiver 56
2.5.2 UHF Antennas 59
2.5.3 UHF Coaxial Transfer Switches 65

2.6 Landing Radar 66
2.6.1 Radar Design 66
2.6.2 Radar Performance 68

2.7 Telecom Hardware Mass and Power Summary 70
2.7.1 X-Band Mass 70
2.7.2 Telecom-Related Spacecraft Power Consumption 71

3 GROUND SYSTEMS 72

3.1 X-Band Operations: The Deep Space Network 72

3.2 EDL Operations 74

4 TELECOM SUBSYSTEM LINK PERFORMANCE 76

4.1 X-Band Performance during Cruise through Separation 76
4.1.1 Initial Acquisition 76
4.1.2 Early Cruise 77
4.1.3 Trajectory Correction Maneuvers 79
4.1.4 Cruise Data Rates 81

4.2 UHF Performance during EDL and Surface Mission 82
4.2.1 EDL (UHF) 82
4.2.2 Surface (UHF Relay) 89

5 FLIGHT OPERATIONS 100

5.1 Phoenix-MEX Mission Operations System 100
5.1.1 Overflight Planning and Forward-Link Concept 100
5.1.2 Telemetry 101

5.2 Surface Ground Operations 102

5.3 Tactical Operations 102

5.4 X-Band Telecom Constraints 103

5.5 UHF Telecom Constraints 103

5.6 Surface Relay Link Strategy and Operations 103
5.6.1 Transceiver Prox-1 Frame Duplication Workarounds 104
5.6.2 Fill-Data Workarounds 104
5.6.3 Data Throughput Workarounds 105

6 LESSONS LEARNED 106

6.1 Spacecraft Design and Hardware 106

6.2 Operations 107

7 ABBREVIATIONS AND ACRONYMS 109

8 REFERENCES 117

List of Figures

Figure 1-1 Mars landing sites 1976–2008. 3
Figure 1-2 Phoenix landing site (actual in RED). 4
Figure 1-3 Phoenix landing site topography 5
Figure 1-4 "Exploded" view of the Delta II 7925 launch vehicle with Phoenix spacecraft. 7
Figure 1-5 Representative launch/ascent sequence of events. 8
Figure 1-6 Interplanetary trajectory. 10
Figure 1-7 Phoenix entry, descent, and landing (EDL) sequence (actual values in RED). 13
Figure 1-8 Phoenix radar timeline (terminal descent and landing phases). 14
Figure 1-9 Lander altitude profile from Entry phase to Landing. 15
Figure 1-10 Lander velocity magnitude profile from Entry phase to Landing. 16
Figure 1-11 "Exploded" view of the Phoenix flight system. 17
Figure 1-12 Phoenix Lander. 21
Figure 1-13 Phoenix science payload elements. 21
Figure 2-1 Ground track for 08/03/2007 window-open (launch Az 93 deg). 28
Figure 2-2 Elevation angles from DSN sites to Phoenix for the first 24 hours after launch 28
Figure 2-3 Phoenix-to-Earth range during initial acquisition. 29
Figure 2-4 Spacecraft-to-Earth range during cruise. 30
Figure 2-5 Sun–Craft–Earth angle during cruise 30
Figure 2-6 Sun-Earth-Probe Angle during cruise. 31
Figure 2-7 Phoenix antenna offpoint angles during cruise. 32
Figure 2-8 Expected Phoenix X-band ranging Pr/No during cruise. 33
Figure 2-9 EDL communications with orbiters and DTE to Green Bank. 36
Figure 2-10 EDL UHF communications. 37
Figure 2-11 Received Pt versus elevation angle for Odyssey relay. 39
Figure 2-12 Received Pt versus elevation angle for MRO relay. 39
Figure 2-13 Phoenix X-band telecom block diagram 40
Figure 2-14 Phoenix Spacecraft Cruise configuration. 41
Figure 2-15 Phoenix SDST from group buy 2. 42
Figure 2-16 Transponder high level functional diagram. 43
Figure 2-17 Modulation parameters and thresholds for (7,1/2) coded telemetry. 45
Figure 2-18 Modulation parameters and thresholds for (15,1/6) coded telemetry. 45
Figure 2-19 X-band SSPA block diagram. 48
Figure 2-20 Receive-band pattern for the Rx-CLGA. 49
Figure 2-21 Transmit-band pattern for the Tx-CLGA. 50
Figure 2-22 X-band MGA receive pattern. 51
Figure 2-23 X-band MGA transmit pattern. 51
Figure 2-24 UHF Telecom block diagram. 54
Figure 2-25 Phoenix entry configuration. 55
Figure 2-26 Phoenix landed configuration. 55

Figure 2-27 Carrier acquisition threshold versus frequency for SN103 transceiver. 57
Figure 2-28 Establishment of Prox-1 relay link with Odyssey. 58
Figure 2-29 Flight UHF wraparound (left) and 1/5-scale test antenna (right). 60
Figure 2-30 UHF wraparound antenna pattern at return-link frequency. 61
Figure 2-31 UHF helix antenna pattern at return-link frequency. 62
Figure 2-32 UHF monopole receive antenna pattern (Lander mockup, 437.1 MHz)..... 63
Figure 2-33 UHF monopole transmit antenna pattern (Lander mockup, 401.6 MHz). ... 63
Figure 2-34 Phoenix UHF antennas among other deck objects. 64
Figure 2-35 (Left) Phoenix Lander mockup; (Right) Phoenix model with ground effect. 65
Figure 2-36 Looking up at the radar patch antennas from below the lander. 66
Figure 2-37 Landing radar antenna (top) and electronics (bottom). 67
Figure 2-38 Radar versus IMU estimated altitude versus time. 69
Figure 2-39 Velocity comparison between radar beams and IMU. 69
Figure 3-1 34-m DSN antenna under construction at Madrid, Spain. 72
Figure 3-2 Completed 34-m antenna at Madrid, Spain. 73
Figure 3-3 Block diagram of Green Bank UHF receiving setup for Phoenix EDL. 75
Figure 4-1 Downlink carrier power at 34-m station during initial acquisition. 77
Figure 4-2 LGA and MGA antenna offpoint angles during cruise. 78
Figure 4-3 Example of measured 34-m carrier signal level compared with TFP predictions. 79
Figure 4-4 LGA offpoint angle during TCM-5 (turn, burn, turn back to cruise). 80
Figure 4-5 Measured versus predicted downlink carrier at 70-m station during TCM-5. 80
Figure 4-6 Predicted supportable data rates and actually used rates during cruise. 81
Figure 4-7 Phoenix arrival geometry. 83
Figure 4-8 MRO Image of Phoenix descending beneath its parachute. 84
Figure 4-9 MEX Melacom recorded open loop RF spectrum during Phoenix EDL. 85
Figure 4-10 Phoenix to Green Bank predicted Doppler. 86
Figure 4-11 Phoenix to Green Bank predicted carrier to noise ratio. 87
Figure 4-12 Cone angle (theta) from Phoenix to each of three orbiters during EDL. 88
Figure 4-13 Relative signal strengths for Phoenix-to-orbiter links. 88
Figure 4-14 Phoenix surface operations concept. 90
Figure 4-15 Overview of daily operations cycle with Odyssey and MRO relays. 90
Figure 4-16 Phoenix-MRO return-link data volume residual (actual minus predicted). . 94
Figure 4-17 Return-link data volume per sol compared with 60 Mb requirement. 95
Figure 4-18 Relay metrics: (top) number of passes per sol, (center) forward-link performance, (bottom) return-link performance. 96
Figure 4-19 Overflight durations between MEX orbiter and Phoenix. 97
Figure 4-20 Phoenix-MEX distance, elevation angle, and off-boresight angle on doy 152. 99
Figure 4-21 Phoenix-MEX return-link performance on doy 152. 99
Figure 5-1 MEX-to-Phoenix overflight planning and forward-link concept. 100
Figure 5-2 Phoenix-MEX telemetry interfaces. (Note: The circled numbers are procedure steps in Ref. [40].). 101
Figure 5-3 Megabits of fill data returned sol by sol during the mission. 105

List of Tables

Table 1-1 Legend for Figure 1-13: Phoenix Science Instruments 22
Table 2-1 Phoenix telecom parameters. 27
Table 2-2 Phoenix ΔDOR campaign schedule. 34
Table 2-3 Acronyms and abbreviations in the X-band telecom block diagram. 41
Table 2-4 SDST RF characteristics. 43
Table 2-5 SDST non-coherent and coherent operating states. 44
Table 2-6 Phoenix transponder uplink modulation and threshold values. 44
Table 2-7 X-band SSPA RF characteristics. 48
Table 2-8 X-band diplexer RF characteristics. 52
Table 2-9 X-band notch filter RF characteristics. 52
Table 2-10 X-band bandpass filter RF characteristics. 53
Table 2-11 X-band and UHF coaxial transfer RF characteristics. 53
Table 2-12 CE-505 transceiver RF characteristics. 56
Table 2-13 RF characteristics of the coaxial transfer switches. 65
Table 2-14 Landing radar characteristics. 68
Table 2-15 Landing radar performance. 68
Table 2-16 X-band mass. 70
Table 2-17 Spacecraft power for SDST, SSPA, UHF transceiver, and landing radar. 71
Table 4-1 UHF pass statistics for MRO, Odyssey, and Mars Express. 89
Table 4-2 UHF data volume (DV) comparison with predictions (30-day period with Odyssey). 93
Table 4-3 Comparison of Phoenix-MRO return link predicted and actual data volumes. 94
Table 4-4 Summary of Phoenix-MEX passes on doy 2008-149, -151, -152. 98

Blank

Foreword

This Design and Performance Summary Series, issued by the Deep Space Communications and Navigation Systems Center of Excellence (DESCANSO), is a companion series to the DESCANSO Monograph Series. Authored by experienced scientists and engineers who participated in and contributed to deep-space missions, each article in this series summarizes the design and performance of major systems, such as communications and navigation, for each mission. In addition, the series illustrates the progression of system design from mission to mission. Lastly, the series collectively provides readers with a broad overview of the mission systems described.

Joseph H. Yuen

DESCANSO Leader

Blank

Acknowledgements

This article was made possible by access to information and documents provided by members of the Phoenix spacecraft development, test, and flight teams. We made particular use of mission and instrument descriptive material by the excellent writers of the Launch and Landing press kits [3, 4] available on the JPL Phoenix public website.

Blank

Preface

About half a year before the robotic arm on NASA's Phoenix Mars Lander began digging into soil and subsurface ice of an arctic plain of Mars, six scientists traveled to one of the coldest, driest places on Earth for soil-and-ice studies that would eventually aid analysis of the Mars data [3]. "We wanted to gain experience with our Phoenix instruments in one of the most Mars-like environments on Earth," said Leslie Tamppari of NASA's Jet Propulsion Laboratory, Pasadena, California. She is the project scientist for Phoenix and principal investigator for the Antarctic Dry Valleys expedition. Soil adjacent to the ice table in the dry permafrost of University Valley does not get warmer than about minus 10 degrees Celsius (14 degrees Fahrenheit). “There's no other place on Earth that combines the dryness and the coldness of the Antarctic Dry Valleys, a combination that presents a difficult challenge to life,” said biologist Susanne Douglas of JPL [5].

In May 2010, the Phoenix Lander project ended operations after repeated attempts to contact the spacecraft were unsuccessful. That month the Mars Odyssey orbiter flew over the Phoenix landing site 61 times during a final attempt to communicate with the lander. No transmission from the lander was detected. Phoenix also did not communicate during 150 flights in three earlier listening campaigns in 2010. An image transmitted by the Mars Reconnaissance Orbiter shows signs of severe ice damage to the lander’s solar panels. Phoenix was not designed to survive the dark, cold, icy Martian winter. However, the slim possibility Phoenix survived could not be eliminated without listening for the lander after abundant sunshine returned [6].

Blank

1 Mission and Spacecraft Summary

The spacecraft for the Phoenix Lander mission to Mars was assembled and tested at Lockheed Martin Space Systems in Denver, Colorado. Its landing system included descent engines for a controlled touchdown, rather than making an airbag-cushioned landing like those of the Mars Pathfinder and the Mars Exploration Rover MER) missions. Control of the engines was supported by a landing radar that provided data to a lower altitude than previous missions. This landing method had not been used successfully on Mars since 1976. [7]

The Phoenix spacecraft and its scientific instruments were well suited to uncover clues to the geologic history and biological potential of the Martian arctic. Phoenix was the first surface mission to return data from either polar region providing an important contribution to the overall Mars science strategy "Follow the Water" and was instrumental toward achieving the four science goals of NASA's long-term Mars Exploration Program [8].

- Determine whether life ever arose on Mars
- Characterize the climate of Mars
- Characterize the geology of Mars
- Prepare for human exploration

The Phoenix Mission had two bold objectives to support these goals, which were to (1) study the history of water in the Martian arctic and (2) search for evidence of a habitable zone and assess the biological potential of the ice-soil boundary.

1.1 Mission Description

1.1.1 Objectives

The Phoenix mission was designed to meet the following two main objectives [8].

- **Objective 1: Study the history of water in all its phases**

Currently, water on Mars' surface and atmosphere exists in two states: gas and solid. At the poles, the interaction between the solid water ice at and just below the surface and the gaseous water vapor in the atmosphere is believed to be critical to the weather and climate of Mars. Phoenix was the first mission to collect meteorological data in the Martian arctic needed by scientists to accurately model Mars' past climate and predict future weather processes.

Liquid water does not currently exist – at least not for long – on the surface of Mars, but evidence from the Mars Global Surveyor, Odyssey, and Exploration Rover missions suggest that water once flowed in canyons and persisted in shallow lakes billions of years ago. However, Phoenix was sent to Mars to probe the history of liquid water that may have existed in the arctic as recently as 100,000 years ago. Scientists will be able to better understand the history of the Martian arctic after analyzing the chemistry and mineralogy of the soil and ice provided by the robust instruments on Phoenix.

- **Objective 2: Search for evidence of habitable zone and assess the biological potential of the ice-soil boundary**

Recent discoveries have shown that life can exist in the most extreme conditions. Indeed, it is possible that bacterial spores can lie dormant in bitterly cold, dry, and airless conditions for millions of years and become activated once conditions become favorable. Such dormant microbial colonies may exist in the Martian arctic, where due to the periodic wobbling of the planet, liquid water may exist for brief periods about every 100,000 years making the soil environment habitable.

Phoenix returned data to assess the habitability of the Martian northern environment by using sophisticated chemical experiments to assess the soil's composition of life-giving elements such as carbon, nitrogen, phosphorus, and hydrogen. Identified by chemical analysis, Phoenix also sent data to look at reduction-oxidation molecular pairs that may determine whether the potential chemical energy of the soil can sustain life, as well as other soil properties critical to determine habitability such as acidity/alkalinity (pH) and saltiness.

Despite having the proper ingredients to sustain life, the Martian soil may also contain hazards that prevent biological growth, such as powerful oxidants that break apart organic molecules. Such oxidants are expected in dry environments bathed in ultraviolet (UV) light, such as the surface of Mars. But a few inches (centimeters) below the surface, the soil could protect organisms from the harmful solar radiation. Phoenix successfully dug deep enough into soil (that was potentially protected from UV) to return data to analyze the soil environment and to look for organic signatures and potential habitability.

1.2 Launch/Arrival Period Selection

1.2.1 Phoenix Landing Site

The Phoenix mission was developed to take advantage of the 2007 launch opportunity by sending a payload of science instruments particularly appropriate for examining an environment of ice and soil.

Favorable opportunities to launch missions to Mars come about every 26 months, but the 2007 Phoenix launch opportunity was the best in several years for sending a surface mission so far north on Mars. NASA’s Mars Odyssey orbiter found evidence in early 2002 that this region shelters high concentrations of water ice mixed with the soil just beneath the surface.

The landing region was a key factor in defining the mission. The region has expanses with little variation on the surface, but a key attraction within arm’s reach underground. This stationary lander with a robotic arm was made for just such a place.

Figure 1-1 shows the landing sites of the two Viking landers in 1976, the Mars Pathfinder in 1997, the two Mars Exploration Rovers in 2004, and Phoenix in 2008. Figure 1-2 shows the planned landing site (blue ellipse) and the actual (red circle). Altitude in meters (m) was generated from data supplied by the Mars Global Surveyor (MGS) Mars Orbiter Laser Altimeter (MOLA). Phoenix landed in an arctic plain comparable in latitude to central Greenland or northern Alaska. The landing area is centered at 68.16 degrees (deg) north latitude, 233.35 deg east longitude. Figure 1-3 shows the topography of the area around the landing site [9].

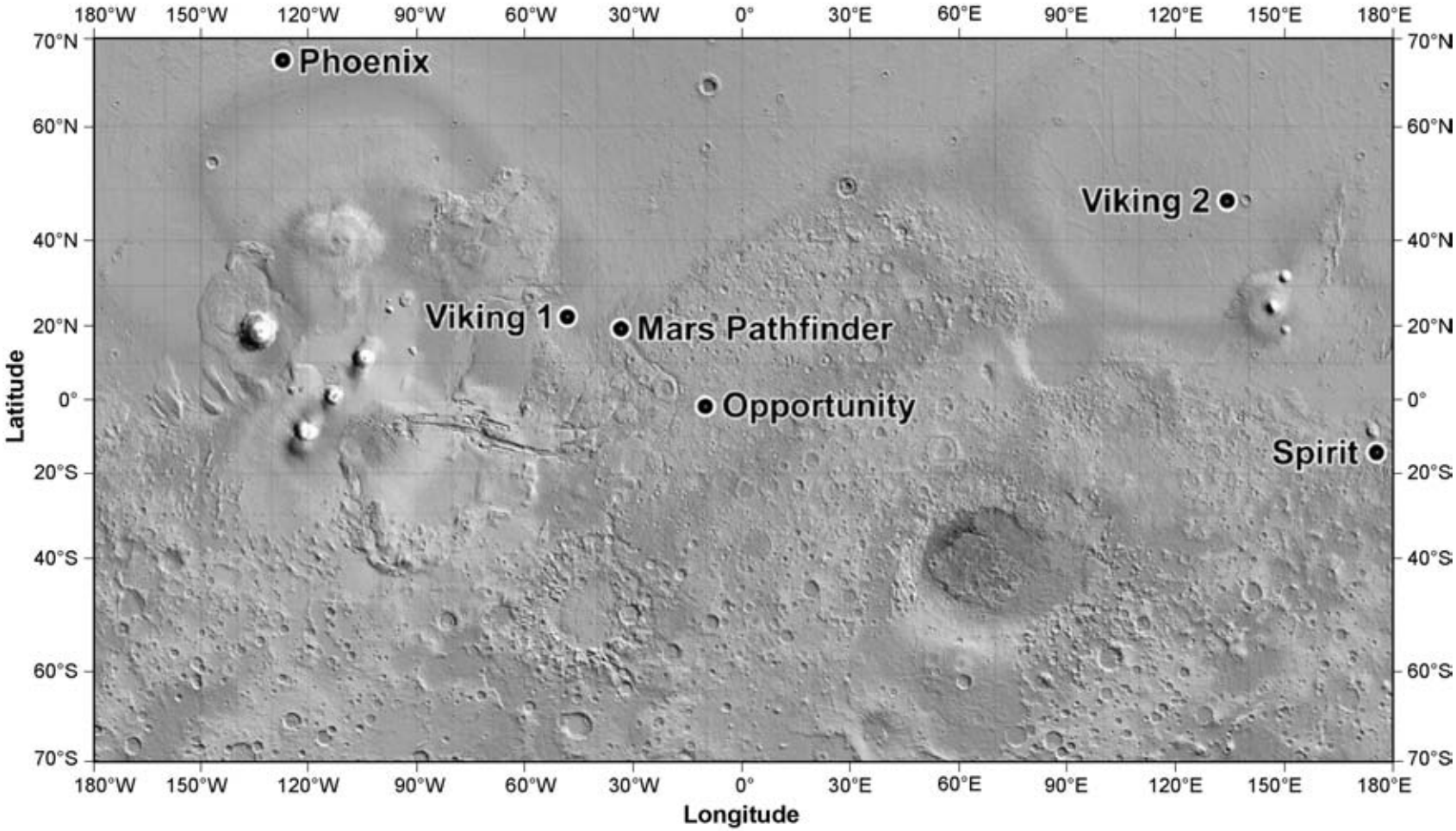

Phoenix	68.2°N	234.3°E	Opportunity	2.0°S	5.9°W
Viking 1	22.5°N	48.0°W	Spirit	15°S	184.7°W
Pathfinder	19.1°N	33.5°W	Viking 2	48.3°N	226°W

Figure 1-1 Mars landing sites 1976–2008.

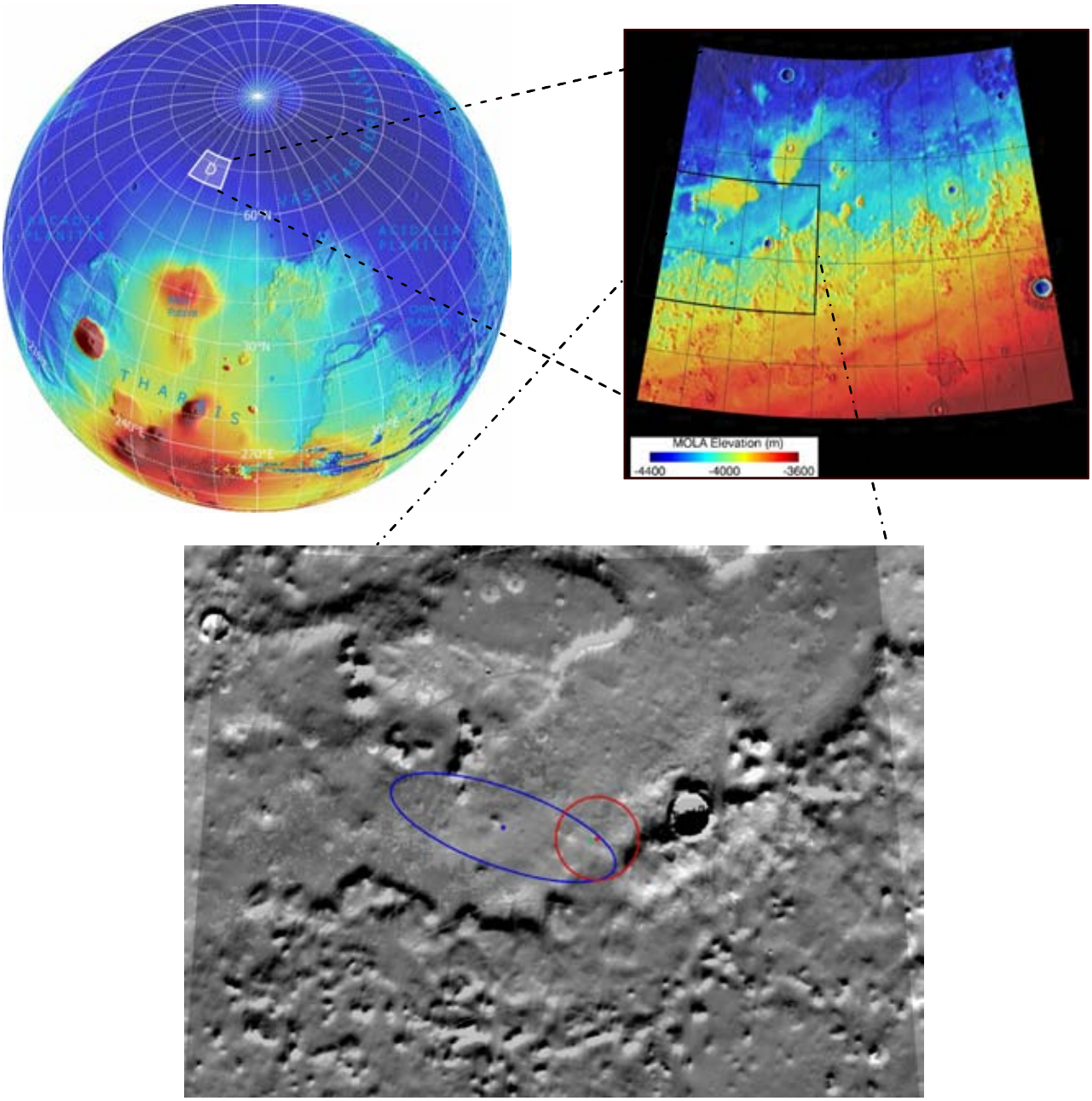

Figure 1-2 Phoenix landing site (actual in RED).

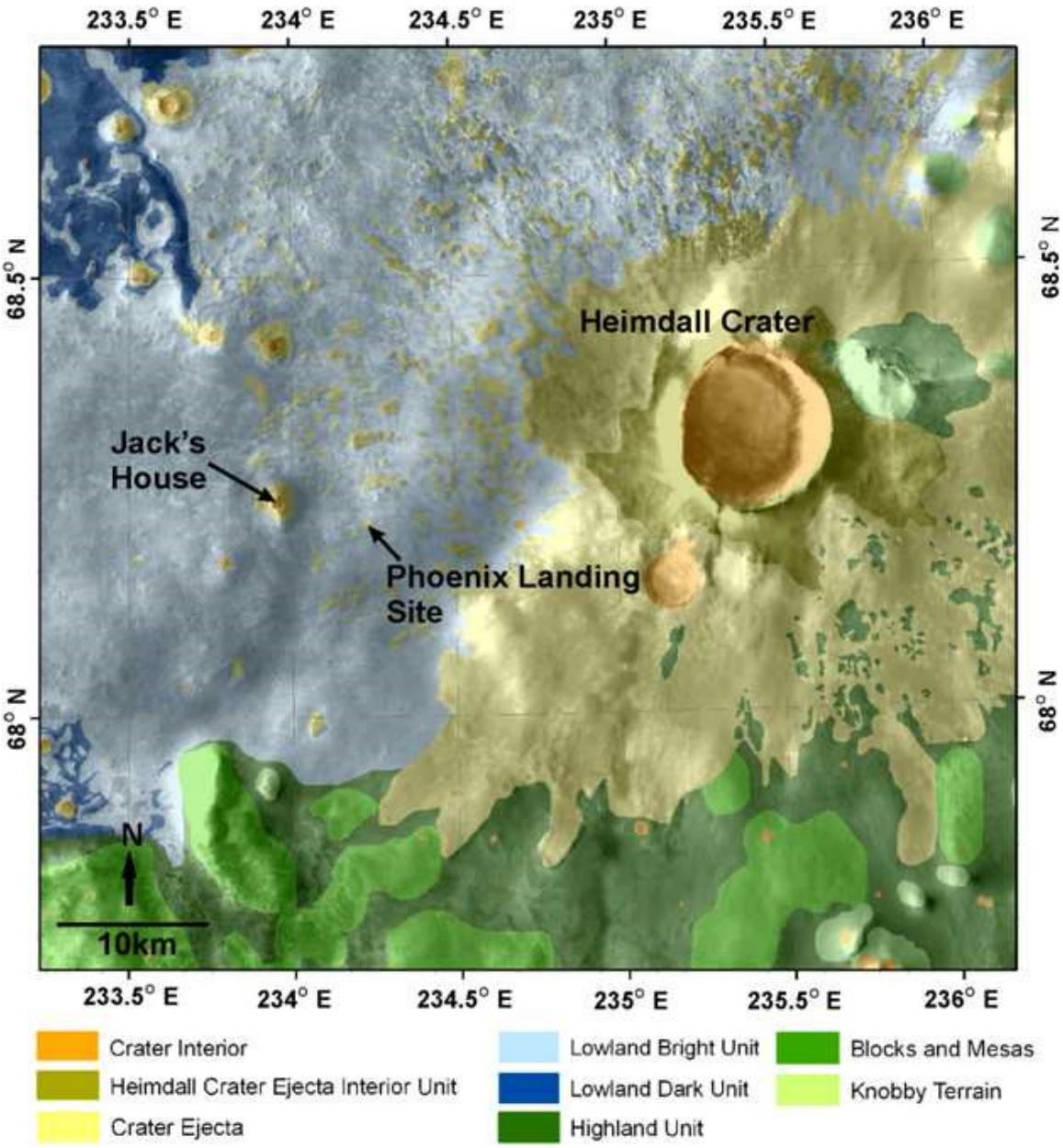

Figure 1-3 Phoenix landing site topography

Topographical mapping by the MOLA indicates a broad, shallow valley about 50 kilometers (km) (about 30 miles) wide and only about 250 m (about 800 feet (ft)) deep. The ground texture shows polygonal cracking, a pattern seen widely in Mars' high latitudes and also observed in permafrost terrains on Earth. It lies in mapped geological units named Scandia and Vastitas Borealis Marginal [10].

1.3 LAUNCH PHASE AND INITIAL ACQUISITION

1.3.1 Launch Vehicle

A three-stage Delta II launch vehicle lofted the Phoenix spacecraft from pad SLC-17A of Cape Canaveral Air Force Station in Florida. Several earlier Mars missions – Mars

Odyssey, the twin Mars Exploration Rovers, Mars Pathfinder and Mars Global Surveyor – have been among the more than 100 payloads carried by Delta II launches.

The Phoenix launch used the 7925 model of Delta II shown in Figure 1-4. This is a so-called "exploded view" that shows the major parts of the vehicle and its payload separately but in positions to indicate their proper relationships to each other and the whole. The launch vehicle had a liquid-fueled first stage with nine strap-on solid-fuel boosters, a liquid-fueled second stage, and a solid-fuel third stage. With its Phoenix payload on top, it stood 39.6 m (130 ft) tall.

The first stage used a Rocketdyne RS-27A main engine that provided nearly 890,000 newtons (N) (200,000 pounds) of thrust by reacting RP-1 fuel (thermally stable kerosene) with liquid oxygen. Hydraulic manipulation of the main engine's nozzle during the ascent controlled the vehicle's pitch and yaw. The nine strap-ons, called graphite-epoxy motors, were each about 13 m (43 ft) tall. Their hydroxyl-terminated polybutadiene propellant provided about 446,000 N (100,000 lb) of thrust apiece.

The Delta's second stage was powered by a restartable Aerojet AJ10-118K engine. The engine used a fuel called Aerozine 50, which is a mixture of hydrazine and dimethyl hydrazine, reacted with nitrogen tetroxide as an oxidizer.

A Star-48B solid-fuel rocket made by Thiokol powered the third stage. Its propellant was made primarily of ammonium perchlorate and aluminum. During launch and ascent through the atmosphere, the Phoenix spacecraft and the third stage were shielded from aerodynamic forces by a payload fairing, or nose cone, that was 2.9 m (9.5 ft) in diameter.

United Launch Alliance, a Denver-based joint venture of Boeing Co. and Lockheed Martin Corp., provided the launch vehicle and related services for the Phoenix mission.

1.3.2 Launch Sequence

Figure 1-5, from the Phoenix mission plan [11], illustrates the sequence of events during the ascent and parking orbit. The values of Alt (altitude in nautical miles, nmi, where 1 nmi = 1.852 km) and V1 (velocity in feet per second) shown in red are representative and varies slightly for the actual launch day and launch azimuth. Note: all other references to miles or miles/hr in this article are statute miles (1 statute mile = 1.609 km).

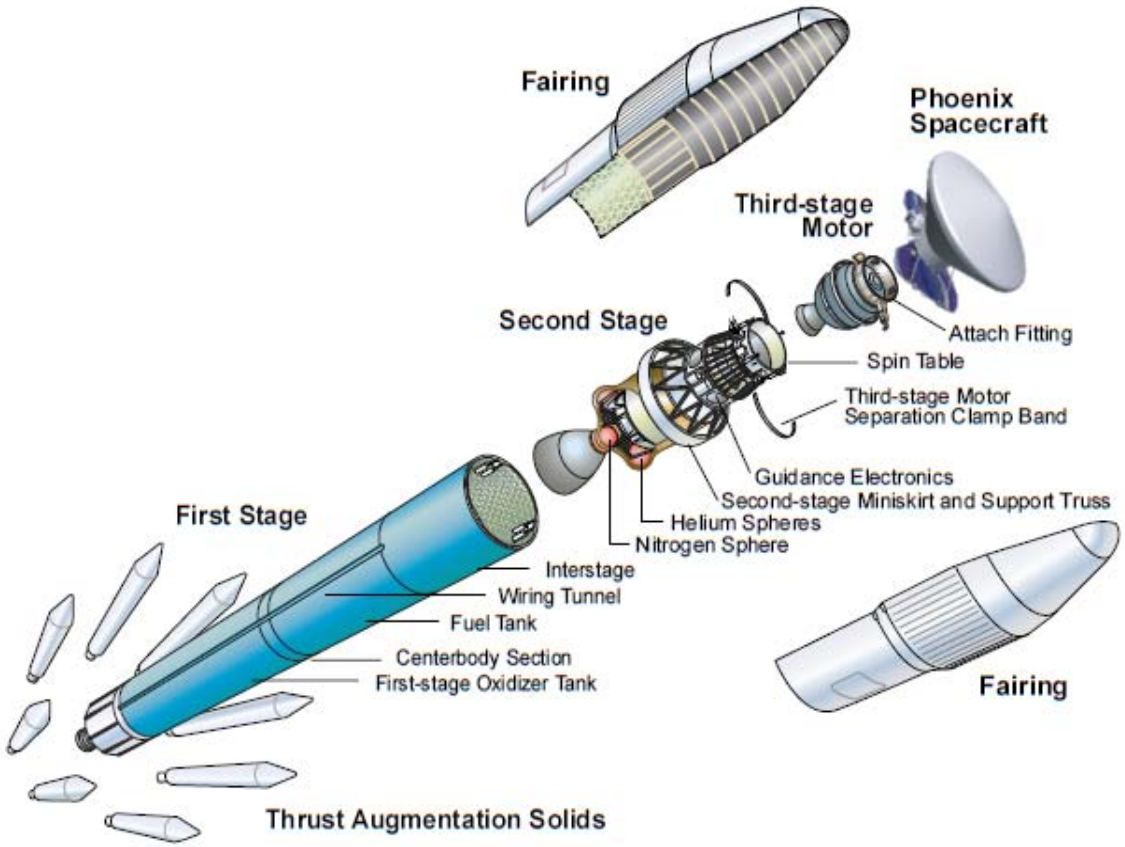

Figure 1-4 "Exploded" view of the Delta II 7925 launch vehicle with Phoenix spacecraft.

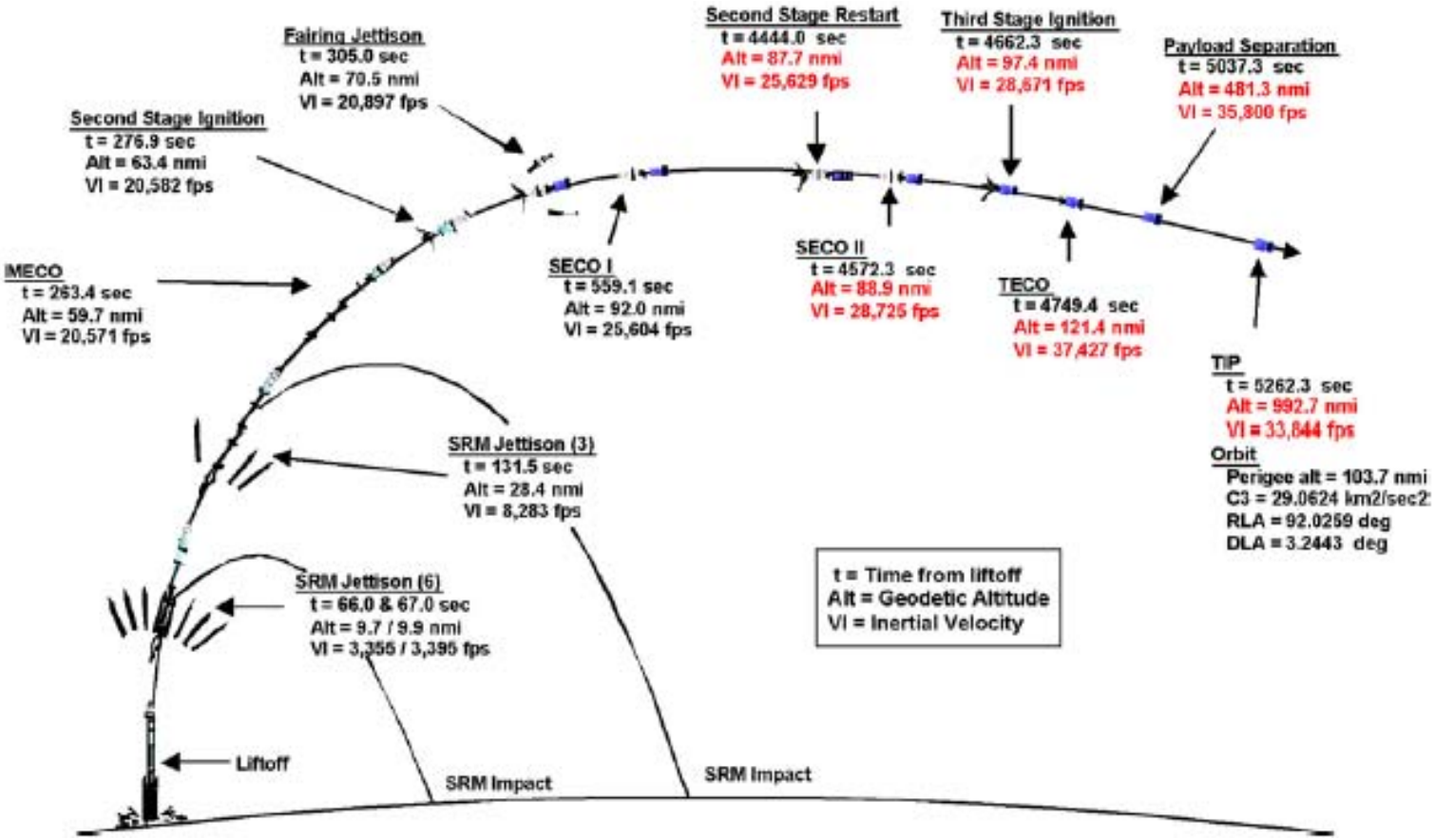

Legend

MECO = main engine cut off, RLA = right ascension of launch azimuth, SECO = sustainer engine cut off, TECO = third stage engine cut off, TIP = target interface point

Figure 1-5 Representative launch/ascent sequence of events.

At Delta II launch, the first-stage engine and six of its nine strap-on boosters ignited at the moment of liftoff. The remaining three boosters ignited following burnout of the first six. The spent casings of the first six boosters were jettisoned about a minute after liftoff. The final three were jettisoned about a minute later.

About 4 minutes, 23 seconds into the flight, at an altitude of about 111 km (69 miles), the main engine's thrust cut off. During the following 40 seconds, the first stage separated from the second, the second stage ignited, and the fairing fell away from the payload. At about 9 minutes, 20 seconds after liftoff, the second-stage engine temporarily stopped firing.

At this point, the spacecraft with the second and third stages of the Delta still attached was in a circular parking orbit planned to be 167 km (104 miles) above Earth. Before completion of even one orbit, however, the Delta's second stage was sequenced to reignite to begin pushing the spacecraft out onto its interplanetary trajectory toward Mars. The amount of time before the restart varied for different dates during the launch period, ranging from 72 minutes to 85 minutes after liftoff. This interval of coasting between the two engine burns by the second stage was longer than in any previous Delta II launch. The second burn of the Delta's second stage lasted about 2 minutes.

Small rockets then fired to spin the Delta's third stage to about 70 rotations per minute on a turntable attached to the second stage. The third stage then separated from the second, firing its engine for about 87 seconds to finish putting the spacecraft on course for Mars. To reduce the spacecraft's spin rate after the third-stage engine finished firing, a set of yo-yo-like weights reeled out on flexible lines.

1.4 Cruise Phase

Phoenix began the portion of its mission called the cruise phase after the spacecraft established radio communications with Earth and sent information that the cruise solar panels were generating electricity and spacecraft temperatures were stable. This phase lasted until 3 hours before Phoenix entered the atmosphere of Mars on May 25, 2008.

Phoenix traveled what is called a Type II trajectory to Mars, meaning the spacecraft is flying more than halfway around the Sun while in transit from one planet to the other. This took longer than the Type I trajectories flown by Mars Odyssey, Spirit, Opportunity and Mars Reconnaissance Orbiter. Figure 1-6 [3] shows the Phoenix trajectory to Mars.

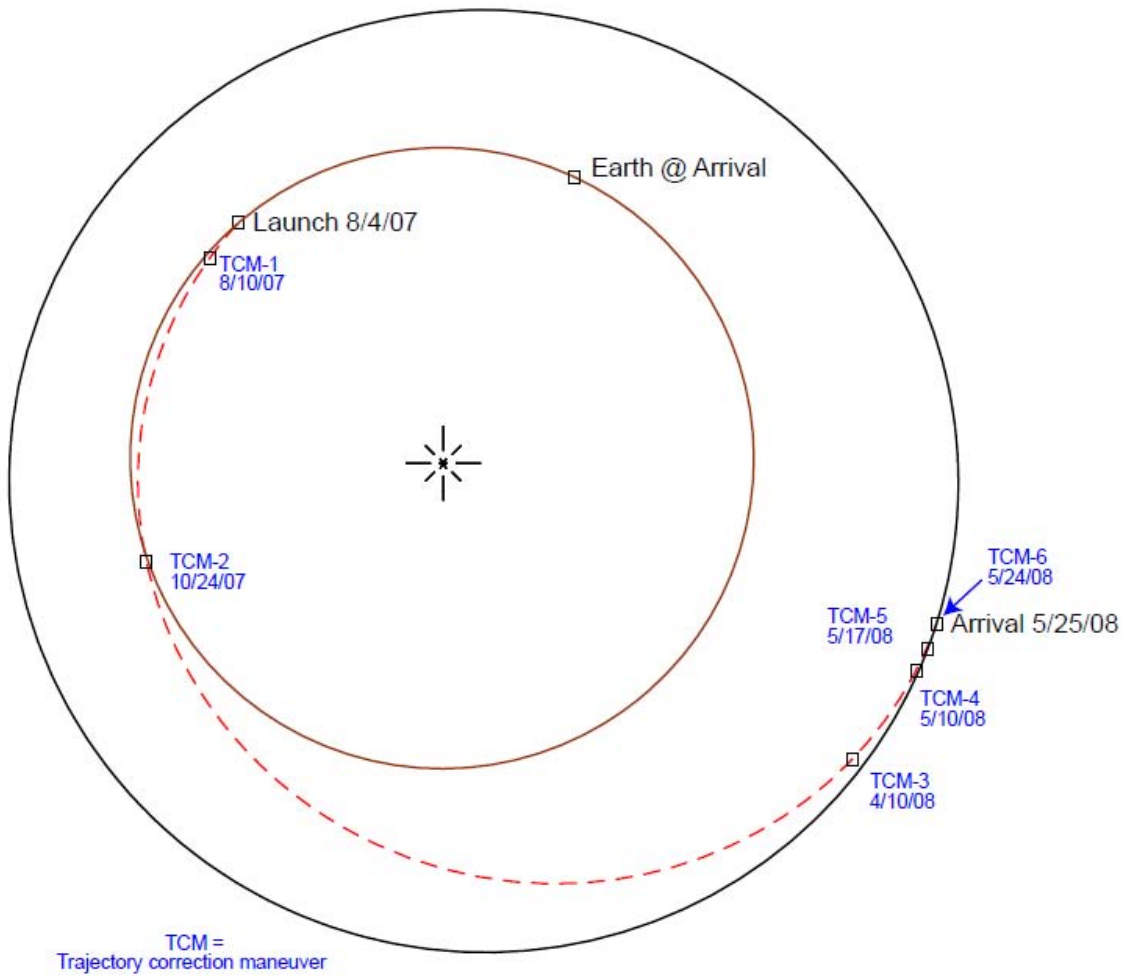

Figure 1-6 Interplanetary trajectory.

During the cruise phase, the Phoenix lander remained tucked inside the aeroshell, with the aeroshell attached to a cruise stage to be jettisoned in the final minutes of flight.

The trip had six scheduled opportunities for firing thrusters to adjust the spacecraft's flight path, or trajectory. Navigation and propulsion engineers designed these maneuvers. Phoenix performed the first and largest of its trajectory correction maneuvers on August 10, just 6 days after launch. The spacecraft fired its four mid-size thrusters for 3 minutes and 17 seconds in trajectory correction maneuver 1 (TCM-1). This changed velocity by 18.5 meters per second (m/s) (41 mph), a small amount in proportion to the spacecraft's velocity relative to the Sun at the time: about 33,000 m/s (74,000 miles per hour).

For the second trajectory correction maneuver (TCM-2), on October 24, 2007, Phoenix fired those same thrusters for 49.5 s. The first two maneuvers were planned from before launch to adjust for a launch day course that was intentionally designed to be slightly offset from Mars. The offset prevented the possibility of the third stage of the launch vehicle hitting Mars. The launch vehicle was not subject to the same rigorous cleanliness requirements that the spacecraft had to meet as a precaution against letting Earth organisms get a foothold on Mars. Before the first maneuver, Phoenix was flying a

trajectory that would miss Mars by about 950,000 km (590,000 miles). After these two maneuvers, it was on course to arrive at Mars.

On April 10, 2008, the mission's third trajectory correction maneuver (TCM-3) put Phoenix on course toward the target landing region in the Martian arctic. The maneuver began by pivoting the spacecraft 145 deg to point the mid-size thrusters in the calculated direction. Those thrusters then burned for about 35 seconds, after which the spacecraft pivoted back to point its main antenna toward Earth.

The final three opportunities for trajectory correction maneuvers, all in May, were for refining just where on Mars the arrival would be. The last one, TCM-6, would have been just 21 hours before landing, and the schedule included a backup opportunity just 8 hours before landing, if needed. TCM-6 was deemed not necessary. This decision resulted in an acceptable predicted landing location 17 km uptrack of the nominal location [12].

Navigators' assessments of the spacecraft's trajectory used three types of tracking information from ground antennas of NASA's Deep Space Network (DSN) at Goldstone, California; Madrid, Spain; and Canberra, Australia. One traditional method is ranging, which measures the distance to the spacecraft by timing precisely how long it takes for a radio signal to travel to the spacecraft and back to the ground station. A second traditional method is Doppler, which measures the spacecraft's speed relative to Earth by the amount of shift in the pitch of a radio signal from the craft.

A newer method, called delta differential one-way ranging (ΔDOR) measurement, adds information about the location of the spacecraft in directions perpendicular to the line of sight. Pairs of antennas on different continents simultaneously receive signals from the spacecraft, and then the same antennas observe natural radio waves from a known celestial reference point, such as a quasar. European Space Agency (ESA) antenna stations (in New Norcia, Australia, and in Cebreros, Spain) were scheduled to supplement the DSN stations in providing the ΔDOR measurements.

The months of the cruise phase also provided time for testing critical procedures, equipment and software in preparation for the spacecraft's arrival at Mars.

1.5 Entry, Descent, and Landing (EDL) Phase

The intense period from three hours before the spacecraft entered Mars' atmosphere until it reached the ground safely was called the entry, descent, and landing (EDL) mission phase. The Phoenix craft hit the top of the atmosphere at a speed of 5.6 kilometers per second (km/s, about 12,500 miles per hour). Within the next six and a half minutes, it used heat-generating atmospheric friction, then a parachute, then firings of descent thrusters, to bring that velocity down to about 2.4 m/s (5.4 miles per hour) just before touchdown.

The EDL system for Phoenix weighed less than the systems for earlier Mars missions, such as the air bags that cushioned the impacts for Mars Pathfinder and the Spirit and Opportunity rovers. This helped to give Phoenix a higher ratio of science-instrument payload (59 kilograms, kg, or 130 pounds, lb) to total launch weight (664 kg or 1,464 lb) than any spacecraft that has previously landed on Mars.

The last three successful landings on Mars before Phoenix used air bags to cushion the impact. Scaling up the air bag landing system from the Mars Pathfinder mission to the

larger Mars Exploration Rover (MER) mission required heavier air bags and stretched the capabilities of that type of landing. For the even larger science payload of the Phoenix mission and the upcoming Mars Science Laboratory [13], an air bag system would become too heavy to be feasible. Compared with the lightweight landing system used by Phoenix, an air bag landing system would have added much more weight to the spacecraft. That extra weight would require eliminating some of the science payload and research capabilities of the mission. Air bags add a safety margin for landing on slopes or rocky ground, but that advantage was deemed not vital for the flat and relatively unrocky terrain targeted for the Phoenix landing.

Like NASA's twin Viking landers in 1976, Phoenix used descent thrusters in the final seconds down to the surface and then set down onto three legs. However, compared to the Vikings, Phoenix used leaner components, such as thrusters controlled by pulse firing instead of throttle-controlled, and more complex interdependence among the components. The calculated tradeoff was more science payload for less leeway to recover if any stage of descent and landing went awry. The system on Phoenix resembled Mars Polar Lander's more than Viking's. Mars Polar Lander (MPL) reached Mars in 1999 but did not land successfully. Engineers for Phoenix remedied all the vulnerabilities identified in reviews of Mars Polar Lander, and also identified and addressed dozens of other potential issues.

The EDL system on Phoenix was a very active one, using radar to continually assess the spacecraft's vertical and horizontal motion during the final minutes and continually adjusted the descent based on that information. Compared with MER Spirit and Opportunity, Phoenix separated from its parachute nearly 100 times farther from the ground. The landing system on Phoenix was designed for the spacecraft to hit the ground at about one-tenth the velocity of Spirit and Opportunity's landings.

Figure 1-7 shows the planned (in black text) and the actual (in red text, from the Ref. [12] reconstruction) events during the preparation, hypersonic, and parachute phases. Figure 1-8 details the events during the terminal descent and landing phases, with an emphasis on radar activities.

From Figure 1-7 seven minutes before it reached the top of Mars' atmosphere, Phoenix jettisoned the cruise-stage hardware that it had relied on during the cruise from Earth to Mars. Half a minute later, the spacecraft began a 90-second process of pivoting to turn its heat shield forward. Five minutes after completing that turn, Phoenix started sensing the top of the atmosphere at an altitude of about 125 km (78 miles). Friction from the atmosphere during the next three minutes took most of the velocity out of the descent. Friction heated the forward-facing surface of the heat shield to a peak of about 1,420 degrees Celsius (2,600 degrees Fahrenheit) at an altitude of 41 km (25.5 miles).

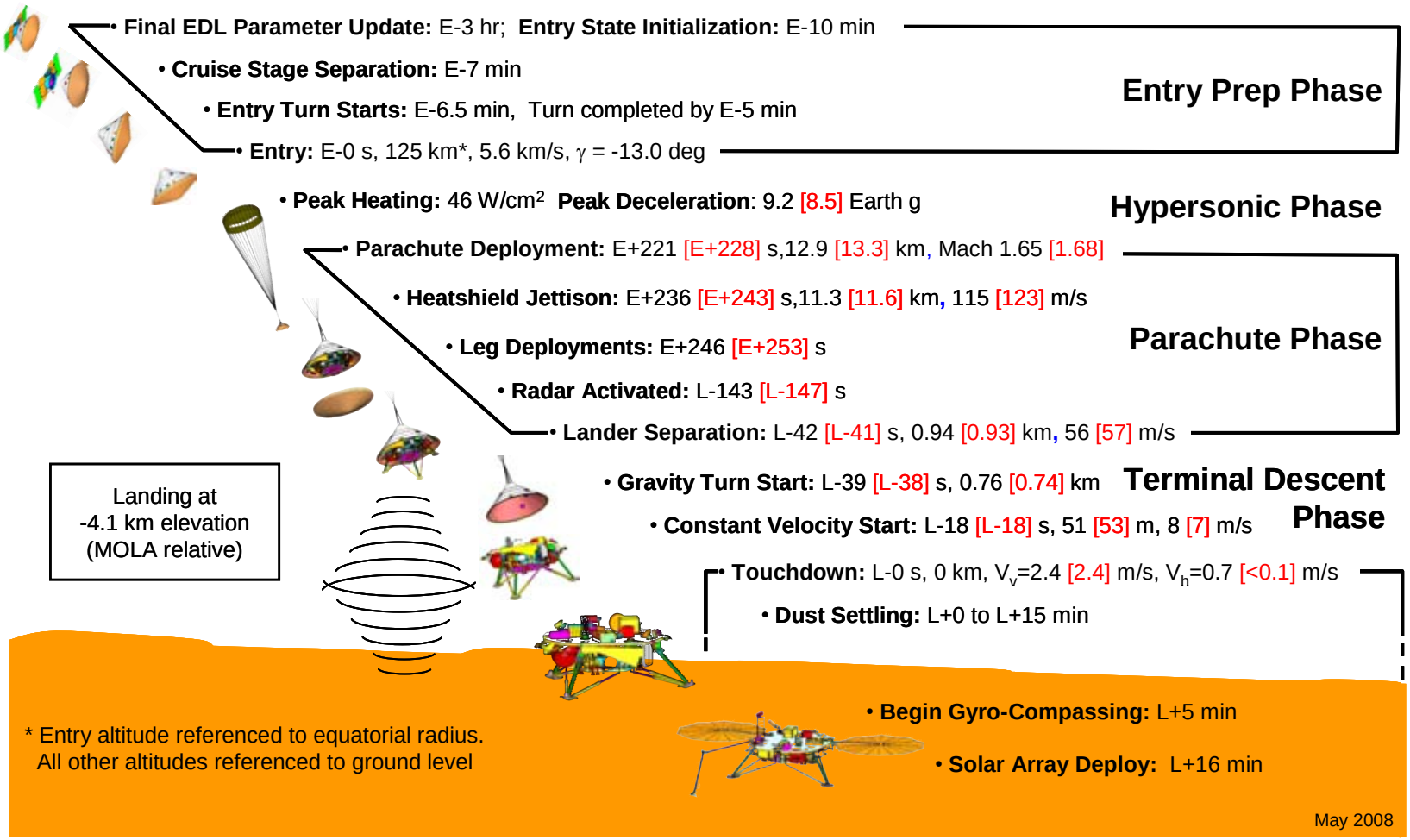

Figure 1-7 Phoenix entry, descent, and landing (EDL) sequence (actual values in RED).

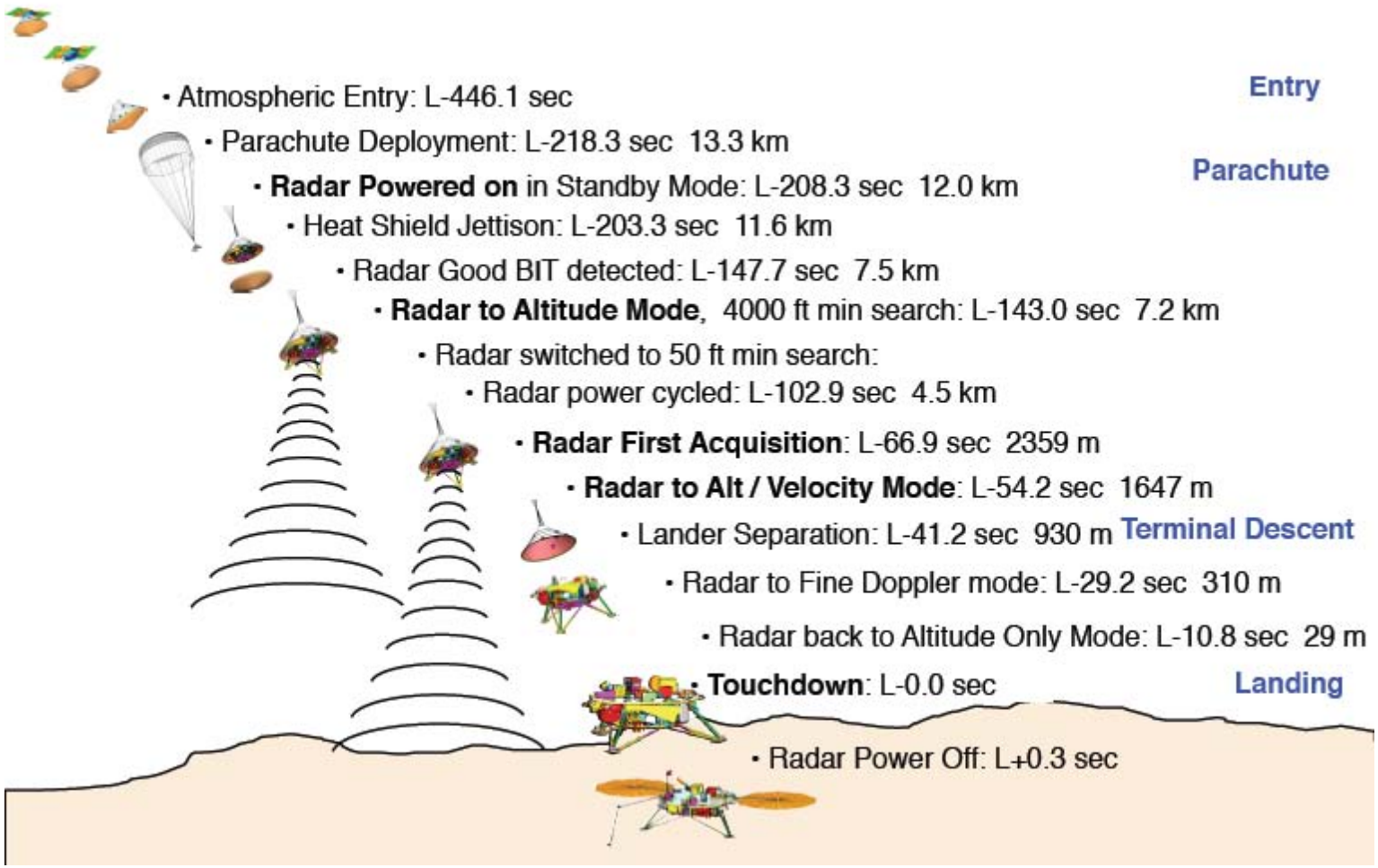

Figure 1-8 Phoenix radar timeline (terminal descent and landing phases).

Figure 1-9 shows the actual altitude profile from the landing radar during EDL, and Figure 1-10 shows the velocity profile. At about 12.6 km (7.8 miles) in altitude and a velocity about 1.7 times the speed of sound, Phoenix deployed its parachute, which was attached to the backshell. The spacecraft descended on the parachute for nearly three minutes. During the first 25 seconds of that, Phoenix jettisoned its heat shield and extended its three legs.

At 78 s after the parachute opened and 147 s before landing, the spacecraft started using its radar. The radar provided information to the onboard computer about distance to the ground, speed of descent, and horizontal velocity. It took readings at a pace of 10 times per second until touchdown.

Descent speed had slowed to 57 m/s (about 128 miles per hour) by the time the lander separated from the back shell and parachute, at 0.93 km (about six-tenths of a mile) above the ground. This was defined as the beginning of the terminal descent phase. The spacecraft was then in free fall for half a second before the landing thrusters began firing. The thrusters increased their thrust 3 s after Phoenix set itself free from the parachute. Touchdown was still 38 s away. The onboard computer used information from the radar to adjust the pulsed firings of the 12 descent thrusters.

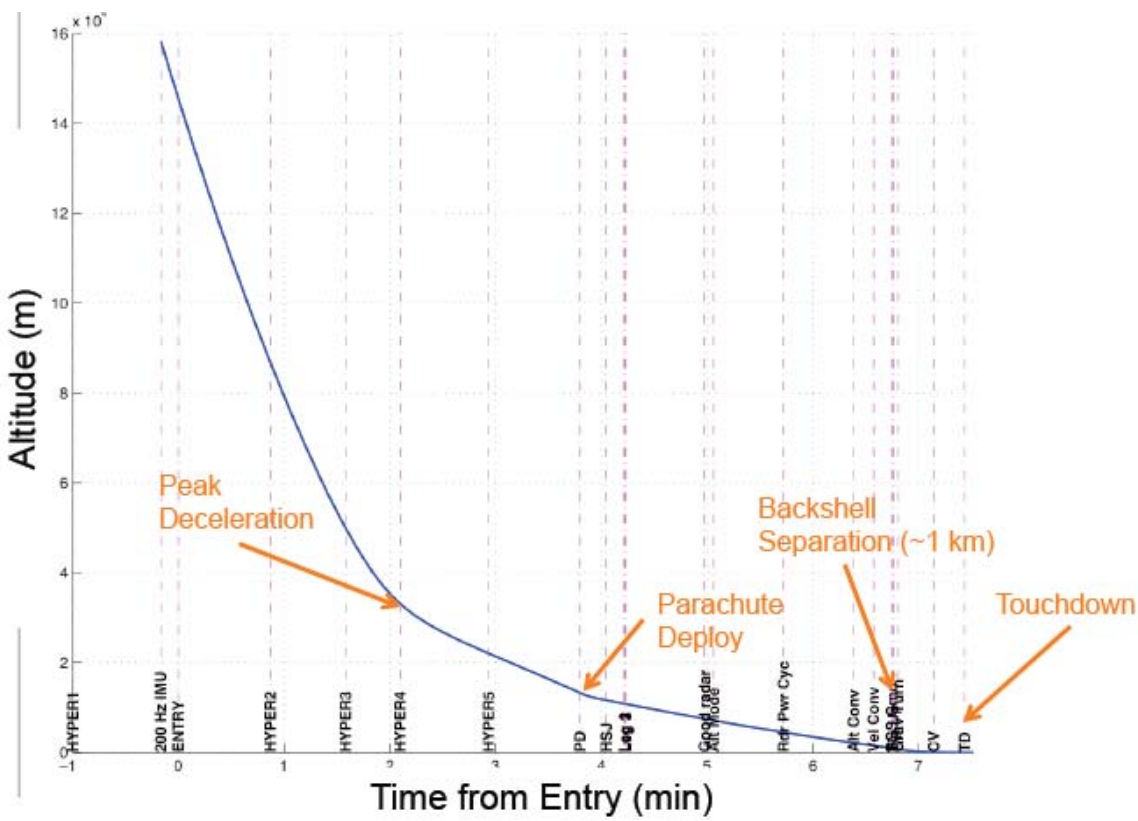

Figure 1-9 Lander altitude profile from Entry phase to Landing.

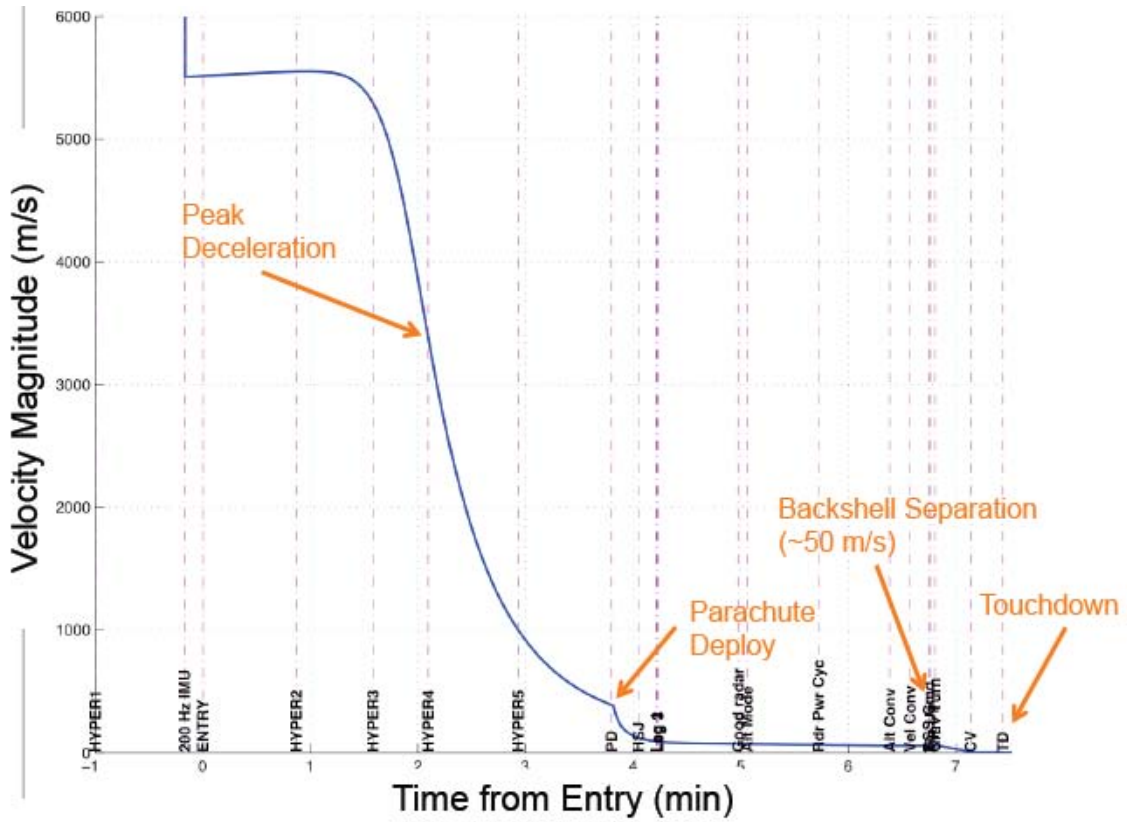

Figure 1-10 Lander velocity magnitude profile from Entry phase to Landing.

To dodge a chance of the parachute following the lander too closely and draping it after touchdown, Phoenix performed a backshell avoidance maneuver. It used the radar "fine Doppler" mode sensing of horizontal motion as an indicator of which way the wind was blowing, and the thrusters shoved the lander in the opposite direction.

By the time the lander got to about 30 m (98 ft) above the surface, it had slowed to about 2.4 m/s (5.4 miles per hour) in vertical velocity. Continuous adjustments to the thruster firings based on radar sensing were also used to minimize horizontal velocity and rocking.

Twelve seconds from touchdown, Phoenix maintained a steady descent velocity with accelerometers until it reached the surface for a soft touchdown. It shut off the thrusters when sensors on the footpads detected contact with the ground.

1.6 Flight System Description

Phoenix flew the existing lander from the Mars Surveyor Program (MSP'01), which was four months into the assembly test and launch operations (ATLO) phase when the mission was cancelled.

The lander's main structure was built for the Mars Surveyor 2001 program, and was then kept in a protective, controlled environment after the lander portion of that program was cancelled. Several modifications were made to the inherited lander, some to meet return-to-flight recommendations from review of Mars mission failures in 1999 and some to adapt to the specific goals and plans for the Phoenix mission.

Figure 1-11 is an exploded view of the major portions of the Phoenix flight system, the parts shown separately but in positions that indicate their proper relationships.

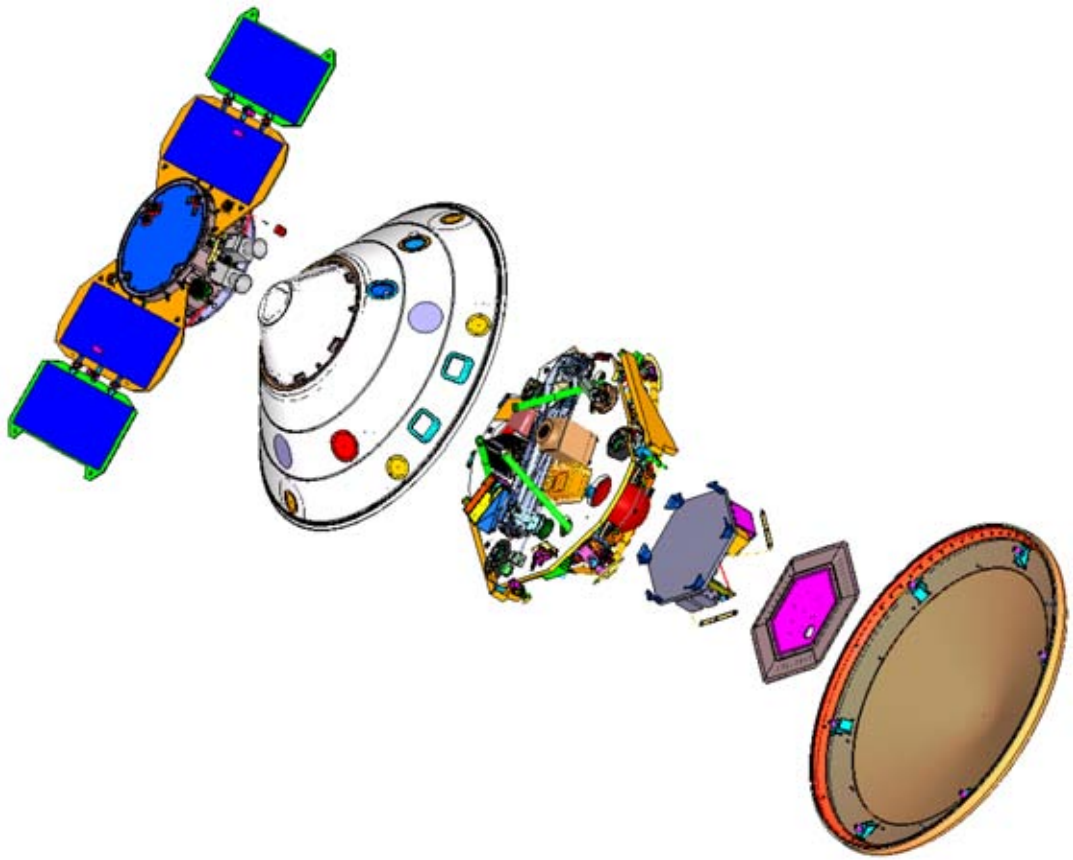

Figure 1-11 "Exploded" view of the Phoenix flight system.

From left to right in the figure, these are the

- Cruise stage
- Backshell
- Lander
- Component deck
- Heat shield

1.6.1 Engineering Subsystems and Functions

The major subsystems of the Phoenix spacecraft were guidance, navigation, and control (GNC), propulsion, power, command and data handling, telecommunications, navigation, thermal control, and flight software (FSW).

1.6.1.1 Guidance, Navigation, and Control (GNC)

The GNC subsystem provided guidance, navigation, and attitude control to the lander spacecraft during cruise and during entry, descent, and landing until touchdown on Mars. Its activities included

- Determining the attitude of the spacecraft, determining the location of desired targets such as the Sun and Earth
- Providing attitude control for rate damping after launch vehicle separation
- Orienting the spacecraft during cruise communication and science periods
- Providing and controlling translational delta-V maneuvers

Attitude determination was nominally accomplished using an inertial measurement unit (IMU) and a star tracker (two of each). Each IMU consisted of three ring laser gyros and three accelerometers. The Star Tracker was a 16.4 × 16.4 deg (full angle) field-of-view star tracker, which provided attitude updates from unknown initial conditions at 10 hertz (Hz). The same type of star tracker is used on Odyssey, a camera that takes pictures of the sky and has computer power to compare the images with a catalog of star positions and recognize which part of the sky it is facing. The subsystem provided an all stellar attitude determination capability by using Star Tracker measurements only, allowing the IMU to be powered down. The subsystem also contained analog Sun-sensor assemblies, which were used for Sun acquisition, pointing, and contingency operations.

The subsystem used a downward-pointing four-beam, 4.3-gigahertz (GHz) Doppler radar during terminal descent to establish altitude and ground relative velocity.

1.6.1.2 Propulsion

Phoenix carried thrusters to adjust its trajectory while it coasted, to control its orientation, and to slow its final descent to the surface of Mars. Attitude control was provided solely using the propulsion system. The propulsion system consisted of one string of four 5.0 pound force (lbf) or 22 newton (N) thrusters and one string of four 1.0 lbf (4.5 N) thrusters for use during cruise and entry, and one string of twelve 68 lbf (300 N) descent engines for use during terminal descent. All 20 of these thrusters used hydrazine, a propellant that does not require an oxygen source. Hydrazine is a corrosive liquid compound of nitrogen and hydrogen that decomposes explosively into expanding gases when exposed to a catalyst in the thrusters.

Twelve thrusters mounted around the bottom edge of the lander slowed the descent during the last half-minute before the legs touched the surface. These could each pulse on and off to fine-tune the velocity and to maintain the lander’s stability – by controlling its pitch, yaw, and roll -- as it approached touchdown. They each provided about 293 N (65.9 lbf) of thrust.

Eight smaller thrusters were used during the cruise phase of the mission, while the lander was enclosed in a protective aeroshell. These eight were also mounted on the lander, but extended through cutaways in the in the backshell. Four were used during the six trajectory correction maneuvers during cruise. These trajectory correction thrusters each delivered about 15.6 N (3.5 lbf). The other four were used for changing the spacecraft's orientation, or "attitude," such as for pivoting the spacecraft so the heat shield faces forward during entry into Mars' atmosphere. Their thrust capacity was about 4.4 N (1 lbf) apiece.

1.6.1.3 Electric Power

The cruise stage, jettisoned 7 minutes prior to entry, incorporates solar arrays. The lander's array stayed folded inside the aeroshell until Phoenix reached Mars. The vehicle then relied on batteries for power until landing, when the lander's array was deployed.

On the surface of Mars, power came from a two-wing solar array. This array was shaped as two nearly circular decagons extending from opposite sides of the lander, with a total of 4.2 square meters (45 square feet) of functional surface area on flexible, lightweight substrate. A pair of rechargeable 25-amp-hour lithium-ion batteries provided power storage.

1.6.1.4 Command and Data Handling

The spacecraft's computing functions were performed by the command and data handling subsystem. The heart of this subsystem was a RAD6000 microprocessor, a version of the PowerPC chip once used on many models of Macintosh computers, but enhanced to endure the natural radiation and other rigors of a space environment. The RAD6000 can operate at three speeds: 5 million, 10 million or 20 million clock cycles per second. Computer memory available to the command and data handling subsystem included more than 74 megabytes of dynamic random access memory, plus flash memory, which allowed the system to maintain data even without power.

1.6.1.5 Telecommunications

Phoenix carried both an X-band telecom subsystem and an ultra-high frequency (UHF) telecom subsystem.

The X-band telecom subsystem used two small deep space transponders (SDSTs), cross-strapped to the two command and data handling (C&DH) boxes. Two MER-heritage 15-watt (W) solid state power amplifiers (SSPAs) provided the radio frequency (RF) output power to the antenna. The cruise stage carried a medium gain antenna (MGA) horn as well as separate transmit and receive low gain antennas (LGAs). Both the MGA and the LGAs were mounted on fixed brackets (that is, not gimbaled).

The X-band telecom subsystem, mounted on the cruise stage of the spacecraft, was used exclusively for launch and cruise phases. Just prior to entry into the Martian atmosphere, the Phoenix cruise stage containing the X-band telecom subsystem was jettisoned. All ensuing communications during EDL and surface operations were from the lander, via the UHF link with the Mars Reconnaissance Orbiter (MRO) and Odyssey.

From the surface of Mars, Phoenix used the UHF (300 to 3,000 MHz) radio band for communications. Communications to and from Earth were relayed by Mars orbiters. NASA's Mars Odyssey orbiter and Mars Reconnaissance Orbiter were the main relay

assets for Phoenix. The system was also compatible with relay capabilities of the European Space Agency's Mars Express (MEX) orbiter.

A helical UHF antenna mounted on the lander deck sent and received all communications starting with the final half-minute of descent. The helical antenna and a monopole UHF antenna, also mounted on the deck, were used for relay telecommunications during the months of operation after landing. The lander could send data at rates of 8,000 bits per second (bps), 32,000 bps, or 128,000 bps. The lower two speeds were the choices for receiving commands relayed to Phoenix from an orbiter. The UHF part of the telecommunications subsystem also included a wrap-around UHF antenna on the back shell. This antenna handled communications during a period beginning when the cruise stage was released (separated) about 5 minutes before landing, and ending when the helical antenna began working, just after the lander separated from the back shell.

During the voyage from Earth to Mars, Phoenix used a set of X-band (7 to 12.5 GHz) communications equipment. It communicated directly with the Deep Space Stations (DSSes) on Earth. A medium-gain X-band antenna mounted on the cruise stage could both transmit and receive. Two low-gain antennas provided backup redundancy, one to transmit and the other to receive. The redundancy also extended to a pair of small deep space transponders (SDSTs) and a pair of solid state power amplifiers (SSPAs). Phoenix could transmit at data rates as great as 2,100 bps and could receive data at up to 2,000 bps.

1.6.1.6 Thermal Control

Thermal controls used a combination of electrical heaters, thermostats, temperature sensors, blanketing, and thermal coatings. The deck of the Phoenix lander doubled as an insulation layer by its honeycomb-composite interior structure and a low-thermal-conductivity surface layer.

At the Phoenix landing site, the main challenge was to prevent components from getting too cold and to prevent the large daily swings in temperature from doing any damage. Enroute from Earth to Mars, overheating was also a concern. The thermal control subsystem conducted heat away from electronics susceptible to becoming too hot.

1.6.1.7 Flight Software

The flight software (FSW) on Phoenix coordinated the spacecraft's execution of commands and organized data to be transmitted to Earth. It protected the spacecraft by checking commands for faults, monitoring the health of subsystems, and being ready to take corrective steps when it detected irregularities. Like other spacecraft, Phoenix had a defined "safe mode" configuration, in which it could remain thermally safe, power-positive, and commandable. Phoenix was intentionally landed in safe mode, and it entered safe mode under FSW control several times during the surface mission.

1.6.2 Payload (Science Instruments)

The Phoenix Mars Lander carried seven science instruments, three of which were suites of multiple tools. Figure 1-12 and Figure 1-13, respectively, show a sketch and an artist's concept of the science payload.

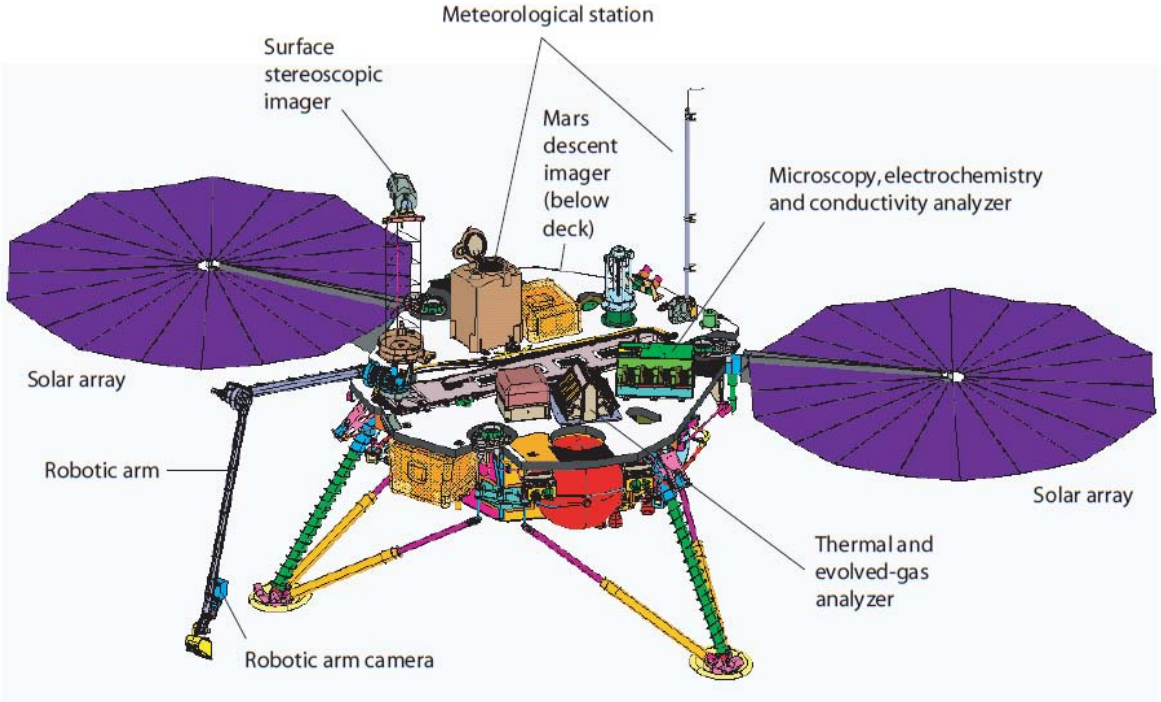

Figure 1-12 Phoenix Lander.

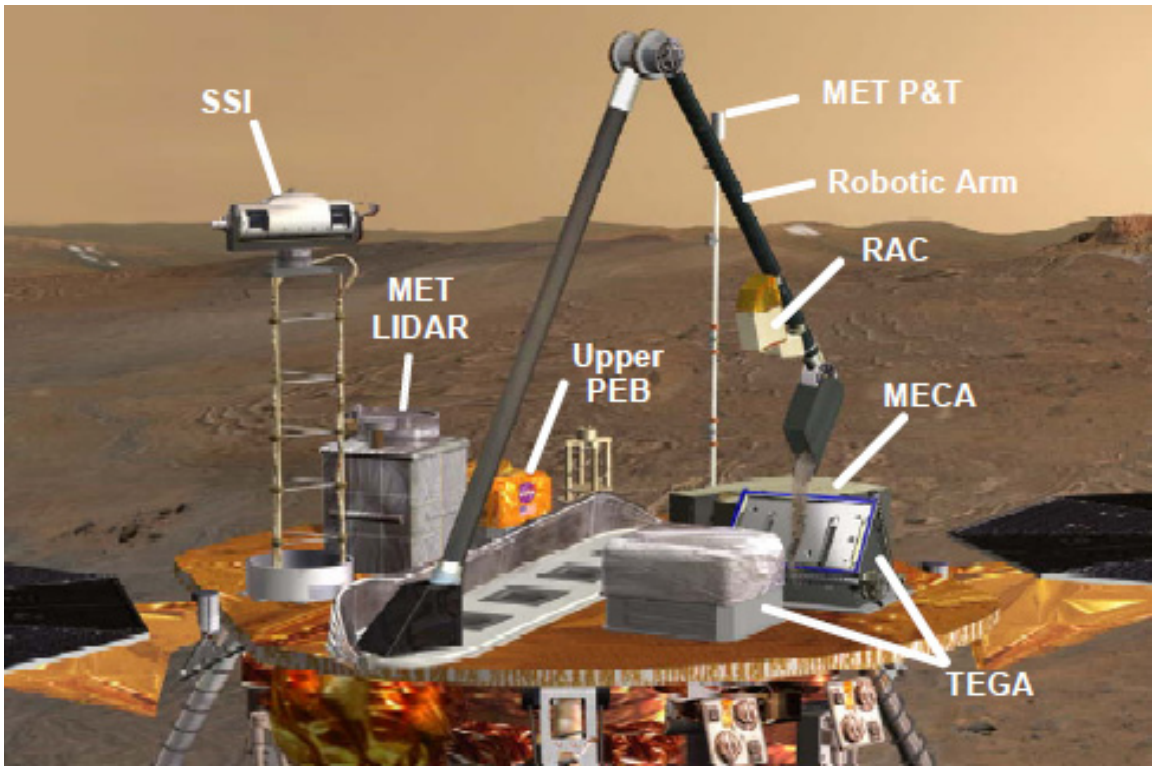

Figure 1-13 Phoenix science payload elements.

Table 1-1 Legend for Figure 1-13: Phoenix Science Instruments

LIDAR	light detection and ranging	P&T	pressure and temperature
MECA	microscopy, electrochemistry, and conductivity analyzer	RAC	robotic arm camera
MET	meteorological	SSI	surface stereo imager
PEB	payload electronics box	TEGA	thermal and evolved gas analyzer

1.6.2.1 The Robotic Arm

The robotic arm allowed Phoenix to explore vertically and to use instruments on the spacecraft deck to analyze samples of Martian soil and ice. The arm dug trenches, positioned arm-mounted tools for studying the soil in place, and delivered scooped-up samples to other instruments.

The aluminum and titanium arm was 2.35 m (7.7 ft) long. One end was attached to the lander's deck. An elbow joint was in the middle. The other end had a scoop with blades for digging into the soil and a powered rasp for breaking up frozen soil. The arm moved like a backhoe, using four types of motion: up-and-down, side-to-side, back-and-forth, and rotating.

The arm could reach far enough to dig about half a meter (20 inches, in.) deep. Researchers anticipated that the icy-soil layer would be about as hard as concrete. Once the excavation by the arm reached that layer, the powered rasp on the bottom of the scoop was used to generate enough loose material for a sample.

Because the arm would be making direct contact with icy soil that is conceivably a habitat where microbes could survive, extra precautions were taken with it to prevent introducing life from Earth. Before the arm was given a sterilizing heat treatment in March 2007, it was enclosed in a biological barrier wrap. This barrier kept microbes off the arm during the subsequent months before launch. It did not open until after Phoenix had landed on Mars.

The robotic arm design was based on a similar arm flown on the 1999 Mars Polar Lander mission, with refinements including enhanced capability for collecting an icy sample.

1.6.2.2 The Robotic Arm Camera (RAC)

The camera rode fastened to the arm just above the scoop. It provided close-up color images of Martian soil at the landing site, of the floor and walls of trenches dug by the arm, and of soil and ice samples before and after they were in the scoop.

Information the camera revealed about soil textures aided in selecting samples to pick for analysis.

The camera had a double Gauss lens system, a design commonly used in 35-millimeter (mm) cameras. Images were recorded by a

charge-coupled device (CCD) similar to those in consumer digital cameras. The instrument included sets of red, green, and blue light-emitting diodes (LEDs) for illuminating the target area.

The focus could be adjusted by a motor, which is a first for a camera on an interplanetary spacecraft. The focus could be set as close as about 11 millimeters about 0.5 in.) and out to infinity. With a resolution of 23 micrometers (microns) per pixel at the closest focus, this camera could show details much finer than the width of a human hair.

1.6.2.3 The Surface Stereo Imager (SSI)

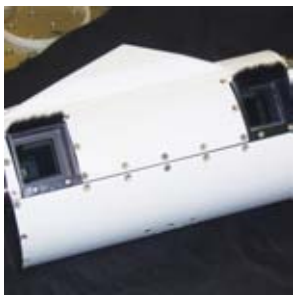

The SSI recorded panoramic views of the surroundings from atop a mast on the lander. Its images from two cameras situated about as far apart as a pair of human eyes provided three-dimensional information for the Phoenix team to use in choosing where to dig and in operating the robotic arm.

A choice of 12 different filters for each eye enabled the instrument to produce images not only in full color, but in a several specific visual and infrared frequencies useful for interpreting geological and atmospheric properties. The twin cameras could look in all directions from a perch about 2 m (7 ft) above Martian ground level. They had about the same resolution as human eyes, though with a much smaller field of view per single glance. The camera captured each view onto 1-megapixel CCDs (a 1,024-by-1,024-pixel CCD for each eye).

The instrument could be pointed upward to assess the amount of dust and water vapor in the atmosphere. When the robotic arm delivered soil and ice samples to deck-mounted instruments, the SSI could look downward to inspect the samples. Views of the spacecraft's deck monitored dust accumulation are of scientific interest for inferences about Martian winds and of engineering interest for effects of dust buildup on the solar panels.

1.6.2.4 The Thermal and Evolved-Gas Analyzer (TEGA)

The analyzer consisted of two tools, a *calorimeter* and a *mass spectrometer*. It had eight tiny ovens for samples, each to be used only once.

The analyzer processed substances that were converted to gases by heating samples delivered to the instrument by the robotic arm. It provided two types of information. One of its tools, called a differential scanning calorimeter, monitored how much power was required to increase the temperature of the sample at a constant rate. This revealed which temperatures are the transition points from solid to liquid and from liquid to gas for ingredients in the sample.

The gases that were released (or "evolved") by this heating then went to a mass spectrometer, which identified what was in these vapors. The mass spectrometer data was used to determine whether the samples of soil and ice contained any organic compounds and to identify the types and amounts of any that were present. The mass spectrometer

measured the atomic weights of molecules. Researchers used that information to identify the substances that were present, as well as their concentrations.

The TEGA could also give information about water and carbon dioxide present either as ices or as molecules attached to minerals. Also, the amount of heat needed to drive off water or carbon dioxide that is bound to minerals is characteristically different for different minerals.

The eight ovens were cylinders about 1 centimeter (cm) (about 0.5 inch) long and 2 millimeters (mm, one-eighth inch) in diameter. At the start of an analysis, sample material was dropped into the oven through a screen. (This was much more difficult than anticipated due to “stickiness” of the soil [14].) The oven was designed to close after a light-beam detector sensed that it is full. The experiment gradually heated samples to temperatures as high as 1,000 deg Celsius (1,800 deg Fahrenheit). The heating process drove off water and any other volatile ingredients as a stream of gases to be directed to the mass spectrometer for analysis.

One of the samples that the TEGA analyzed was a special material that the lander carried from Earth, specially prepared as a “blank” to be as free of carbon as possible. This served as an experimental control for comparison with samples of Martian soil and ice. The control material was made of a machinable glass ceramic substance named Macor, from Corning Inc.

The mass spectrometer part of the TEGA also examined samples of atmosphere at the landing site, in addition to the evolved gases from scooped-up samples and the blank. The atmospheric measurements added information about humidity to the weather data monitored by the spacecraft’s Meteorological Station.

1.6.2.5 The Microscopy, Electrochemistry, and Conductivity Analyzer (MECA)

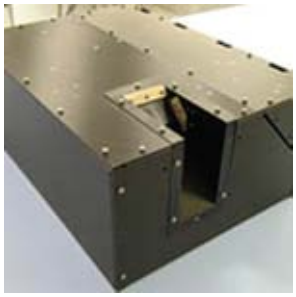

The MECA used four tools to examine soil. Three of the tools -- a *wet chemistry laboratory* and two types of microscopes -- analyzed samples of soil scooped and delivered by the robotic arm. The fourth tool (mounted near the end of the arm) had a row of four small spikes that the arm pushed into the ground to examine electrical conductivity and other soil properties.

The wet chemistry laboratory had four teacup-size beakers. Each was intended to be used only once. Samples from the Mars’ surface and from three lower depths could be analyzed and compared. The instrument provided data on soluble chemicals in the soil by mixing water -- brought from Earth -- with the sample to a soupy consistency and keeping it warm enough to remain liquid during the analysis.

On the inner surfaces of each beaker were 26 sensors, mostly electrodes behind selectively permeable membranes or gels. Some sensors gave information about the pH of the soil -- the degree to which it is acidic or alkaline. Other sensors gauged concentrations of such ions as chlorides, bromides, magnesium, calcium, and potassium to assess the level of the sample’s oxidizing potential.

The wet chemistry setup added specific substances to each beaker in a choreographed two-day sequence. The first addition was about 25 cubic centimeters (cc) (nearly two

tablespoons) of ice from Earth with dilute concentrations of several ions. This was slowly melted in a special container, a process that took one to two hours before providing baseline measurements at this starting point. The first of five pill-size crucibles of prepared chemicals was then added to increase ion concentrations by a known amount in order to calibrate the measurements. Next, a drawer above the beaker extended to receive the soil sample, and the scoop on the robotic arm dropped as much as 1 cc (one-fifth of a teaspoon) of soil into the drawer, which then retracted and dumped the sample into the beaker. A paddle stirred the soup for hours while the sensors took measurements. The next day, the second crucible added nitrobenzoic acid to the beaker to test how ions from the soil reacted to increased acidity. The last three crucibles held barium chloride. As they were added, one at a time, any sulfate from the soil would react with the barium to make an insoluble compound, taking both the barium and the sulfate out of solution. The amount of sulfate in the soil sample would be determined by measuring the amount of unreacted barium left behind.

The "microscopy" part of the Microscopy, Electrochemistry and Conductivity Analyzer (MECA) was intended to examine soil particles and possibly ice particles with both an *optical microscope* and an *atomic force microscope*. The robotic arm delivered soil samples to a wheel that rotated to present the samples to the microscopes. Along the perimeter of the wheel were substrates with different types of surfaces, such as magnets and sticky silicone. This allowed the experiment to provide data from the particles' interaction with the various surfaces, as well as about the sizes, shapes, and colors of the particles.

Images from the optical microscope covered an area 2 mm by 1 mm (about 0.08 in. by 0.04 in.); so, the biggest particles the optical microscope could view are just over a millimeter across. The smallest it could see were about 500 times smaller -- about 2 microns across, the smallest scale ever seen on Mars. Even so, the atomic force microscope could reveal details down to another 20 times smaller than that -- as small as about 100 nanometers (nm), one one-hundredth the width of a human hair.

The optical microscope obtained color information by illuminating the sample with any combination of four different light sources. The illumination comes from 12 LEDs shining in red, blue, green or ultraviolet parts of the spectrum.

The atomic force microscope assembled an image of the surface shape of a particle by sensing it with a sharp tip at the end of a spring, which has a strain gauge indicating how far the spring flexes to follow the contour of the surface.

The "*conductivity*" part of the MECA assessed how heat and electricity move through the soil from one spike to another of a four-spike electronic fork or probe pushed into the soil at different stages of digging by the arm. For example, a pulse of heat could be put onto one spike, and the rate at which the temperature increased on the nearby spike could be recorded, along with the rate at which the heated needle cooled off. The conductivity probe also served as a humidity sensor when held in the air. In addition, slight temperature changes from one spike to the next allowed it to estimate wind speed. The device, called the Thermal and Electrical Conductivity Probe, adapted technology used in commercial soil-moisture gauges.

The microscopy and wet chemistry tools were based on an instrument developed for the Mars Surveyor 2001 Lander mission, which was canceled in 2000. The conductivity probe and other improvements were added to the earlier design for Phoenix.

1.6.2.6 The Meteorological Suite (MET) with scanning LIDAR

This first high-latitude weather station on Mars tracked daily weather and seasonal changes using pressure and temperature (P&T) sensors, and it also had a laser-reflection instrument.

The laser tool, called a LIDAR for "light detection and ranging," used powerful laser pulses in a way comparable to radio pulses emitted by a radar instrument. The laser beam was emitted vertically into the atmosphere. Atmospheric dust and ice particles in the beam's path reflected the light, sending it in all directions, including straight back to the instrument. A telescope integrated into the instrument detected the downward-reflected light. Analysis of the strength and time-delay of the reflections can reveal information about the sizes and altitudes of the particles.

The weather station included a 1.2-m (4-ft) mast bearing sensors at three heights to monitor how temperature varies with height near the surface. The temperature sensors were thin-wire thermocouples that measured temperature by its effect on the flow of an electrical current through a closed circuit of two metals with different thermal properties. The thermocouples used the metals chromel (a nickel and chromium alloy) and constantan (a copper and nickel alloy). Also, hanging from the top of the mast was a wind telltale. This was a small tube that was deflected by the wind. The science payload's stereo camera recorded images of the telltale that were used to determine wind direction and speed. The top of the meteorology mast, at 1.14 m (3.75 feet) above the deck, was the highest point on the lander.

1.6.2.7 Mars Descent Imager (MARDI, on-board but not used)

It was planned that the MARDI would play a key science role during Phoenix's descent to the Martian arctic. Beginning just after the aeroshell was jettisoned (shown in Figure 1-7, parachute phase) at an altitude of about 8 km (5 miles), MARDI would acquire a series of wide-angle, color images of the landing site all the way down to the surface [15].

The imager was included in the payload to take downward-looking images during the three minutes just before touchdown. However, spacecraft tests identified a potential problem, not with the camera itself but in handling data from the camera during crucial moments of final descent. The risk to a safe landing was deemed unacceptable, and the MARDI was not used [16].

2 Telecom Subsystem Overview

Table 2-1 summarizes some of the Phoenix telecom parameters.

Table 2-1 Phoenix telecom parameters.

Parameter	Value	Notes	Source
Spacecraft ID	84		
Uplink Frequency (X-band)	7151.909722 MHz	DSN channel 5	[17]
Downlink Frequency (X-band)	8402.777778 MHz	DSN channel 5	[17]
Cruise EIRP	46.0 dBm (LGA) 57.7 dBm (MGA)		
Cruise Gain-to-Noise Ratio (G/T)	–21.9 dBi/K (LGA) –13.8 dBi/K (MGA)		
UHF Transmit Frequency	401.585625 MHz	CCSDS channel 0	[18]
UHF Receive Frequency	437.1 MHz	CCSDS channel 0	[18]
UHF EIRP	42.0 dBm (Helix)		

2.1 Telecom for Launch and Cruise

2.1.1 Initial Acquisition

For telecom, initial acquisition occurred when the DSN first established contact with Phoenix after separation from the launch vehicle. The X-band downlink was configured for 2100 bps during initial acquisition [19].

The first opportunity to acquire the Phoenix spacecraft occurred almost immediately after separation, which was roughly 88 minutes after liftoff. For the initial acquisition, the project scheduled two 34-m beam waveguide (BWG) antennas at Goldstone (DSS-25 and DSS-26). A 1.2-m X-band acquisition aid antenna was used to assist in initial pointing of the 34-m antenna. This antenna provides a wider beamwidth (2.1 deg) than the 34-m main antenna (0.066 deg)

For mission planning purposes, many of the launch-related figures were generated in advance for the first possible (“window open”) launch date of August 3, 2007. This article uses these planning figures for illustration. The quantities for the actual August 4 launch differ little from the planning quantities.

For a launch near the open of the launch window, the Goldstone Deep Space Control Center had the first opportunity for initial acquisition, with Madrid and then Canberra following (Figure 2-1).

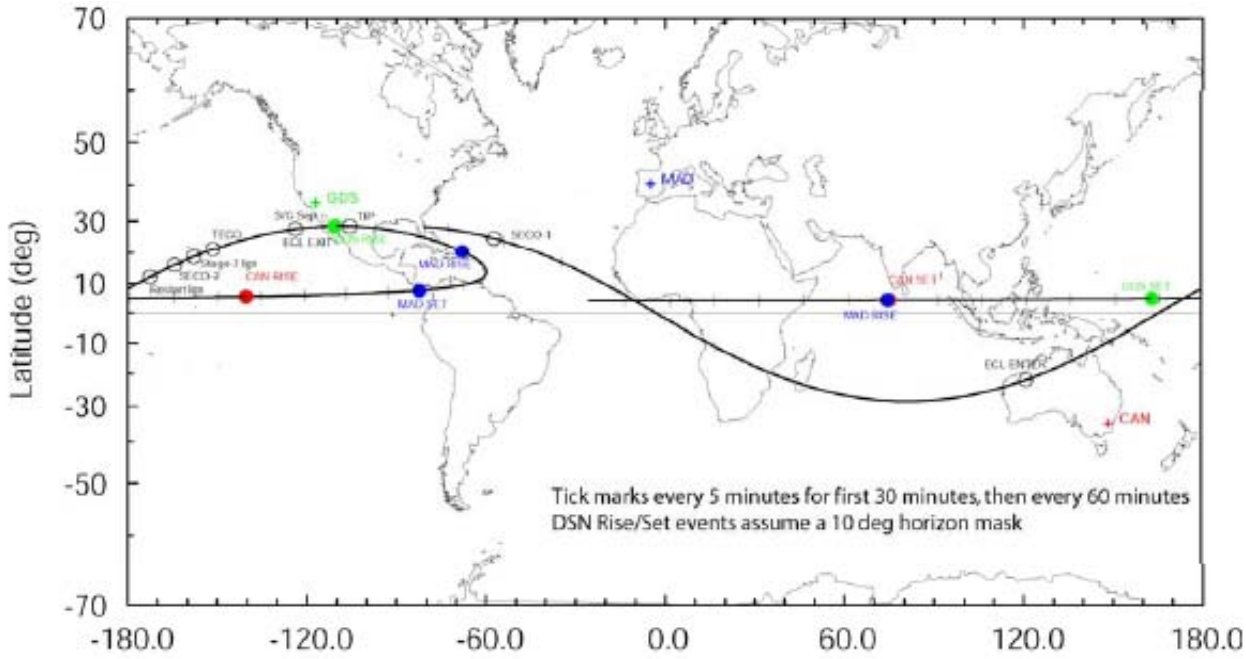

Figure 2-1 Ground track for 08/03/2007 window-open (launch Az 93 deg).

Figure 2-2, a prelaunch planning graphic, shows the DSS elevation angles for the first 24 hours after launch. The figure is labeled DSS-14 to represent the Goldstone site, DSS-43 to represent the Canberra site, and DSS-63 to represent the Madrid site.

Figure 2-3, another planning graphic, shows how the distance from the spacecraft to the Earth would change during the first 48 hours after launch. The August 3 label is the most representative of the Phoenix-Earth distance versus time profile that occurred.

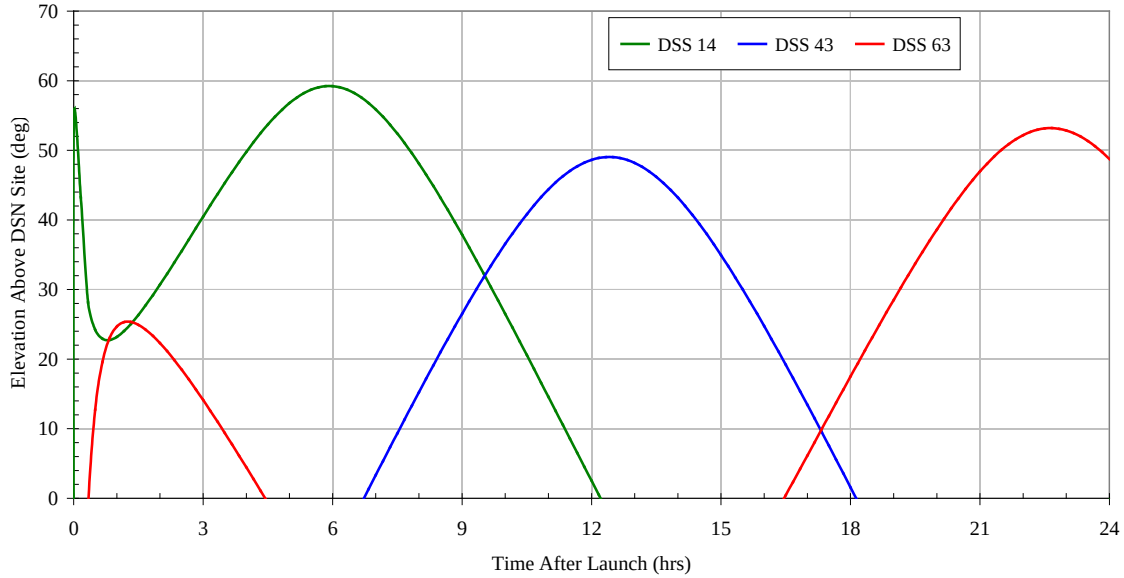

Figure 2-2 Elevation angles from DSN sites to Phoenix for the first 24 hours after launch

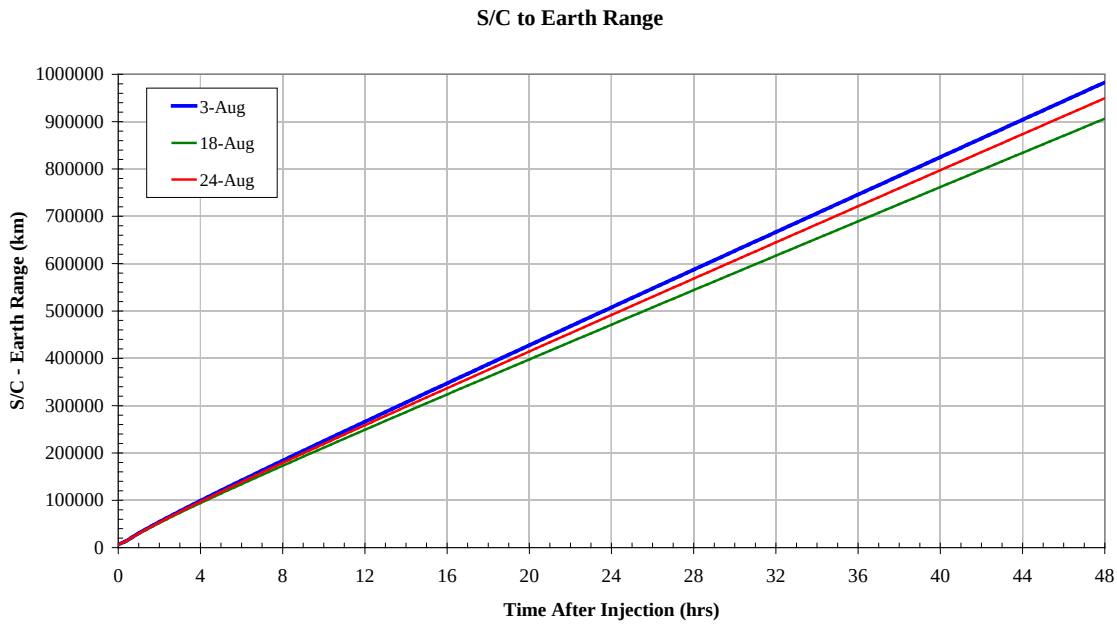

Figure 2-3 Phoenix-to-Earth range during initial acquisition.

During initial acquisition, the DSS X-band transmitter was operated at 200 W instead of the standard 20 kW to avoid exceeding the specified maximum –70 decibels referenced to milliwatts (dBm) total uplink received power at the SDST.

2.1.2 Cruise

The cruise portion of the mission began after initial acquisition had been completed and the spacecraft state had been verified.

Figure 2-4 shows the spacecraft-Earth range during cruise, and Figure 2-5 shows the Sun-spacecraft-Earth angle (labeled with its traditional or historical name Sun-Probe-Earth angle[1] or SPE angle) during cruise.

[1] The SPE angle has the spacecraft at its vertex. Historically, for a spacecraft with fixed solar panels to be pointed generally toward the Sun and a fixed antenna aligned with the solar panels, the SPE angle defined how far off the antenna's boresight the Earth would be.

A related angle, the Sun-Earth-probe angle (SEP angle) has the Earth at its vertex. The SEP angle is a useful indicator of the amount of solar noise interference received at the ground station antenna when that antenna is pointed toward the spacecraft.

The term "probe" in the historical angle names was an attempt to avoid two different meanings for the letter S in the same term, "spacecraft" or the Sun.

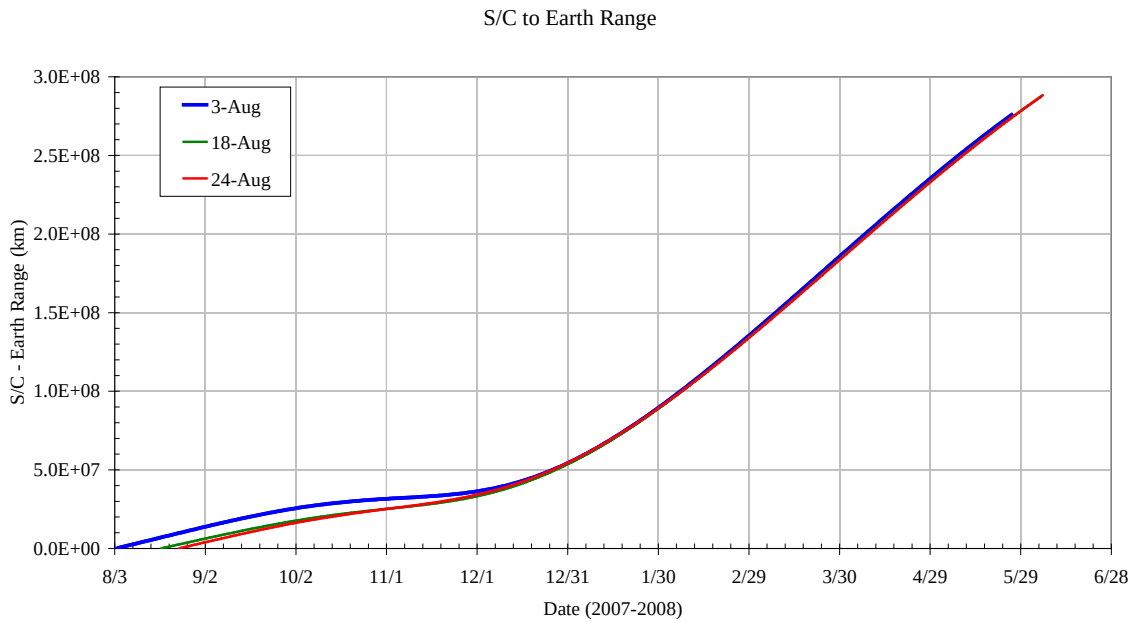

Figure 2-4 Spacecraft-to-Earth range during cruise.

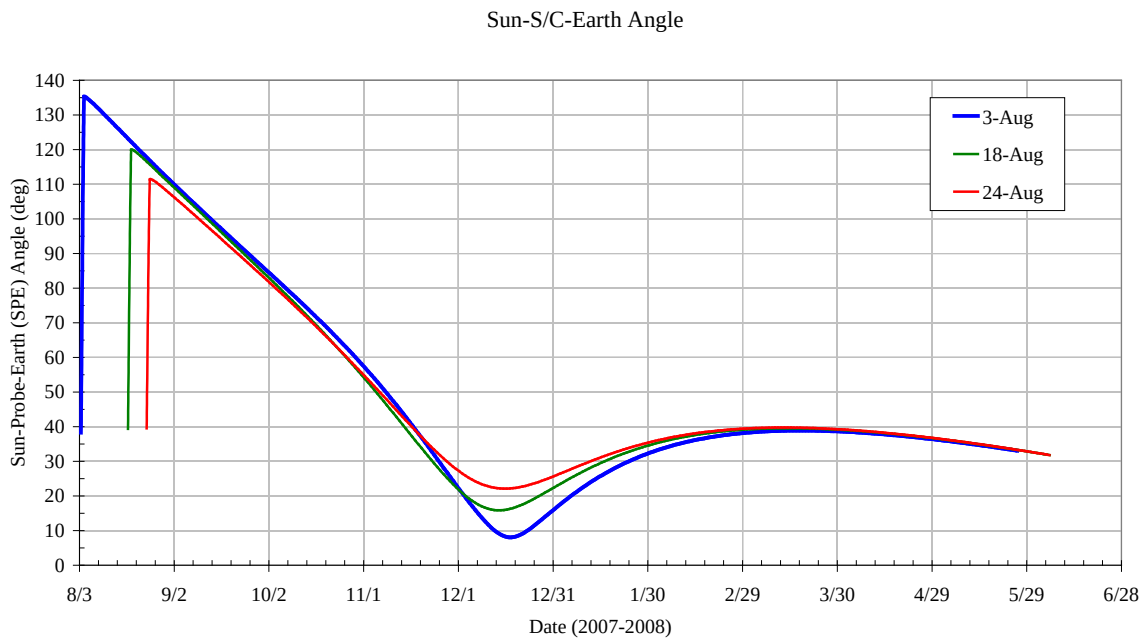

Figure 2-5 Sun–Craft–Earth angle during cruise

Figure 2-6 shows the Sun-Earth-Probe (SEP) angle during cruise. Since the SEP angle never got below 40 deg, solar scintillation effects to the X-band downlink or uplink were negligible.

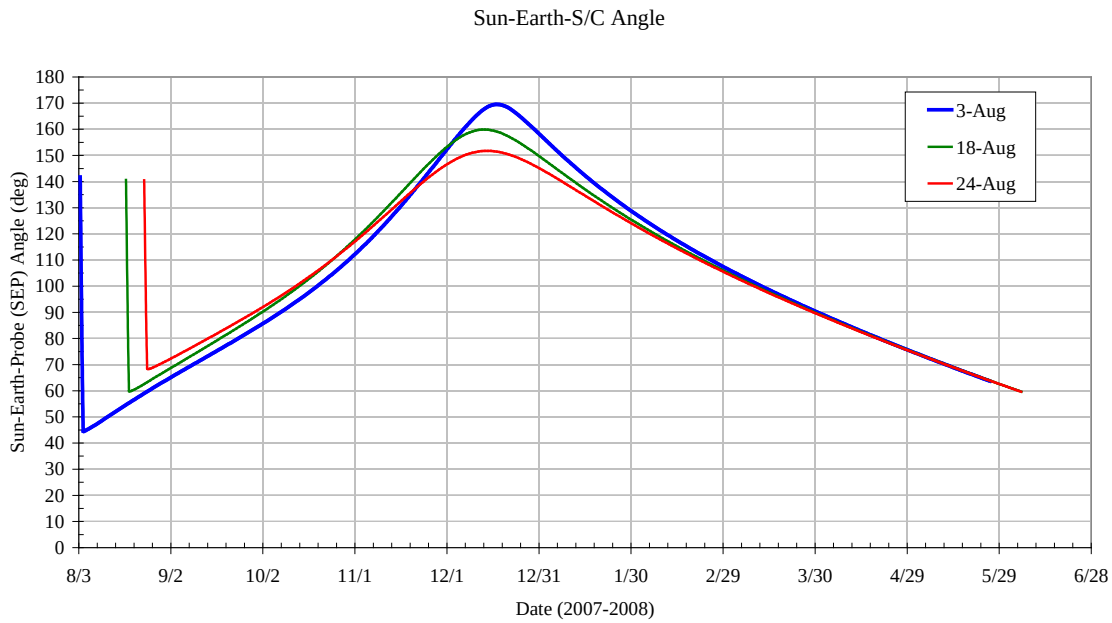

Figure 2-6 Sun-Earth-Probe Angle during cruise.

During cruise, the spacecraft transmitter and receiver were planned to be on continuously. Due to the MGA offpoint angle from Earth, the cruise low-gain antenna (CLGA) was used for both transmitting and receiving until about 160 days after launch. This corresponded of a distance from Earth of about 0.55 astronomical units (AU).

After 160 days, the medium-gain antenna (MGA) was used for transmitting and receiving even for safe mode operations until cruise stage separation. This spanned a time period of about 120 days. Beyond 0.55 AU, the CLGA could not provide sufficient antenna gain to close the link for nominal data rates. The spacecraft pointing requirements were that the MGA would have adequate field-of-view to cover Earth during safing. However, the CLGA could be used at the emergency downlink rates (10 bps and 40 bps) to a 70-m antenna if needed.

Figure 2-6 shows the nominal Phoenix antenna off-point angles for the launch window open. Because the antennas are body mounted and not gimbaled, the off-point angles depended on spacecraft orientation. The sharp increase in offpoint angle around day 70 was due to the solar arrays going on-point to the Sun at that time.

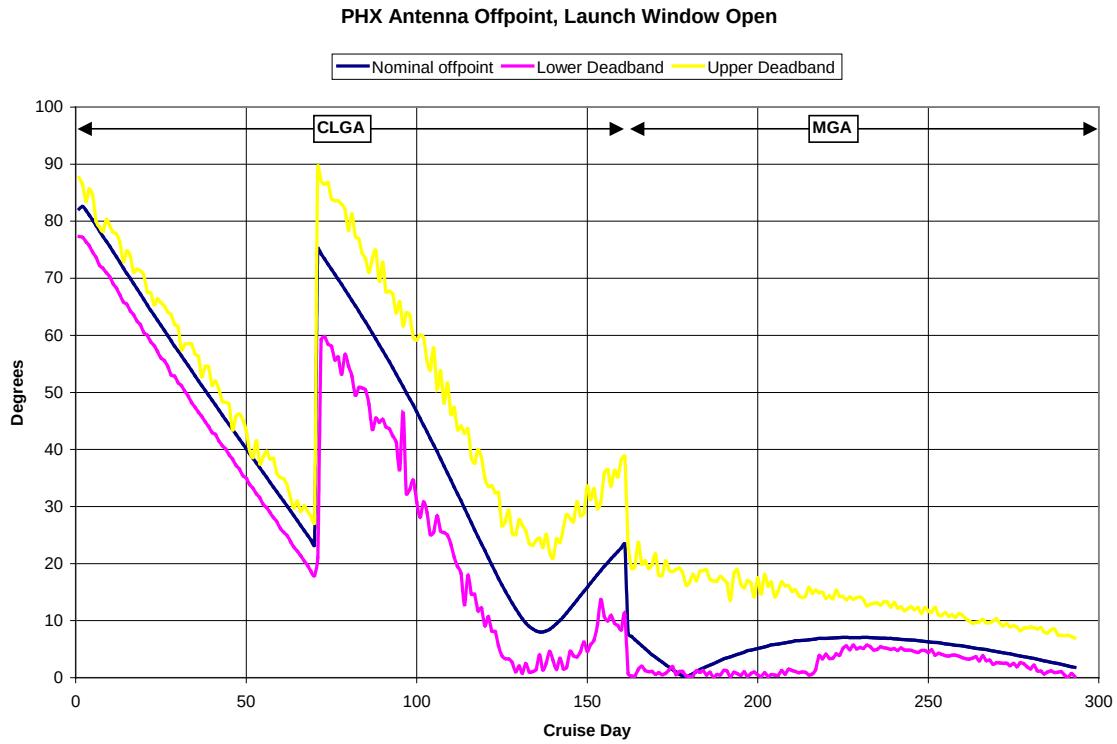

Figure 2-7 Phoenix antenna offpoint angles during cruise.

2.1.2.1 Uplink (Command) Capability

The command rate requirement during cruise was 125 bps from a 34-m antenna at maximum range (at arrival) for an MGA Earth-pointed configuration. The maximum cruise range was about 1.95 AU. The 125-bps uplink rate was also possible through the cruise low gain antenna (CLGA) with nominal offpointing almost all the way to cruise stage separation at EDL.

2.1.2.2 Downlink (Telemetry) Capability

The cruise downlink rates were 10 bps, 40 bps, 100 bps, 395 bps, 700 bps, 1400 bps, and 2100 bps. These bit rates are defined at the telemetry data input to the SDST and as such include all Reed-Solomon (RS) code symbols, the frame sync marker, and the packet overhead. However, it does not include the (7,1/2) or (15,1/6) convolutional encoding which occurred in the SDST, thus the channel symbol rate was two times or six times the above values.

The requirement for cruise downlink was to provide 40 bps through the MGA at maximum cruise range for an Earth-pointed configuration. The transition to the MGA was planned to occur 160 days after launch, after which the MGA could support 40 bps to a 34-m HEF until arrival at Mars.

When in safe mode the spacecraft would go into a Sun coning mode. In this mode the spacecraft Sun sensors determined the direction of the Sun, and rotated about this vector. At any time during cruise, the Sun-spacecraft-Earth angle defined the size of the cone.

The angle was such that the field-of-view of the LGA or MGA intersected with the Earth at some point in the rotation, and a downlink could be established. The telecom subsystem was required to be capable of providing 10 bps for this defined Sun-coning configuration. This requirement translated into antenna gain and beamwidth and transmitter power requirements to achieve this data rate.

The safemode 10 bps could be supported by the CLGA to a 34-m high efficiency (HEF) station until roughly 220 days after launch.

2.1.2.3 Cruise Ranging Performance

As one example of cruise X-band signal levels, Figure 2-8 shows the predicted ranging Pr/No (ratio of ranging power to noise power spectral density) at the tracking station during Phoenix cruise assuming different downlink ranging modulation index values and DSN antennas. Only the effects of thermal noise are considered; other effects such as calibration error and media effects will increase variation in the ranging measurement.

The Pr/No thresholds needed for one-sigma 2-m ranging accuracy are shown for integration times (called T1) of 60 s, 180 s, and 600 s. The shorter the T1, the more ranging acquisitions can be accomplished during a given tracking duration. Early in cruise, with large Pr/No, the T1 could be short (less than 1 min). During late cruise, as the Pr/No decreased, it was necessary to use T1 as large as 10 min.

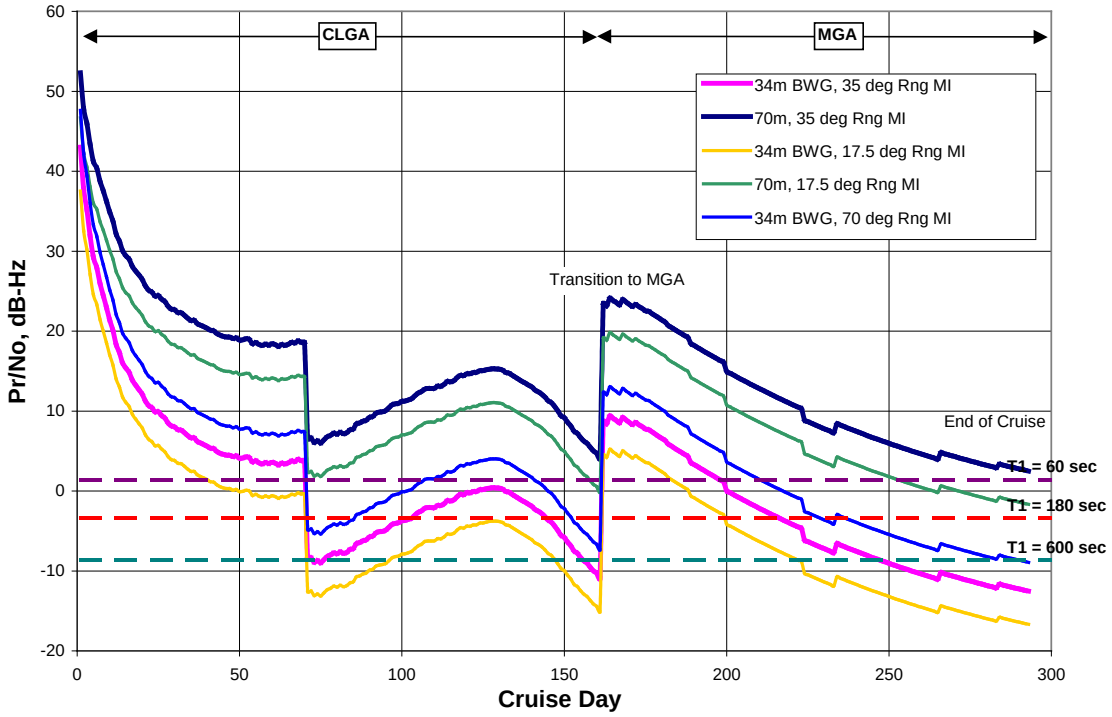

Figure 2-8 Expected Phoenix X-band ranging Pr/No during cruise.

2.1.2.4 Delta Differential One-way Ranging (ΔDOR)

Delta (or 'differenced') differential one-way ranging (ΔDOR) is a form of delta very long baseline interferometry (ΔVLBI)., ΔDOR provides an observation of the plane-of-sky position of the spacecraft using signals received simultaneously at two or more DSN antennas. These signals, known as DOR tones, are two or more unmodulated frequencies separated from the carrier by a large offset (tens of megahertz). The tones are received and recorded at each station. The same pair of DSN stations observes a quasar shortly before and after the spacecraft measurements are made. The spacecraft measurements can be combined to yield an unambiguous measure of the phase delay in the transmitted signal (called differential one-way range), and the differential delay between the spacecraft and the quasar – termed ΔDOR – yields a highly accurate measure of the spacecraft's angular position in the radio source reference frame.

In the process of determining the spacecraft trajectory from Earth to Mars, ΔDOR data was included with other radio navigation data types (Doppler and range). Doing so desensitized the trajectory solutions to errors in modeling the effect of small forces on the spacecraft, considerably improving spacecraft position knowledge. Five ΔDOR campaigns were planned, according to the schedule in Table 2-2.

Table 2-2 Phoenix ΔDOR campaign schedule.

Campaign	Start	End	Pass Frequency
Period 1	L + 17 days	L + 35 days	1 pass/week
Period 2	L + 36 days	L + 42 days	1 pass/day
Period 3	L + 43 days	E – 63 days	1 pass/week
Period 4	E – 62 days	E – 19 days	3 passes/week
Period 51	E – 18 days	Entry	2 passes/day

2.2 Entry, Descent, and Landing

The Entry, Descent, and Landing (EDL) phase had many critical events occurring over a short period of time, including cruise stage separation, entry into the Martian atmosphere, parachute deployment, lander separation, and terminal descent. The X-band telecom subsystem was jettisoned with the cruise stage upon separation, with all subsequent EDL (and surface) communications through the UHF subsystem.

Figure 1-7 shows the three stages of EDL

- Entry preparation
- Hypersonic flight
- Parachute
- Terminal descent
- Lander preparation

Roughly 5 minutes prior to Phoenix entry, the cruise stage containing the X-band telecom subsystem was jettisoned. During the entry phase, the spacecraft rapidly heated up due to the Martian atmosphere and plasma formed, leading to a possible blackout period

(resulting in loss of signal being received from the spacecraft). In fact, as discussed later in the article, no blackout occurred, though post-track analysis showed severe fades, dubbed “brownout”.

About 4 minutes after entry into the Martian atmosphere, the Phoenix parachute deployed to slow the rate of descent. Shortly after parachute deployment (~ 10 s), the heat shield was jettisoned. Then the lander separated from the backshell and began the terminal descent. Touchdown on the Martian surface was about 7 minutes after entry.

In order for the flight team back on Earth to receive spacecraft health information during these critical events, the Phoenix lander was required to provide UHF carrier as well as 8-kilobits per second (kbps) engineering data to both the MRO and Odyssey relay orbiters. During terminal descent, the lander transmitted at 32 kbps. Phoenix had a requirement to transmit UHF data during EDL to support identification of the probable fault should a catastrophic failure occur. The EDL data would be used in the event of failure to help determine most probable cause in post-analysis. The definition of the end of the EDL phase was a safe successful landing, confirmation that at least one landed solar array was deployed and positive power/thermal balance existed, a functional UHF radio link had been established, and surface fault protection has been enabled. [19]

As many as three communications blackouts were anticipated during EDL, the first at cruise stage separation, the second during hypersonic entry, and the third at lander separation from the backshell.

Figure 2-9 shows the planned use of the Odyssey, MRO, and MEX orbiters and a direct to Earth (DTE) UHF link to Green Bank during Phoenix EDL. The actual EDL communications are described later in the article.

The EDL orbiter links are labeled 1 through 3, and the Green Bank DTE is labeled 4. Figure 2-10 is an overview of the UHF communications implementation plan for EDL.

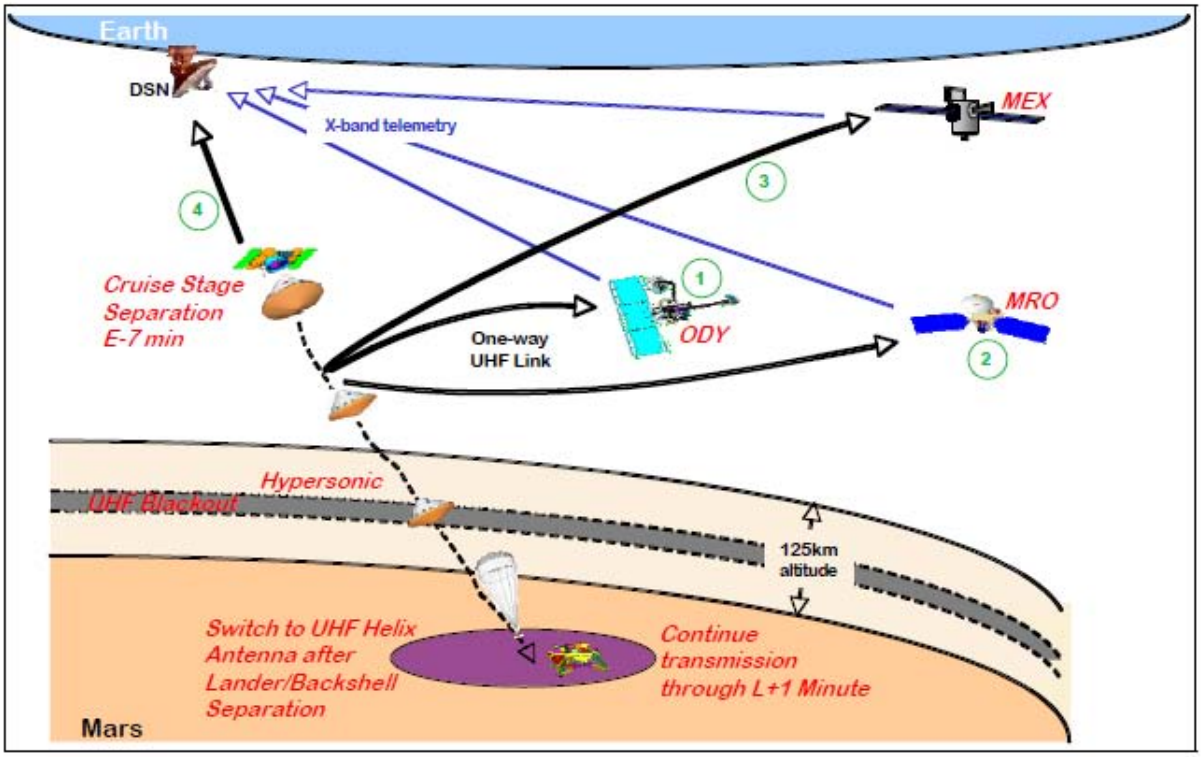

Figure 2-9 EDL communications with orbiters and DTE to Green Bank.

Prior to separation, Phoenix transmitted an X-band carrier over the LGA on the cruise stage. The X-band downlink ended at cruise stage separation (CSS). After CSS, using the UHF wrap-around patch antenna located on the parachute cone at the tip of the backshell, the lander started an unmodulated UHF carrier (called CW) to assist MRO and Odyssey in acquiring the signal. The presence of a UHF carrier confirmed that cruise stage separation was successful, and Doppler confirmed aeroshell performance. For the entry phase, Phoenix transitioned to 8 kbps in the "unreliable bit stream" mode.

The Odyssey and Mars Express orbiters were configured in an open-loop "canister mode" to record carrier and Doppler information only. The term "canister mode" refers to the means by which the data is collected. The term goes back to a NASA plan in roughly 2000 for a Mars sample return device housed in a protective canister and placed in orbit around Mars. The canister mode signal does not carry telemetry bits because the link design deemed it too weak to do so. The signal is a tone beacon that is digitized by the orbiter, but there is nothing to decode. The resulting raw data is relayed to Earth where processing is performed [20]. Canister mode, previously used in attempts to detect the Beagle Lander on the surface of Mars by the MEX orbiter in 2003–2004, was the most sensitive surface-to-orbiter mode available for lander signals to MEX.

The Mars Reconnaissance Orbiter (MRO) was configured for open-loop record as well. However, sampling fidelity on MRO was high enough to recover the data and carrier by processing the samples sent to the ground. The plan assumed a UHF plasma blackout was likely during hypersonic entry. This blackout was expected to last about 100 s. If the blackout had occurred, data would not have been received by any orbiter during the blackout.

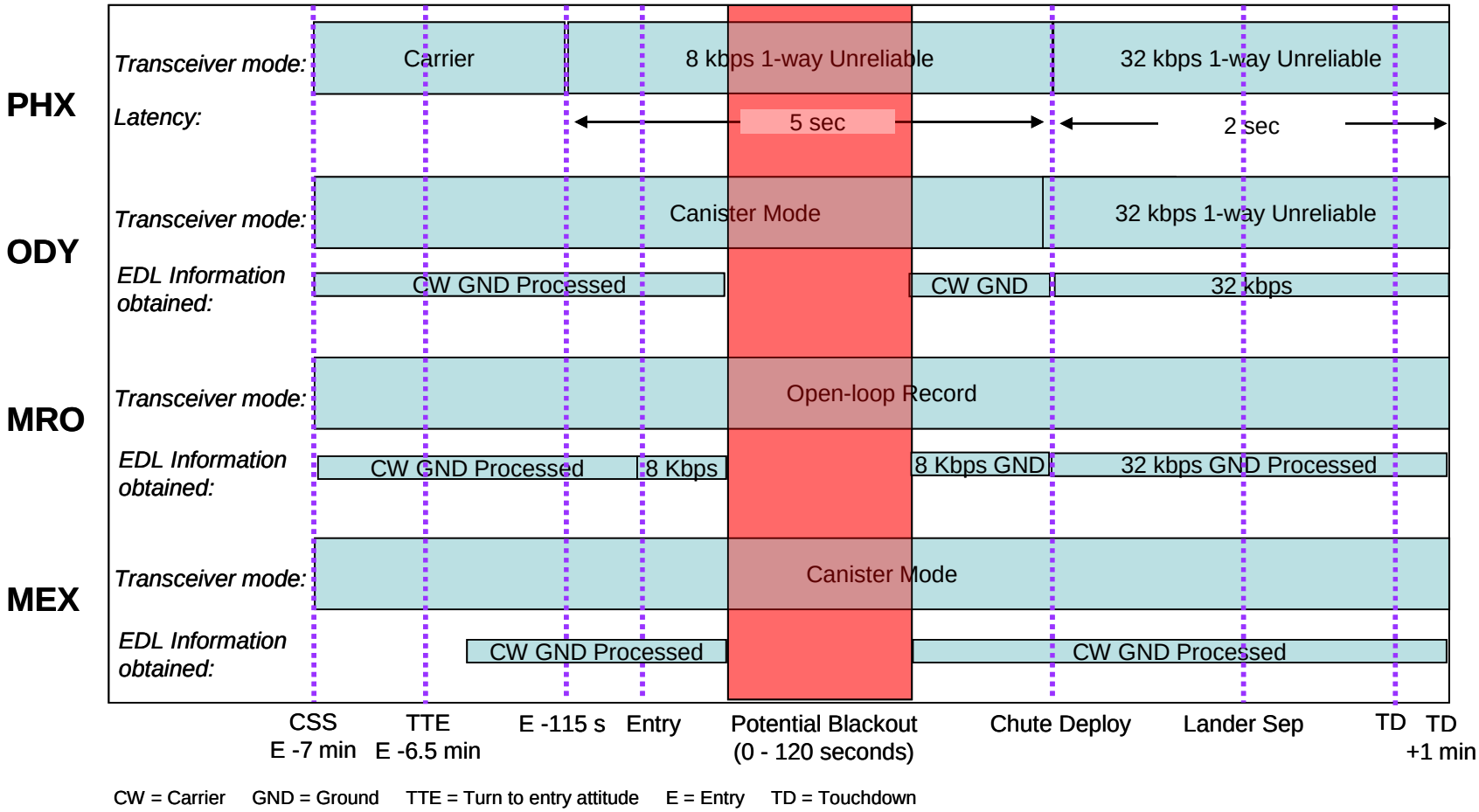

Figure 2-10 EDL UHF communications.

Phoenix was planned to transmit at 8 kbps until slightly after parachute deployment in order to collect parachute performance data. Following parachute deployment, Phoenix transmitted unmodulated carrier for a brief period to assist MRO and Odyssey in reacquiring the UHF carrier. Phoenix then transitioned to 32 kbps again in the bit stream mode. Odyssey was configured to receive 32 kbps data in its phase-lock loop (bit stream) mode. MRO remained in its open loop record mode throughout EDL. The higher data rate allowed for MRO and Odyssey to collect separation and terminal descent performance data. Phoenix used the helix antenna for UHF transmission after lander separation from the backshell.

The plan was to keep data latency short during EDL because a catastrophic failure would have terminated transmission and caused the loss of engineering data not yet transmitted from the buffer prior to the failure. The Phoenix requirement was for data latency from the flight software (FSW) push to the C&DH uplink downlink (ULDL) buffer to RF transmission to be less than 5 s at 8 kbps, and less than 2 s at 32 kbps. In contrast, the normal data latency for the UHF transceiver buffer was about 32 s at 8 kbps and 8 s at 32 kbps. The shorter latency was through a FSW change to "starve" the transceiver buffer (that is, instead of waiting for the buffer to be half-full before transmitting, the transmitter would be triggered when the buffer had 400 bytes). The remaining delay was in the C&DH hardware and not accessible via FSW. However it would be reduced as the rate was increased. With the FSW change, Phoenix met its data latency requirements of < 5 s at 8 kbps, and < 2 s at 32 kbps.

2.3 Surface Operations

The surface phase included the digging and polar climate subphases. During the digging phase, Phoenix collected subsurface samples using robotic arm-based trenching. It analyzed the soil samples using its MECA and TEGA science instruments. Phoenix also conducted Mars polar climate observations using its meteorological package. The nominal surface phase ended 90 sols after landing. In fact, Phoenix entered safemode due to a lower-power fault from deteriorating weather conditions on October 28, 2008 [21], returning science data for more than 150 sols.

During the surface phase, all communications to the lander was through the Phoenix UHF transceiver. MRO and Odyssey served as the relay orbiters, receiving Phoenix UHF transmissions and sending them back to the DSN at X-band, as well as relaying commands from the DSN back to Phoenix.

Figure 2-11 shows the predicted total power (labeled Ptotal) received from Phoenix by Odyssey for different elevation angles. Similarly, Figure 2-12 shows the predicted total power received by MRO under similar conditions. Each figure includes the Ptotal thresholds for Odyssey or MRO for 8 kbps, 32 kbps, 128 kbps, and 256 kbps. The figures assume worst-case lander tilt of 16 deg.

The large change in received signal level with elevation angle was due to the increasing range to the orbiter implicit as the elevation angle decreased.

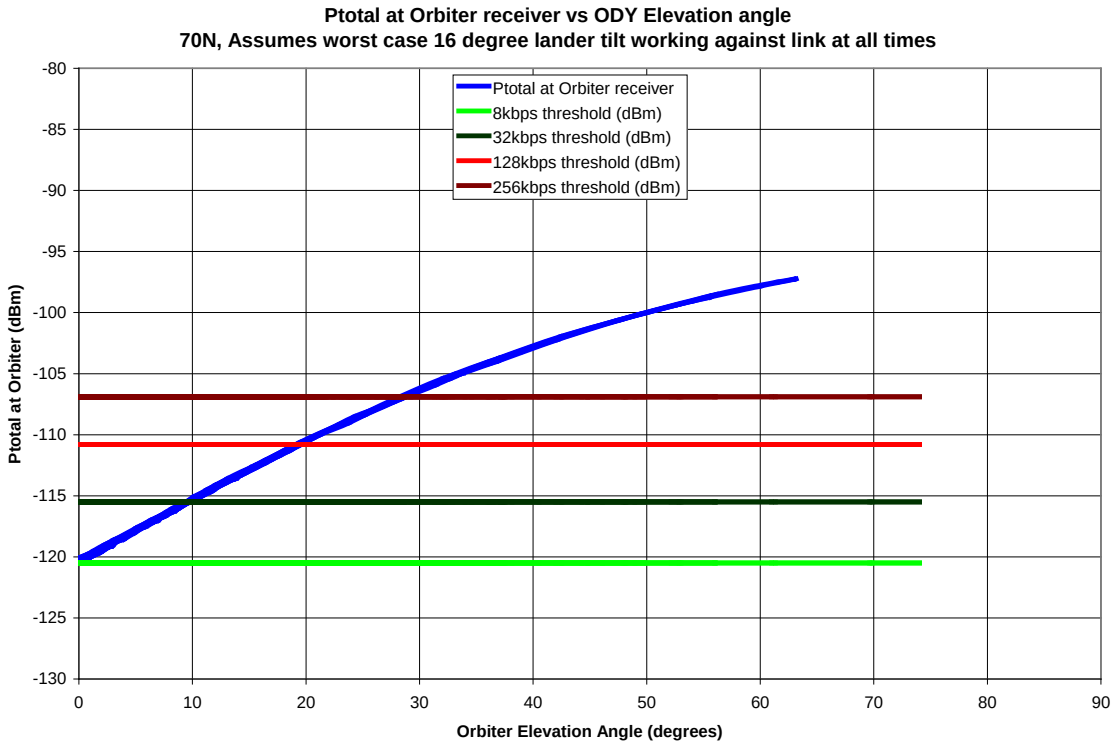

Figure 2-11 Received Pt versus elevation angle for Odyssey relay.

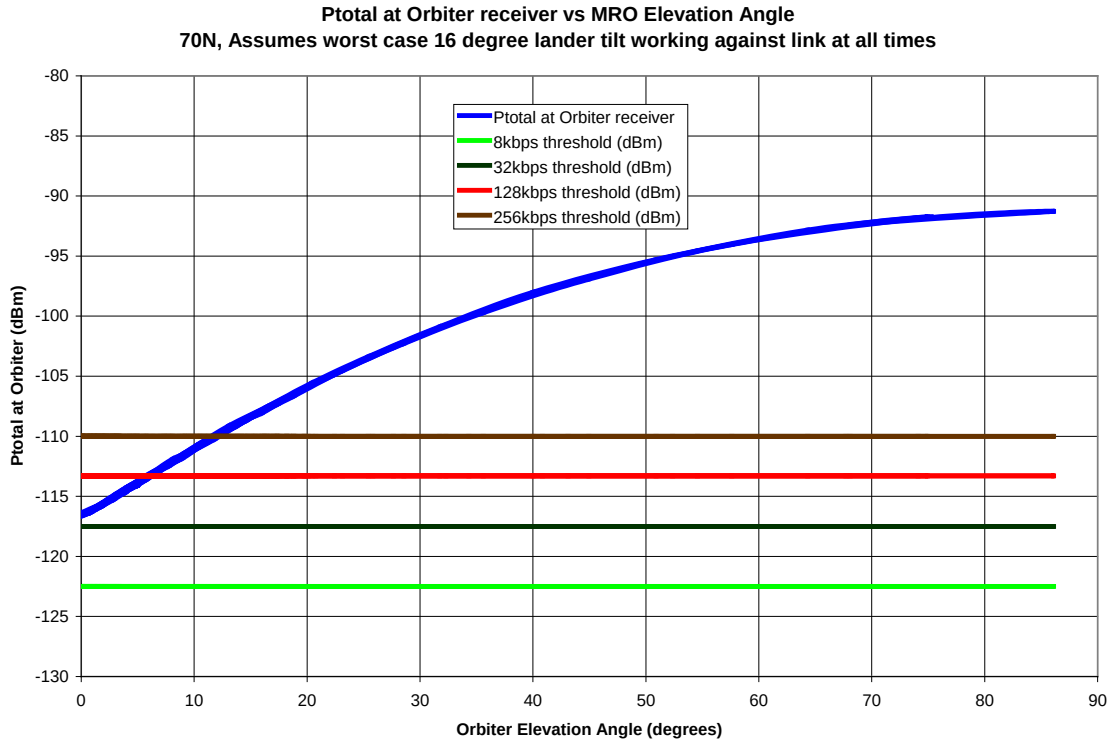

Figure 2-12 Received Pt versus elevation angle for MRO relay.

2.4 X-Band Flight Subsystem Description

The Phoenix X-band telecom subsystem is shown in Figure 2-13**Error! Reference source not found.**.

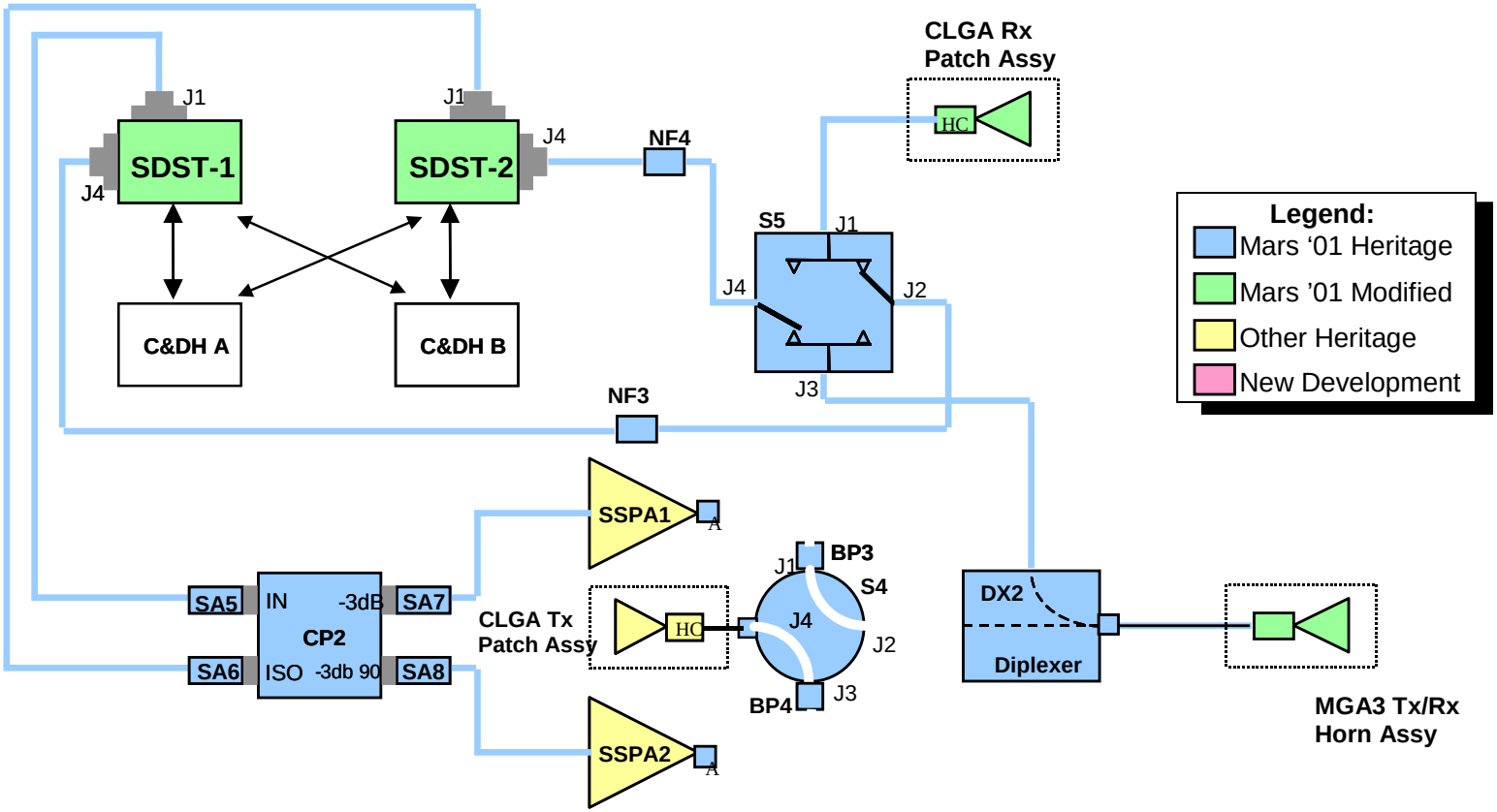

Figure 2-13 Phoenix X-band telecom block diagram

Table 2-3 Acronyms and abbreviations in the X-band telecom block diagram.

Acronym	Meaning	Acronym	Meaning
BP	Bandpass	MGA	Medium gain antenna
C&DH	Command & data handling	NF	Notch filter
CLGA	Cruise low gain antenna	Rx	Receive
CP	Coupler	SDST	Small deep space transponder
ISO	Isolator	SSPA	Solid state power amplifier
		Tx	Transmit

The X-band telecom subsystem had two small deep space transponders (SDST) that were cross-strapped to two C&DHs. Two MER-heritage 15-W solid state power amplifiers (SSPA) provided the necessary RF power. The Phoenix X-band telecom subsystem was mounted on the cruise stage which was jettisoned shortly before entry into the Martian atmosphere. The cruise stage carried a medium gain antenna (MGA) horn as well as separate transmit and receive low gain antennas (LGA). The MGA and the LGAs were fixed in orientation, that is, not gimbaled.

Figure 2-14 shows a picture of the Phoenix cruise configuration, showing the locations of the SDSTs and SSPAs inside the cruise stage and the medium gain antenna directed away from the aeroshell. X-band was used to support initial acquisition and cruise operations.

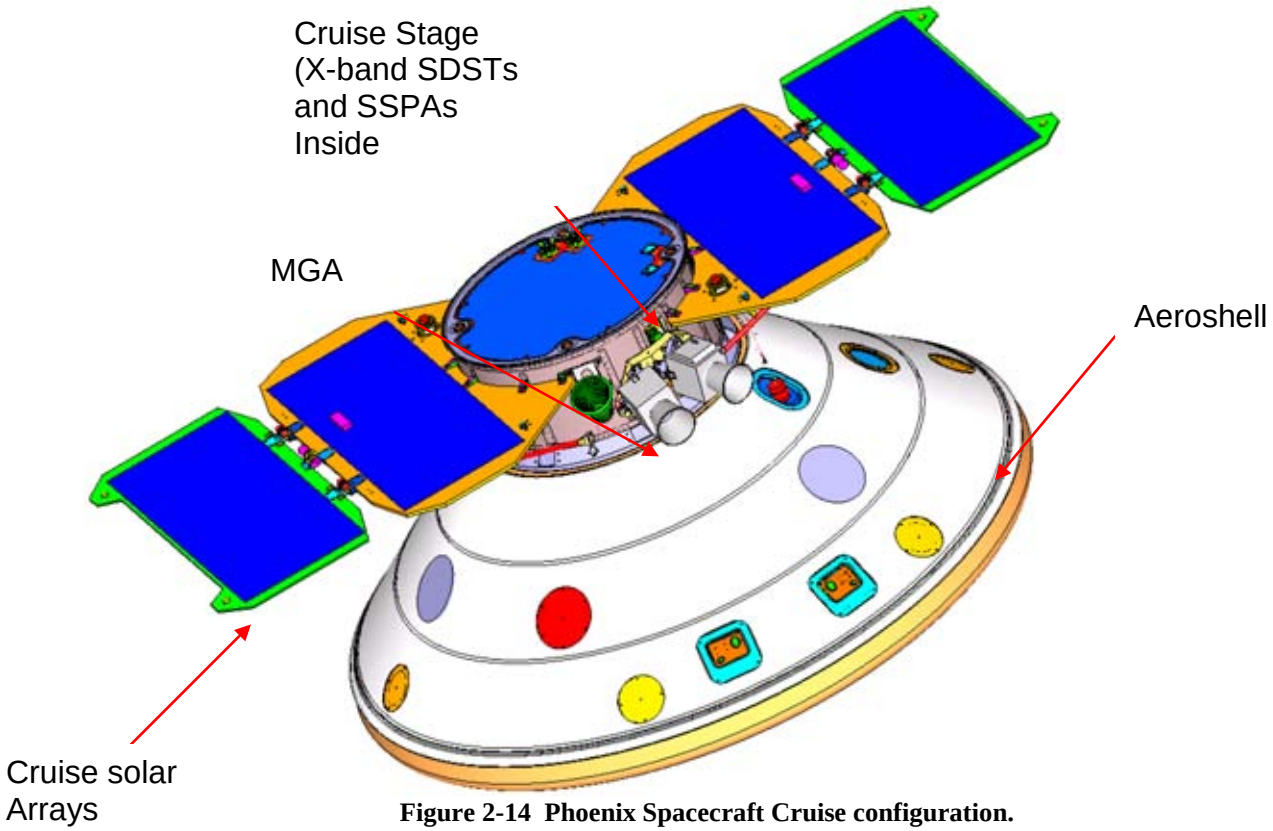

Figure 2-14 Phoenix Spacecraft Cruise configuration.

2.4.1 Small Deep Space Transponder (SDST)

Phoenix had two SDSTs (Figure 2-15) for X-band communications during cruise.

Figure 2-15 Phoenix SDST from group buy 2.

The SDSTs were manufactured by General Dynamics. They included retrofitted Mars'01 digital processing modules (DPM) with new power converters, downconverters, and power converters [22]. SDST SN102 and SDST SN103 were mounted on the spacecraft while SN101 was kept as a flight spare.

Figure 2-16 shows the function of each of the modules in the SDST. In this figure, the term f1 refers to an RF signal at a basis frequency of approximately 19.1 MHz.

The downconverter module handled the received RF signal, and the exciter module provided generation of the transmitted RF signal. The digital processor provided control of the transponder as well as demodulation of the command symbol stream and ranging signal from the received carrier and modulation of the ranging signal and telemetry symbol stream onto the transmitted carrier. The power converter module provided power to the other modules at the required voltage and current levels.

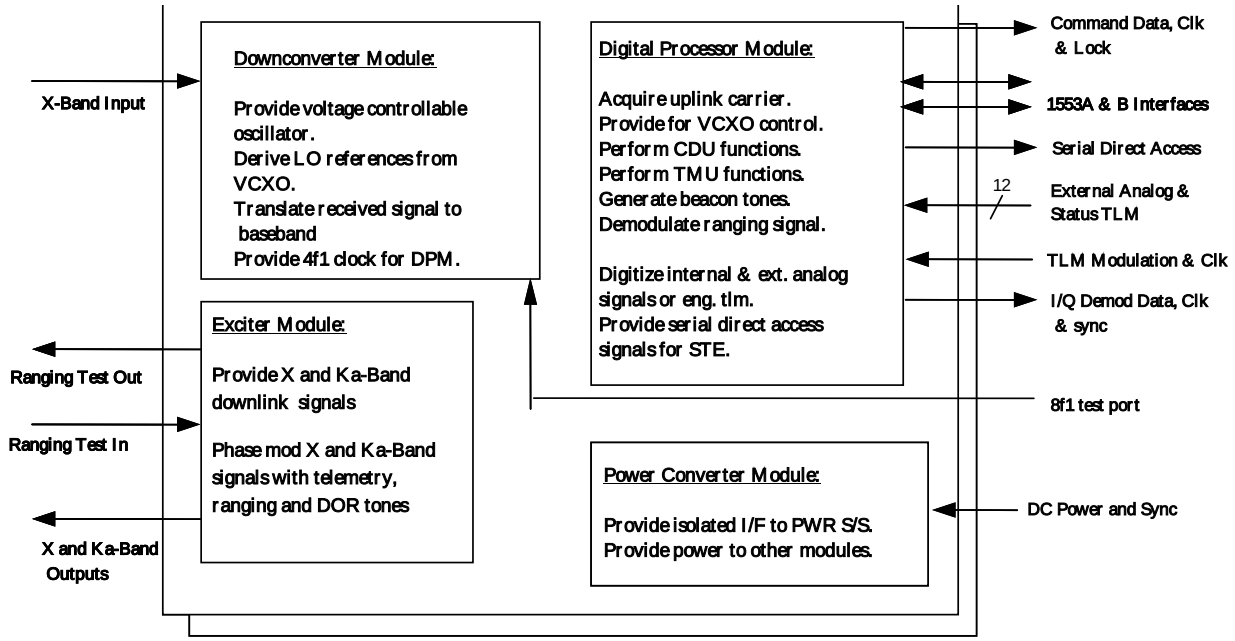

Figure 2-16 Transponder high level functional diagram.

Table 2-4 describes the RF characteristics of the Phoenix SDSTs.

Table 2-4 SDST RF characteristics.

SDST parameter	SN101	SN102	Conditions
Carrier Tracking Threshold	–155 dBm	–155 dBm	
Best Lock Frequency (BLF)	7151.904897 MHz	7151.903162 MHz	TVAC, 25 deg C
Aux Osc Frequency (after warm-up)	8402.777480 MHz	8402.758975 MHz	Ambient pressure, 25 deg C
Noise Figure	2.18 dB	2.19 dB	25 deg C
Exciter Output Power	13.04 dBm	12.81 dBm	TVAC, 25 deg C
DOR Mod Index	68.9 deg	70.2 deg	25 deg C

The Phoenix transponder had the same standard non-coherent and coherent operating modes of other SDSTs. These modes use an auxiliary oscillator as the downlink frequency source and a voltage controlled crystal oscillator (VCXO) that provides a downlink frequency that is coherent with the uplink carrier when the SDST is locked to an uplink carrier. Table 2-5 summarizes these modes.

Table 2-5 SDST non-coherent and coherent operating states.

SDST State	Transponder Mode	Coherency	U/L carrier lock status	D/L Freq Ref
State 1	Normal Mode 1-way Non-Coherent	N/A	Unlocked	Aux Osc
State 2	Normal Mode, 2-way Non-Coherent	Inhibit	Locked	Aux Osc
State 3	Normal Mode, 2-way Coherent	Enable	Locked	VCXO

2.4.1.1 Uplink Modulation and Threshold

Table 2-6 shows that all standard SDST uplink command rates were available to Phoenix and that standard station modulation index values were to be used. With these values, the Pt thresholds for each SDST and the Pt/No threshold appear in the columns to the right.

Table 2-6 Phoenix transponder uplink modulation and threshold values.

CMD Rate bps	Mod Index radians	Mod Index deg	Carrier Suppression dB	SN101 P_t Threshold dBm	SN102 P_t Threshold dBm	Pt/No Threshold (inflight)
7.8125	0.94	53.9	-2.04	**-146.6**	**-146.3**	25.9
15.625	1.2	68.8	-3.46	-141.8	-141.9	30.7
31.25	1.3	74.5	-4.15	-141	-141.1	31.5
62.5	1.3	74.5	-4.15	**-141.5**	**-140.1**	31.0
125	1.5	85.9	-5.82	**-137.8**	**-138**	34.7
250	1.5	85.9	-5.82	-134.2	-134.2	38.3
500	1.5	85.9	-5.82	-131.9	-132	40.6
1000	1.5	85.9	-5.82	-128.9	-129	43.6
2000	1.5	85.9	-5.82	**-126.1**	**-126.2**	46.4

2.4.1.2 Downlink Modulation and Threshold

Figure 2-17 shows the optimum telemetry mod index and Pt/No thresholds for the (7,1/2) convolutional code concatenated with the Reed-Solomon (RS) code.

Near maximum cruise range, the (15,1/6) code could be used to support higher telemetry rates as needed. Figure 2-18 shows the optimum telemetry mod indices and Pt/No thresholds for the (15,1/6) convolutional code concatenated with the RS code.

							DTT Configuration			Threshold Pt/No, dB-Hz		
Code Type	C&DH Output Coded Bit Rate	SDST Output Symbol Rate	Subcarrier Frequency	Opt TLM Mod Index deg	SN101 Mod Index DN	SN102 Mod Index DN	Carrier Loop BW	Subcar Loop BW	Sym Loop BW	TLM only	TLM + RNG Lo	TLM+Rng Hi
(7,1/2)+RS(I=5)	10	20	25 kHz	38	24	25	3	0.5	0.05	17.78	18.08	18.61
(7,1/2)+RS(I=5)	40	80	25 kHz	56	35	36	3	0.5	0.05	20.78	21.08	21.61
(7,1/2)+RS(I=5)	100	200	25 kHz	66	42	43	3	0.5	0.05	23.76	24.06	24.59
(7,1/2)+RS(I=5)	395	790	25 kHz	72	46	47	3	0.5	0.2	29.09	29.40	29.92
(7,1/2)+RS(I=5)	700	1400	25 kHz	72	46	47	3	0.5	0.2	31.48	31.78	32.31
(7,1/2)+RS(I=5)	1400	2800	25 kHz	72	46	47	3	0.5	0.2	34.46	34.76	35.29
(7,1/2)+RS(I=5)	2100	4200	25 kHz	72	46	47	3	0.5	0.2	36.24	36.54	37.07

Figure 2-17 Modulation parameters and thresholds for (7,1/2) coded telemetry.

							DTT Configuration			Threshold Pt/No, dB-Hz		
Code Type	C&DH Output Coded Bit Rate	SDST Output Symbol Rate	Subcarrier Frequency	Opt TLM Mod Index deg	SN101 Mod Index DN	SN102 Mod Index DN	Carrier Loop BW	Subcar Loop BW	Sym Loop BW	TLM only	TLM + RNG Lo	TLM+Rng Hi
(15,1/6)+RS(I=5)	10	60	25 kHz	34	22	22	3	0.5	0.05	17.86	18.16	18.69
(15,1/6)+RS(I=5)	40	240	25 kHz	51	32	33	3	0.5	0.05	20.26	20.56	21.09
(15,1/6)+RS(I=5)	100	600	25 kHz	62	39	40	3	0.5	0.05	22.88	23.18	23.71
(15,1/6)+RS(I=5)	395	2370	25 kHz	72	46	47	3	0.5	0.2	27.93	28.24	28.76
(15,1/6)+RS(I=5)	700	4200	25 kHz	72	46	47	3	0.5	0.2	30.27	30.57	31.10
(15,1/6)+RS(I=5)	1400	8400	25 kHz	72	46	47	3	0.5	0.2	33.22	33.52	34.05
(15,1/6)+RS(I=5)	2100	12600	25 kHz	72	46	47	3	0.5	0.2	34.99	35.29	35.82

Figure 2-18 Modulation parameters and thresholds for (15,1/6) coded telemetry.

2.4.1.3 SDST Idiosyncrasies

These idiosyncrasies are similar to those documented for other Group Buy 1 and Group Buy 2 SDSTs described in other telecom articles in this series. For a comprehensive example with similar idiosyncrasies, see article 13, Dawn Telecommunications [23].

Subcarrier frequency

The SDST downlink subcarrier frequency was not precisely 25 kHz. Because of the narrow subcarrier tracking loop bandwidths used at low data rates, an inaccurate subcarrier frequency predict could cause the station's Block V receiver (BVR) subcarrier loop not to lock up. The tested frequency was about 25,000.3 Hz, similar to other SDSTs.

Receiver automatic gain control (AGC) telemetry

There were three measures of received signal level, wideband AGC (wb_agc), carrier lock accumulator (cla_agc), and narrowband AGC (nb_agc). The wb_agc measured total power while the other two measured carrier power. The wb_agc and cla_agc interacted with one another, so wb_agc was good only at strong signal levels and cla_agc at weaker levels.

Because the CLA was implemented in series with the wb_agc it did not read correctly for a modulated uplink until the uplink was weak enough (below about –135 dBm) so that the wb_agc gave only a noise signal. When the uplink was above –135 dBm and modulated by command or ranging, the cla_agc measure saw a large power change in carrier power but not the wb_agc measure, which was designed to keep its gain constant. This caused a big change between modulation on and modulation off in the cla_agc when the uplink was saturated.

Digital to analog converter (DAC) rollover glitch

When the DAC counter for receiver static phase error (rcvr_spe) rolled over to a data number (dn) that was a power of two (typically greater than 32; for example, 64, 128, or 255), there could be a hardware glitch which would cause the SDST to drop lock. The glitch could be caused when a large number of registers changed states at the 'rollover' points. It was particularly noticeable for large rcvr_spe that was a power of two (that is, the problem was worse for a rcvr_spe represented by a data number near 128 than for one near 32), and it became worse at high uplink power levels (total received power >–110 dBm at the receiver) and at cold temperatures (< 0 deg C). These conditions affected the frequency sweeps (in terms of end-to-end sweep range in kHz and sweep rate in Hz/s) to ensure SDST receiver acquisition of the uplink carrier.

The Phoenix SDST had a commandable carrier loop bandwidth (either 50 Hz or the power-on-reset value of 20 Hz). Phoenix was flown with the 50-Hz bandwidth from initial acquisition until a spacecraft safing (not related to the SDST) returned it to 20 Hz. At 50 Hz, the DAC rollover issue was of less significance (allowing uplink transmitter frequency sweeps of 2 kHz/s in either direction), but the wider bandwidth raised the carrier lock threshold by 4 dB relative to the threshold at 20 Hz.

Occasional invalid command frame sync words between commands

Periodically, engineering telemetry from the C&DH would indicate a command error. These errors would occur in between commands approximately once every 100 commands. The errors were caused by the SDST sending noise to the C&DH uplink downlink (ULDL) card for a short period before the SDST command subcarrier dropped lock at the end of a command session. Periodically, the ULDL card erroneously registered this noise as the frame synchronization word which placed the hardware command decoder (HCD) in decode mode. Because the HCD never received a valid code block to link to the frame sync word, upon uplinking the next command, the ULDL card would send out a loss of lock and invalid frame error. This idiosyncrasy did not cause loss of commands. No invalid commands or error counts were associated with this event.

Flight software interaction with SDST 1553 bus "busy bit"

Phoenix flight software monitored the SDST configuration every 5 s to verify the SDST telemetry state agreed with commanded state. Independently, the SDST refreshed its configuration every 10 minutes (the State 1 timeout, or S1) when it was without an uplink signal. During this brief refresh period, the SDST set its "busy bit". If flight software issued a telemetry request command during the refresh period, the 1553 driver would return all zeros for the telemetry and cause the 1553 bus to be declared suspect and then change sides. This condition not only caused an error count in the telemetry, but also tripped the SDST component fault protection algorithms named SDST Under Current and SDST Voltage. The 1553 bus on the other side would then query the SDST and work nominally. No Phoenix system fault protection was tied to the 1553 bus errors, thus localizing the problem to within the SDST only.

Ranging pedestal effect

The SDST ranging channel has a bandwidth of about 2.2 MHz. When the channel is powered on but there is no uplink ranging modulation (tones), the noise in the uplink ranging channel was modulated onto the downlink and caused an elevated noise floor (a "pedestal") in the 4.4-MHz bandwidth around the downlink carrier frequency. As a result, the station receiver reported a lower Pc/No than predicted by a simple link calculation that does not take into account the pedestal effect. When uplink ranging tones were present, the pedestal effect decreased, making the downlink Pc/No increase. This effect was mainly noticeable right after launch and in early cruise. At larger ranges the pedestal became small compared to the thermal noise on the downlink.

Ranging polarity

The Phoenix SDST ranging polarity was non-inverted, in contrast to that in some other transponders such as MRO's. Configuring the station receiver for the wrong ranging polarity would cause the range measurement to be wrong by a half cycle.

2.4.2 X-Band Solid State Power Amplifier (SSPA)

The Phoenix X-band system had two MER-heritage 15-W X-band SSPAs on its cruise stage. One MER flight spare General Dynamics solid state power amplifier (SSPA) and one upgraded MER engineering development unit (EDU) SSPA were used in the cross-strapped X-band cruise stage subsystem. Both units performed flawlessly during the cruise mission. SSPA engineering telemetry was limited to a baseplate temperature.

Table 2-7 shows the measured RF output power for EDU003 and SN102. EDU003 was a development unit, but it was subsequently flight qualified for use on Phoenix. Figure 2-19, from Ref. [24], is a block diagram of the SSPA (© 2005 IEEE).

Table 2-7 X-band SSPA RF characteristics.

SSPA parameter	EDU003	SN102
RF Output Power	42.2 dBm (25°C)	42.3 dBm (25°C) 42.1 dBm (0°C) 42.1 dBm (–20°C)
Efficiency (25 deg C, Pin = 1 dBm)	28.6%	29%

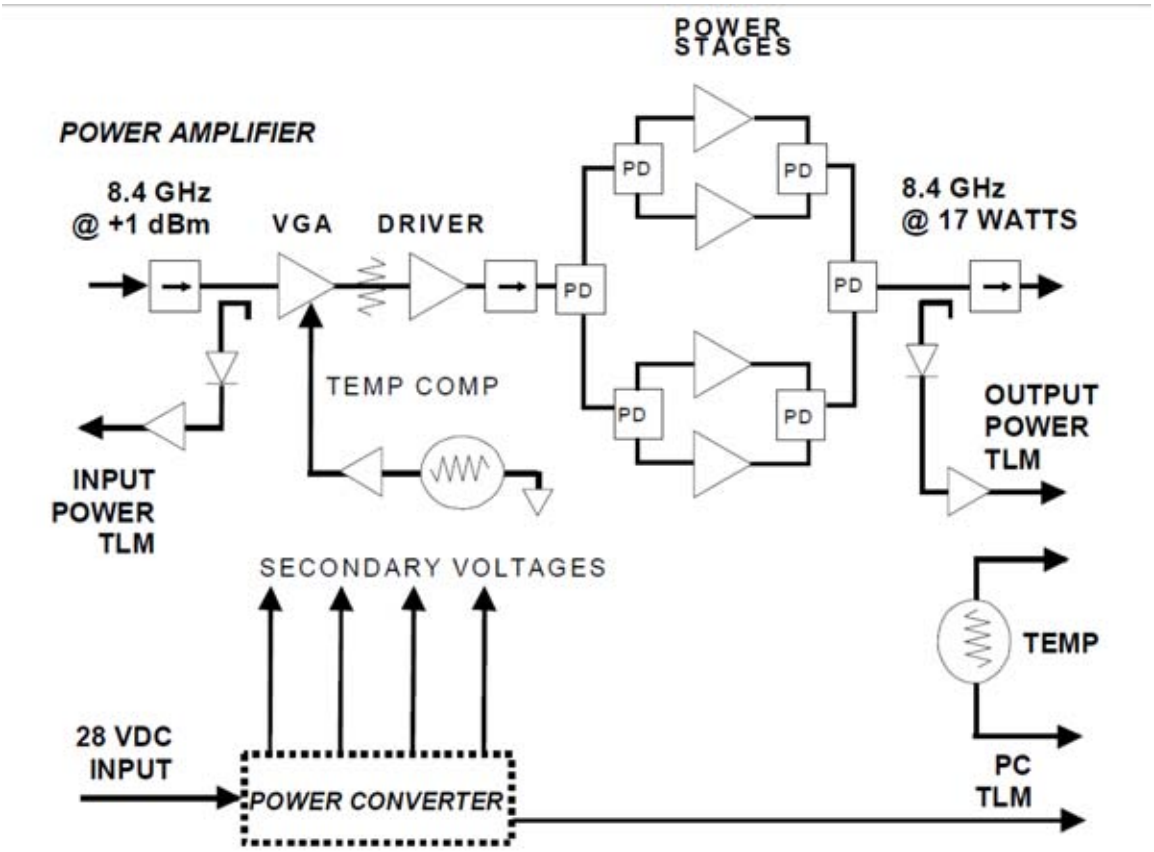

Figure 2-19 X-band SSPA block diagram.

2.4.3 Antennas

Three antennas were included in the cruise subsystem: one receive-only low gain microstrip patch antenna (CLGA Rx); one transmit-only low gain microstrip patch antenna (CLGA Tx); and one dual frequency medium gain horn antenna for both receiving and transmitting (MGA Tx/Rx). The transmit LGA and the receive LGA were inherited from the Stardust program and environmentally tested to Phoenix thermal and vibration requirements as well as RF pattern tested. The LGAs were embedded in the auxiliary solar panel which was located in the top of the cruise ring. The auxiliary solar

panel worked well as an extended ground plane and imparted little beam deformation on the ± 90 deg antenna field of view.

2.4.3.1 Cruise Low-Gain Antennas (Rx-CLGA and Tx-CLGA)

The CLGA polarization is right circular polarization (RCP), and had heritage from MSP98, Spitzer, and Odyssey. The average on-boresight gain for the receive-only CLGA was 6.7 dBi. Figure 2-20 shows the pattern as a function of angle from boresight.

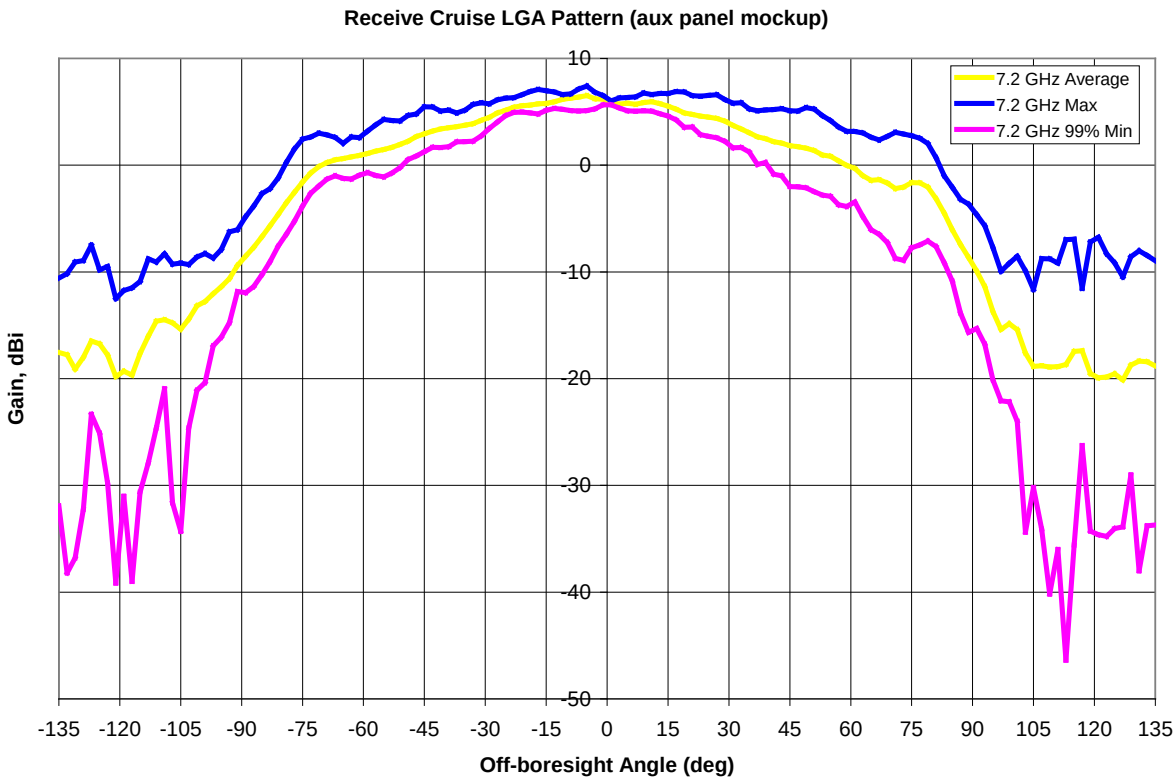

Figure 2-20 Receive-band pattern for the Rx-CLGA.

The transmit CLGA was inherited from the Stardust mission. The transmit polarization was RCP. The on-boresight transmit gain from this antenna was slightly less than the receive gain of the receive CLGA. Figure 2-21 shows the pattern as a function of angle from boresight.

Although the LGA mockup pattern data proved the LGAs provided good hemispherical coverage, at large antenna off-point angles and near the edge of the auxiliary panel, nulls were present. The pattern proved a strong variation in gain versus roll (clock) angle at off-point angles (cone angles) greater than 55 deg. Consequently, small variability in spacecraft roll angle at large antenna off-point angles created variation in signal strength of as much as 10 dB, which made accurate link predictions during spacecraft roll maneuvers more critical. Fortunately, this gain variation was not significant enough to cause unpredicted signal drop-outs. The poor axial ratio of these antennas was a likely contributor to the gain variations at large off-point angles.

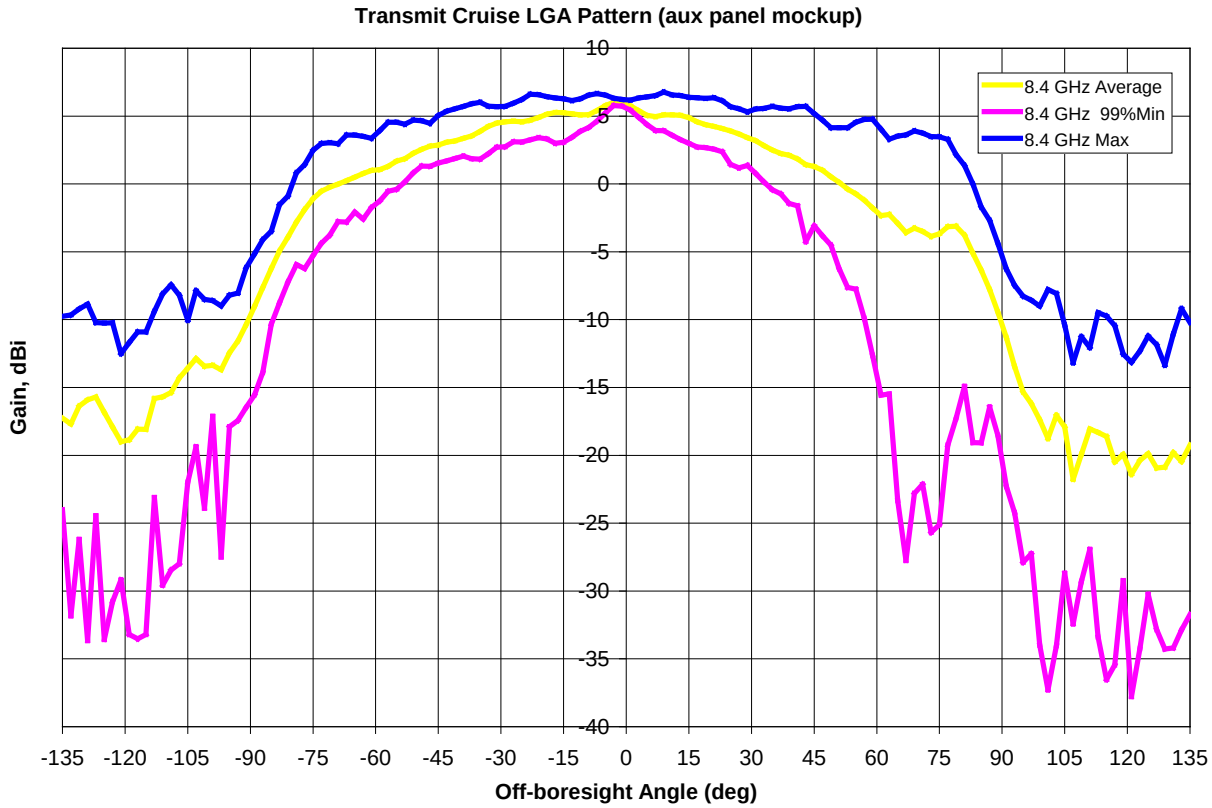

Figure 2-21 Transmit-band pattern for the Tx-CLGA.

2.4.3.2 Medium-Gain Antenna (MGA)

The medium gain horn antenna was inherited from Mars01. The average on-boresight gain was 15.9 dBic receive, and 17.25 dBic transmit. The MGA polarization was also RCP. Figure 2-22 shows the MGA receive antenna pattern, and Figure 2-23 shows the MGA transmit antenna pattern.

The MGA was not gimbaled and therefore, attitude control had to balance between the requirements from the telecom, power and thermal subsystems. The MGA horn bracket was shimmed to match the Sun-probe-Earth (SPE) geometry of the Phoenix spacecraft at Mars arrival. This geometry allowed the solar arrays to point normal to the Sun vector while the MGA boresight remained Earth pointed, which provided the perfect balance between power and communications. The MGA worked without issue throughout all of late cruise.

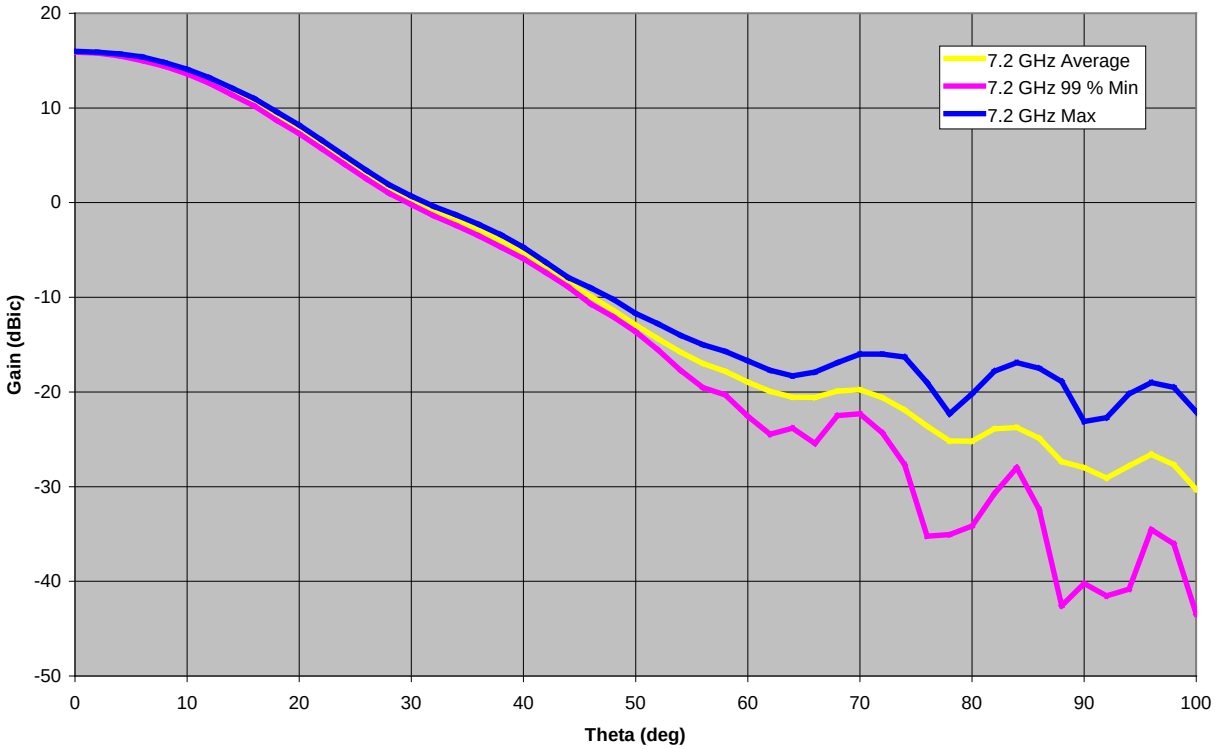

Figure 2-22 X-band MGA receive pattern.

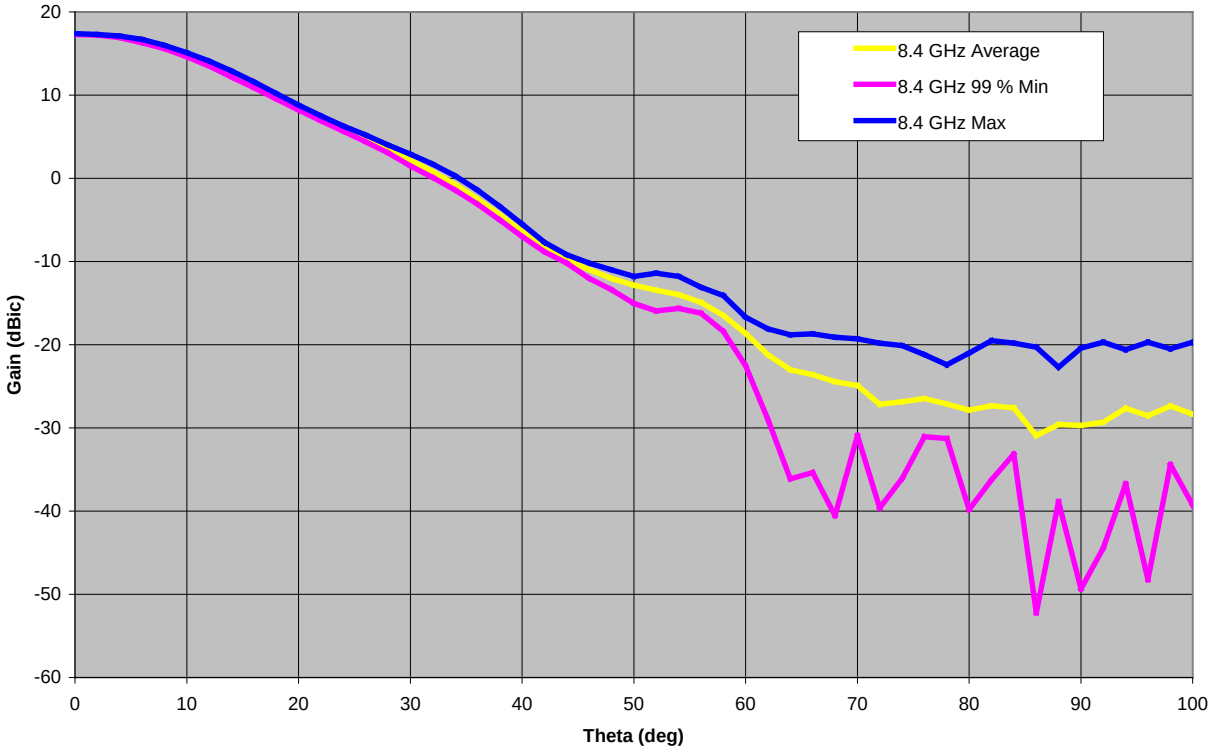

Figure 2-23 X-band MGA transmit pattern.

2.4.4 X-band Microwave Components

The waveguide, bandpass and notch filters, waveguide adaptors, and attenuators were all inherited from the Mars01 Lander program.

2.4.4.1 Hybrid Coupler

In deep space missions, a hybrid coupler is most often used to provide cross-strapping between the SDSTs and the SSPAs, so that either SDST can provide an RF input to either SSPA. However, Phoenix did not implement a cross-strapped design due to lack of available relays to independently power the four units. As a result, the only function of the hybrid coupler in Phoenix was to attenuate the input signal level to the SSPA.

The Phoenix flight unit, manufactured by Merrimac Industries, was inherited from MSP01. The insertion loss is 0.8 dB not including the 3-dB loss for power division.

2.4.4.2 Diplexer

The diplexer, manufactured by Microwave Communications Corp., served the usual purpose of making it possible to receive and transmit simultaneously. SN103 is the flight unit, and SN101 is the flight spare. Table 2-8 describes the diplerxer's RF characteristics.

Table 2-8 X-band diplexer RF characteristics.

Diplexer parameter	Value
Transmit insertion loss (8.4 GHz)	< 0.1 dB
Receive insertion loss (7.1 GHz)	< 0.2 dB
Isolation between Tx and Rx ports	> 40 dB
Group delay	< 4 ns (8.4 GHz) < 4 ns (7.1 GHz)

2.4.4.3 Notch Filter and Bandpass Filter

The purpose of the notch filter was to block leakage of the X-band transmit spectrum into the spacecraft receive path. The manufacturer was Microwave Communications Corp., with SN 003 and SN 004 in the spacecraft. Table 2-9 and Table 2-10 show the RF characteristics.

The bandpass filter was used to filter out harmonics of the downlink frequency spectrum as well as to block other spurious emission in the receive band. The manufacturer was Microwave Communications Corp., with SN001 and SN002 in the spacecraft.

Table 2-9 X-band notch filter RF characteristics.

Notch filter parameter	Value
Receive band insertion loss (7.145 GHz to 7.195 GHz)	< 0.2 dB
Transmit band attenuation (8.4 to 8.5 GHz)	> 70 dB
Group delay (7.145 GHz to 7.195 GHz)	< 4 ns

Table 2-10 X-band bandpass filter RF characteristics.

Bandpass filter parameter	Value
Transmit band insertion loss (8.4 – 8.45 GHz)	< 0.2 dB
Stop band attenuation	> 70 dB (7.145 - 7.195 GHz) > 50 dB (16.8 - 16.9 GHz) > 50 dB (25.2 - 25.4 GHz)
Group delay (8.4 - 8.5 GHz)	< 4 ns

2.4.4.4 Waveguide Transfer Switch (WTS)

The waveguide switch was inherited from the Mars01 Lander program. The unit was procured from Comdev, installed on the Mars01 spacecraft cruise stage, and stored in a clean room until the Phoenix mission inherited it. Both the flight and spare units were inspected and performance tested; then the flight unit was installed on the spacecraft.

The Mars01 Lander environments enveloped those of Phoenix for the WTS, so the unit was not re-tested environmentally at the unit level but instead at the system level. The switch was activated during ATLO in order to measure both transmit paths; however, the switch was never used in flight. In contrast to the operational principle stating that a working component shall never be powered down, the Phoenix mission opted to switch SSPAs in lieu of the activating the waveguide switch when antenna switches were necessary[2]. The flight team swapped SSPAs during the planned switch from the LGA to the MGA on doy 2008-008, when the LGA link margins became slim and during the third and fourth TCMs without issue.

2.4.4.5 Coaxial Transfer Switch (CTS)

The X-band double pole double throw (DPDT) coax transfer switches (CTS) were manufactured by Sector Microwave. This unit is the same model as the DPDT CTS used in the lander UHF telecom subsystem. Table 2-11 provides the switch RF characteristics.

Table 2-11 X-band and UHF coaxial transfer RF characteristics.

Switch parameter	Requirement	SN101 value	SN102 value
Insertion Loss	< 0.4 dB	0.15 dB	0.15 dB
Isolation	> 60 dB	76 dB	73 dB
Return Loss	–17.7 dB max	26.3 dB max	24.3 dB max

[2] The Phoenix constraint resulted from an in-flight anomaly with the MRO WTS (the switch failed in August 2006 to move fully, resulting in about 1 dB loss in the HGA RF path).

The EPOXI mission (an extended mission using the Deep Impact flyby spacecraft) also chose to swap its RF power amplifiers (traveling wave tube amplifiers, TWTAs), rather than using a WTS, when necessary to select between antennas. The reason is similar to Phoenix's: a concern about the integrity of the waveguides or other microwave elements after an anomaly in April 2008 caused the RF output received at the station to decrease by 8 dB for several months. The cause of this anomaly has not been determined, and the output has subsequently returned to normal, but the EPOXI mission believes the lesser risk is still to swap the TWTAs.

2.5 UHF Flight Subsystem Description

The UHF telecom subsystem block diagram is shown in Figure 2-24 [25] which also indicates the heritage of the components. During EDL, UHF transmission prior to lander separation was through the wraparound antenna [26] that the figure shows to the left of the separation (Sep) interface. The helix antenna was used during terminal descent and as the primary UHF antenna during surface operations. The UHF monopole antenna was the secondary antenna for surface operations.

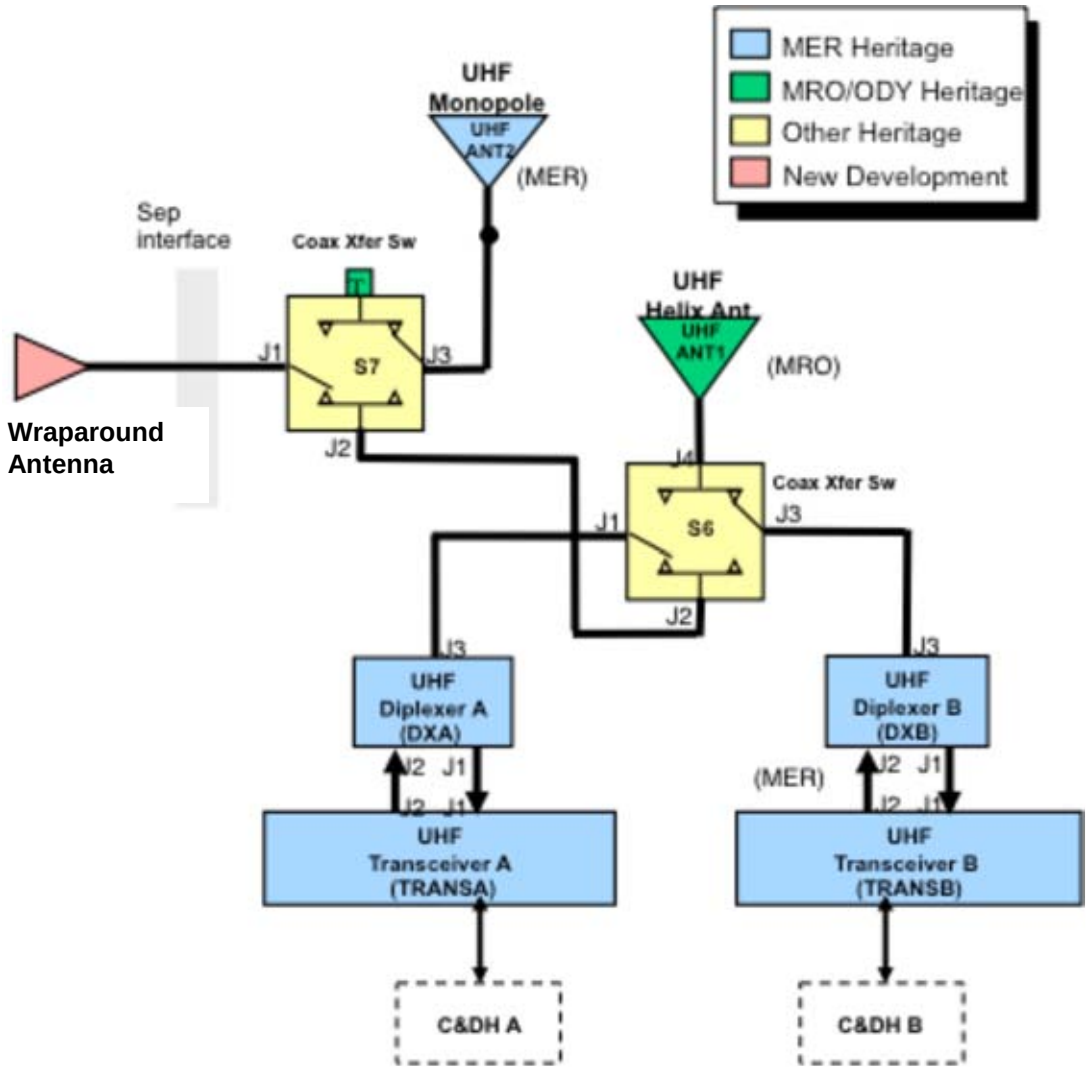

Figure 2-24 UHF Telecom block diagram.

Figure 2-25 shows the Phoenix configuration during entry. At this time, the cruise stage had already been jettisoned. The UHF wraparound antenna was mounted on top of the parachute cone of the aeroshell. The angle theta defines the cone angle between the spacecraft axis and the direction of the receiving orbiter or Green Bank.

Figure 2-26 shows the landed Phoenix configuration with the solar arrays deployed. The UHF components including the CE-505 transceiver were inside the thermal enclosure.

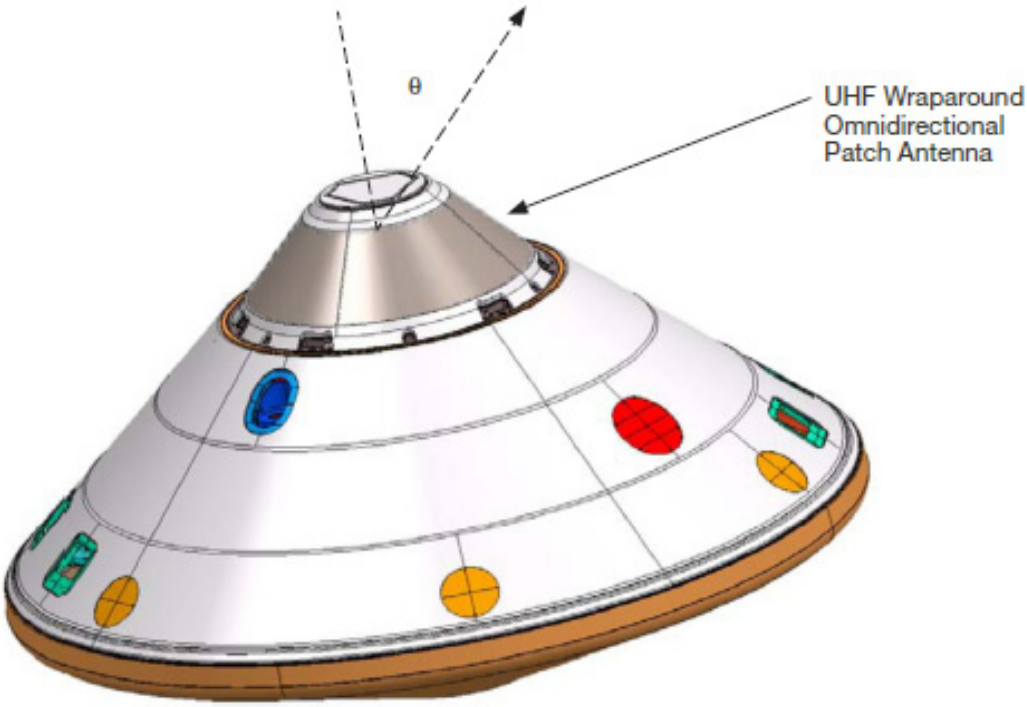

Figure 2-25 Phoenix entry configuration.

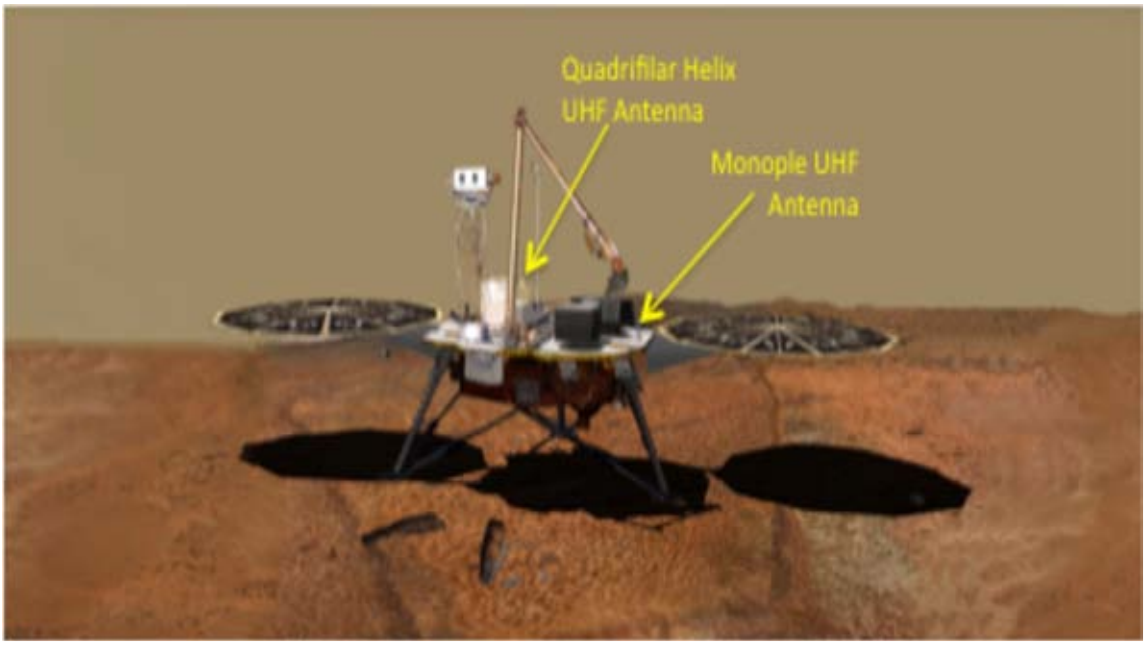

Figure 2-26 Phoenix landed configuration.

2.5.1 UHF Transceiver

The Phoenix lander carried a redundant CE-505 transceiver, made by Cincinnati Electronics. The transceiver (SN103) was the type as used on the two MER rovers.

Table 2-12 summarizes the RF characteristics of the Phoenix transceiver.

Table 2-12 CE-505 transceiver RF characteristics.

Parameter	Value	Notes
Data Rates	8, 32, 128, 256 kbps on forward and return links	
Mod Index	60.5 deg (128 kbps, 25 deg C)	
RF power	40.6 dBm (25 deg C)	
Frame Length	1024 bytes (1019 bytes data + 5 bytes header)	
Frame Sync Marker	FAF320	
Error Correction/Detection	(7,1/2) convolutional code 32-bit CRC appended to end of each frame	G2 symbol not inverted Can be bypassed for uncoded operations
Modulation	PCM/Bi-phase-L/PM, Residual Carrier 60 deg mod index FSK NRZ-L (uncoded only)	
UHF Frequency	Forward link from orbiters: 437.1 MHz Return link to orbiters: 401.585625 MHz	CCSDS channel 0 CCSDS channel 0

Figure 2-27 shows the carrier acquisition measured for SN103. This was the lowest signal power level that the unit could acquire within 1 s. The nominal forward-link operating frequency was 437.1 MHz.

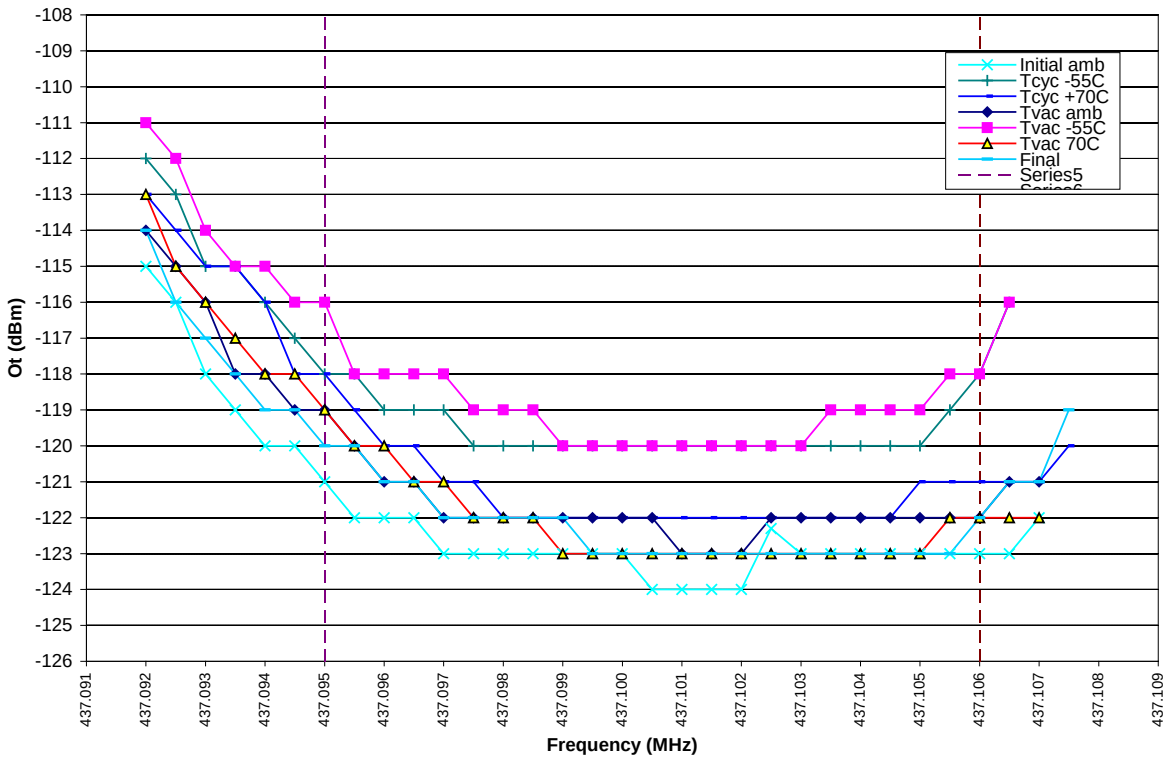

Figure 2-27 Carrier acquisition threshold versus frequency for SN103 transceiver.

2.5.1.1 Establishing a Prox-1 Relay Link with Odyssey

Figure 2-28 shows the sequence of events for establishment of a full-duplex link between the Phoenix lander and Odyssey, using the Proximity-1 (Prox-1) protocol [27]. The top part of the figure shows the initial timing, before lander response. An Odyssey relay link began with a hail sequence initiated by the orbiter. The hail sequence consisted of three parts, starting with a 1-s carrier only signal to aid carrier acquisition by the lander. Next an idle sequence consisting of 4096 alternating 1's and 0's was transmitted at 8000 bps to aid bit sync. Third, an 8-kbps hailing message consisting of 17 bytes was transmitted:

- 3-byte attached synchronization marker (ASM),
- 5 byte transfer frame header,
- 5 byte directive PDU,
- 3 byte ASM, and
- 1 byte pad.

The bottom half of the figure shows the synchronization that occurred after the lander responded. Odyssey would switch its transmitter and receiver to the values specified in the hailing message. To assist the lander in locking to the new bit rate, 1 s of carrier-only was transmitted following by 4096 bits of alternating 1's and 0's at the bit rate specified in the hailing message. If no response was received, the Odyssey transmitter was turned off for 2 s, and the hailing sequence was repeated until a link was established or the Odyssey transceiver was turned off by the spacecraft controller. If the orbiter received a response from the surface element and thus was able to establish bit sync, Odyssey considered the link to be established.

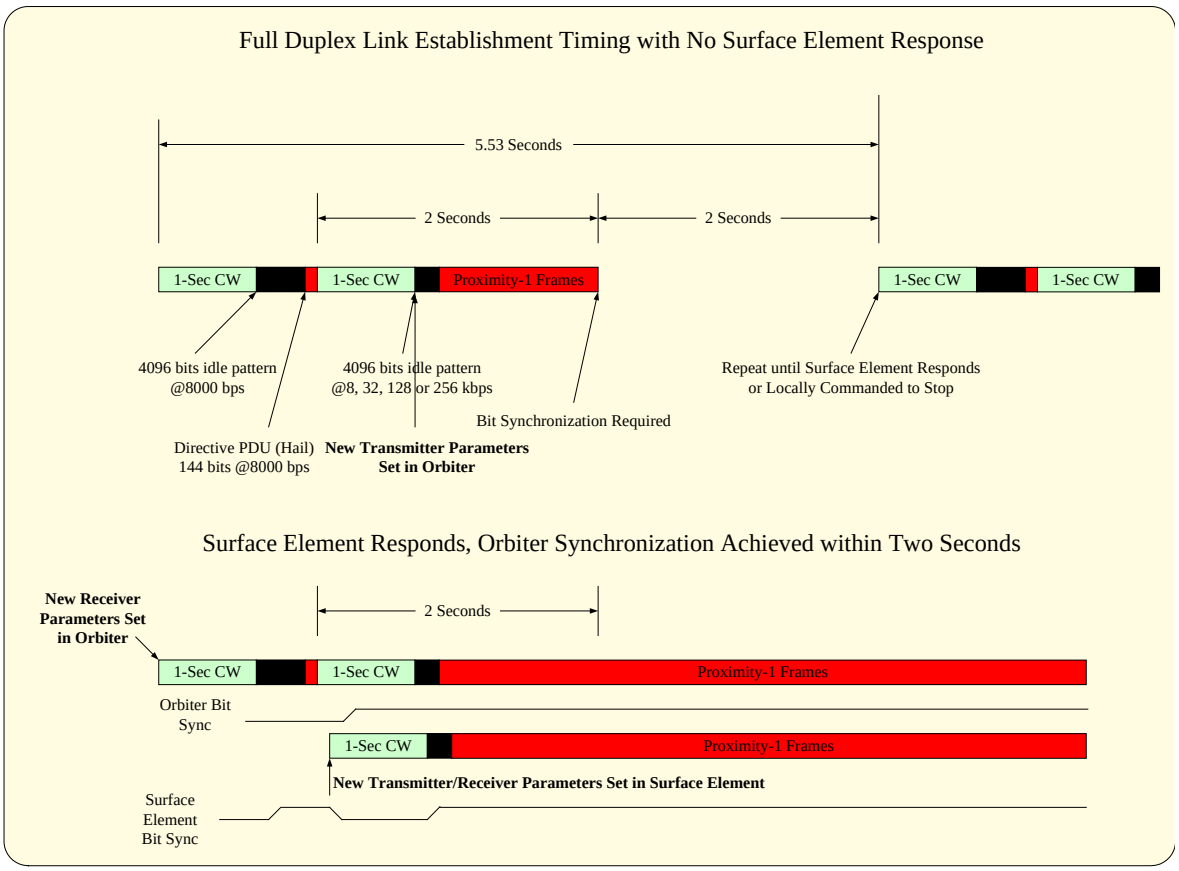

Figure 2-28 Establishment of Prox-1 relay link with Odyssey.

2.5.1.2 Transceiver Idiosyncrasies

Excessive retransmissions to MRO

The CE-505 used a fixed Go-Back-2 protocol [27]. This meant the CE-505 had to receive an acknowledgement from the other end (in this case, either MRO or Odyssey) for the packet before the last one it transmitted before it would send a new packet (call the new one packet N). Otherwise it would go back and start retransmitting packets starting with packet (N-2). Due to the transmit buffer delay in the MRO Electra radio, this could have caused unnecessary retransmissions when Phoenix was relaying to MRO. A workaround was implemented in the MRO Electra radio to reduce transmission delays in the acknowledgement.

Extra byte after each frame (not per Prox-1)

Odyssey inserted one byte of pad after each frame is transmitted. This byte is not defined in the Prox-1 standard and should have been ignored by the lander upon reception. Similarly, the lander was not required to insert the one byte pad when transmitting to Odyssey.

Frame duplication (in Prox-1 mode)

This problem occurred only in the Prox-1 reliable mode. A momentary link drop or low signal-to-noise ratio (SNR) could cause the Prox-1 content to be repeated in the

subsequent UHF frame transmission. This would cause duplication of forward-link commands passed to the lander. This problem could be solved by a frame sequence control mechanism on the lander; similarly, or a frame repeat capability could be implemented on the ground.

False bit lock (without carrier lock)

Under certain conditions, the CE-505 radio could achieve bit sync lock without carrier lock. In this scenario, the transceiver would no longer try to acquire the signal because it considered it in lock even though it was not. The workaround was to reset the UHF to standby after the link had been inactive for 10 s (inactive in this case meant that no proximity frames have been successfully transferred in either the forward or return links).

The false bit-sync idiosyncrasy ended up being a benefit to the Phoenix mission in a Phoenix mode called fixed time-step safemode (FTS). Due to this idiosyncrasy, the link could stagnate if the radio achieved bit sync lock without carrier lock. To counter this, Phoenix implemented the recommended mitigation that used fault-protection software to monitor the transmit-and-receive Proximity-1 advance counters, which only incremented when data was being sent and received successfully. If bit synchronization was registering locked for 5 consecutive samples at 2-s increments and the advance counters had not incremented during this time, the radio was “reset” (asserted to receive standby) to configure it for re-establishment of another link. During FTS while the Phoenix radio was cycling through various communications modes and sleep/wake cycles, the orbiters could be configured for a single hail configuration (either Proximity-1 reliable mode or unreliable mode with a bit rate of 8 kbps) and still establish a link with the lander. In this case, the lander could be hailed out of a Proximity-1 unreliable mode even though the orbiters were configured for a reliable mode.

Data left untransmitted at end of relay pass

At the end of the UHF pass, data in the transmit buffer that was not yet sent (about 32 kilobytes) would be lost. The solution was to program the Phoenix C&DH to stop sending data to the CE-505 before the expected loss or planned termination of the link.

Missing bits in coded data

The missing bits occur at the beginning of link lock. The Phoenix workaround was to repeat packets sent at the beginning of the pass. Also key data packets could be repeated.

2.5.2 UHF Antennas

The wraparound antenna, on the parachute cone, was used during EDL only. The helix antenna was used during landed operations, with a UHF monopole as the backup.

2.5.2.1 Wraparound Antenna

The UHF wraparound antenna was a major new development required for EDL communications. This critical component allowed the spacecraft to transmit carrier and telemetry while the spacecraft experienced cruise stage separation, entry into Mars

atmosphere, parachute deployment, and backshell separation. Because the system had to return information regardless of spacecraft orientation, the antenna pattern accuracy was crucial to the link analysis.

Figure 2-29 (left) shows the Phoenix wraparound antenna on a parachute cone model and (right) an S-band wraparound antenna (which was 1/5 scale for Phoenix UHF) on an aeroshell model at the Haigh-Farr antenna range.

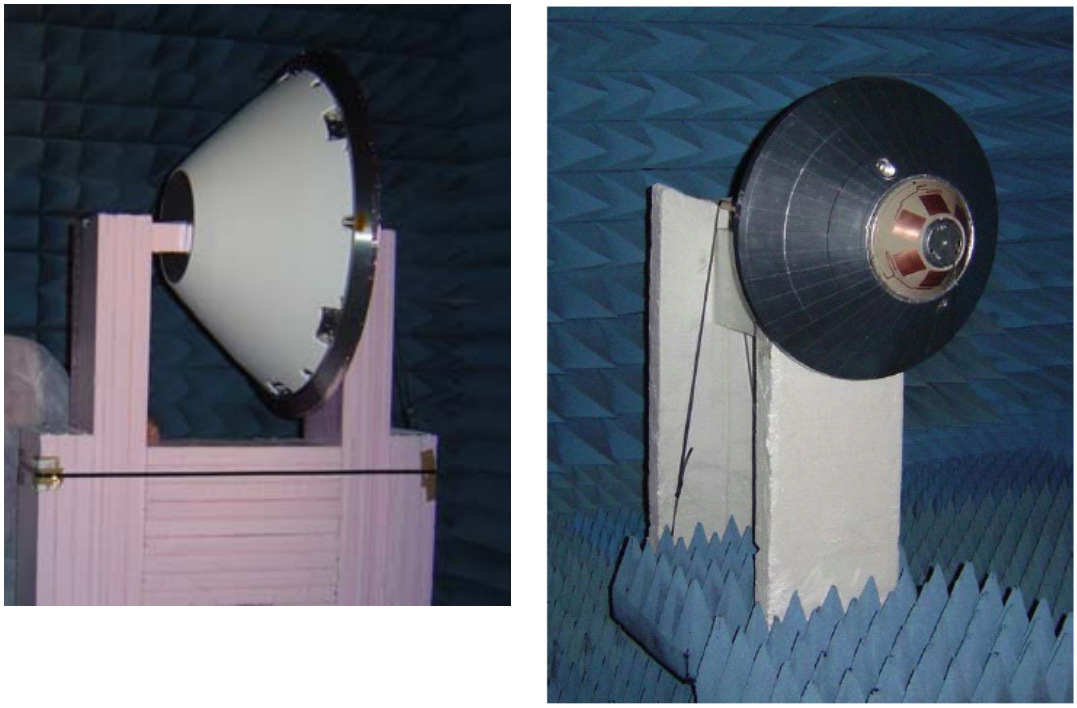

Figure 2-29 Flight UHF wraparound (left) and 1/5-scale test antenna (right).

The verification plan was to measure the flight antenna on the parachute cone only, excluding the rest of the aeroshell in the measurement. The 1/5th scale model would then be used to validate the computer-generated UHF antenna pattern that was a result of the flight hardware free-space parachute cone pattern projected on a three-dimensional (3D) model of the aeroshell.

Figure 2-30 shows the pattern of the wraparound antenna at the transmit frequency of the return link. The best gain is in the region 30–90 deg from the axis of the backshell.

Additional antenna pattern measurements were made at Lockheed Martin on the antenna mounted only on the parachute cone which verified that a null about 135 deg from boresight existed, but not to the depth that the Haigh-Farr Range had measured. Additionally, an independent electromagnetic analysis was performed using the measured pattern projected on a computer generated model of the aeroshell. This analysis proved the null moved out of the field of view when mounted in flight configuration.

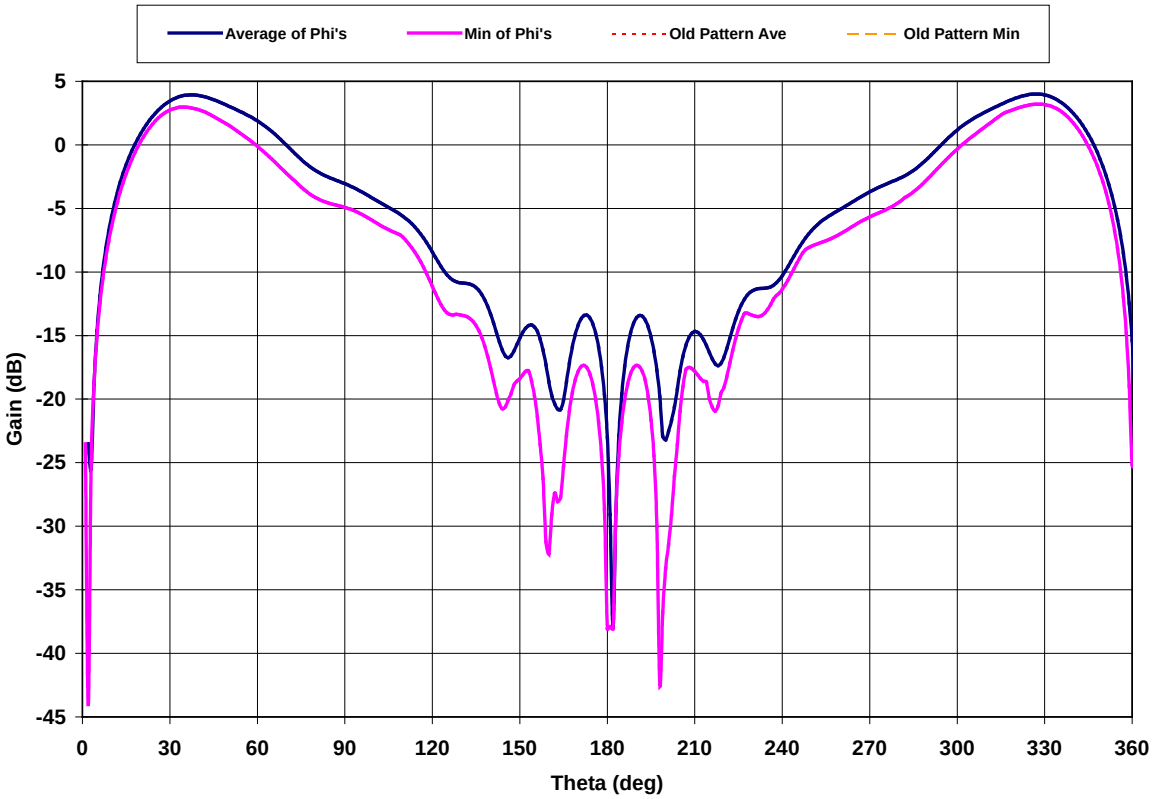

Figure 2-30 UHF wraparound antenna pattern at return-link frequency.

2.5.2.2 Helix Antenna

The helix antenna consisted of four helices connected to a ground plane supported by dielectric rods. It was mounted on the lander deck, and it was designed to have a wide beamwidth to accommodate various lander tilt angles.

The helix antenna was inherited hardware built by Northrop Grumman (formerly Litton-Amecom) for both the Mars01 programs in 1999 and for the MRO program in 2003.

Three antennas of this design were available: the Mars98 Engineering Model (test usage only), the Mars01 protoflight unit (PF-1), and the MRO spare. When tested for directivity and gain, the MRO spare was almost 2 dB better than the Mars01 protoflight in transmit efficiency. Based on this, the MRO flight spare became the Phoenix flight antenna.

Figure 2-31 shows the pattern of the helix antenna at the return link frequency, as measured on a mockup. The nominal pattern had good gain from boresight (vertical from the deck) out to about 70 deg. Due to blockages, the adverse (minimum) pattern had up to 6 dB decrease about 30 deg from the boresight.

The operating polarization of the orbiters and the lander helix was RCP.

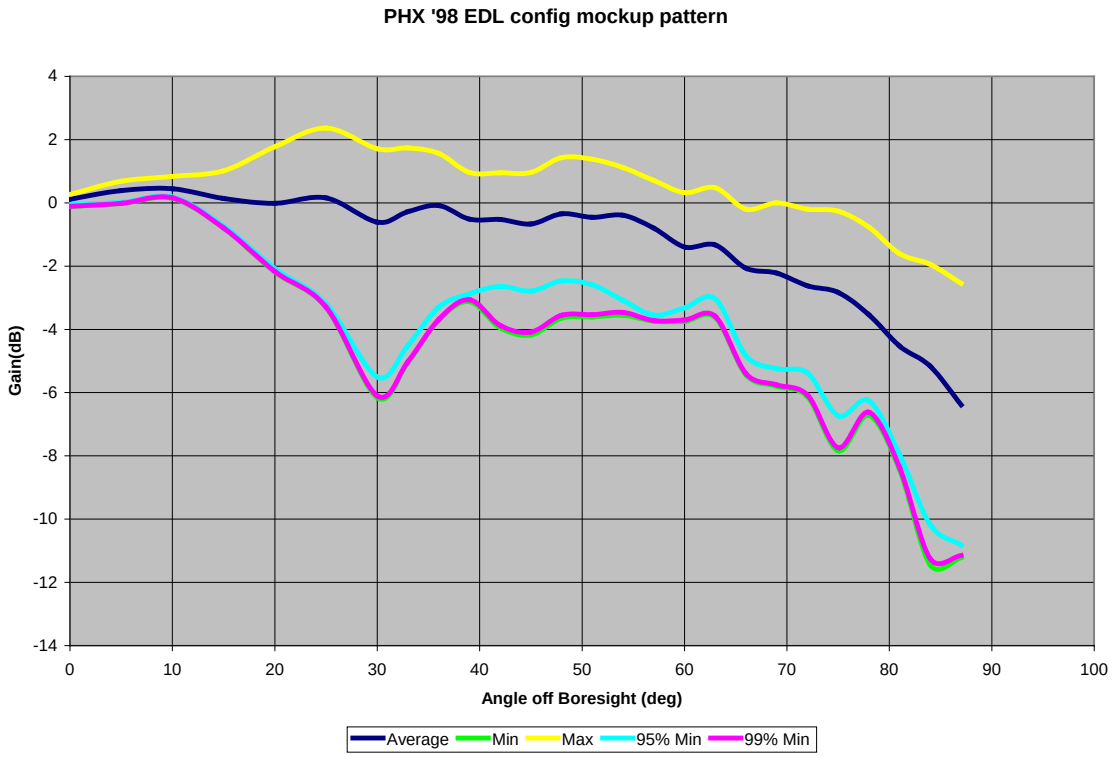

Figure 2-31 UHF helix antenna pattern at return-link frequency.

2.5.2.3 Monopole Antenna

The UHF monopole antenna design was based on the MER monopole design. The Phoenix antenna was shortened by approximately an inch (2.5 cm) compared to the MER design to compensate for the addition of a mounting bracket, and that changed its tuning slightly.

This antenna was used to meet the Phoenix UHF forward command data volume requirement, which could not be met with only the helix antenna. Figure 2-32 and Figure 2-33, respectively, show the forward link and return link gain patterns of the monopole antenna using the lander mockup. The peak monopole antenna gain was 4.62 dB forward and 6.13 dB return.

The monopole was linearly polarized, as was the MER UHF relay antenna upon which it was based.

2.5.2.4 UHF Antenna Modeling and Measurements

The chosen position for the helix antenna, shown in Figure 2 34, was expected to cause significant pattern distortion. Phoenix had a requirement to land with the digging arm side pointing north to within ±5 deg. It was evident that due to deck objects the helix pattern would be obscured in the north-northwest direction at low elevation angles. The operations plan included commanding the lander in the Martian mornings, using low-elevation orbiter passes, which are predominantly to the north-west, near 7 a.m. local solar time. For this, and also for redundancy reasons, a second MER-type monopole antenna was positioned on the northwest corner of the deck [28].

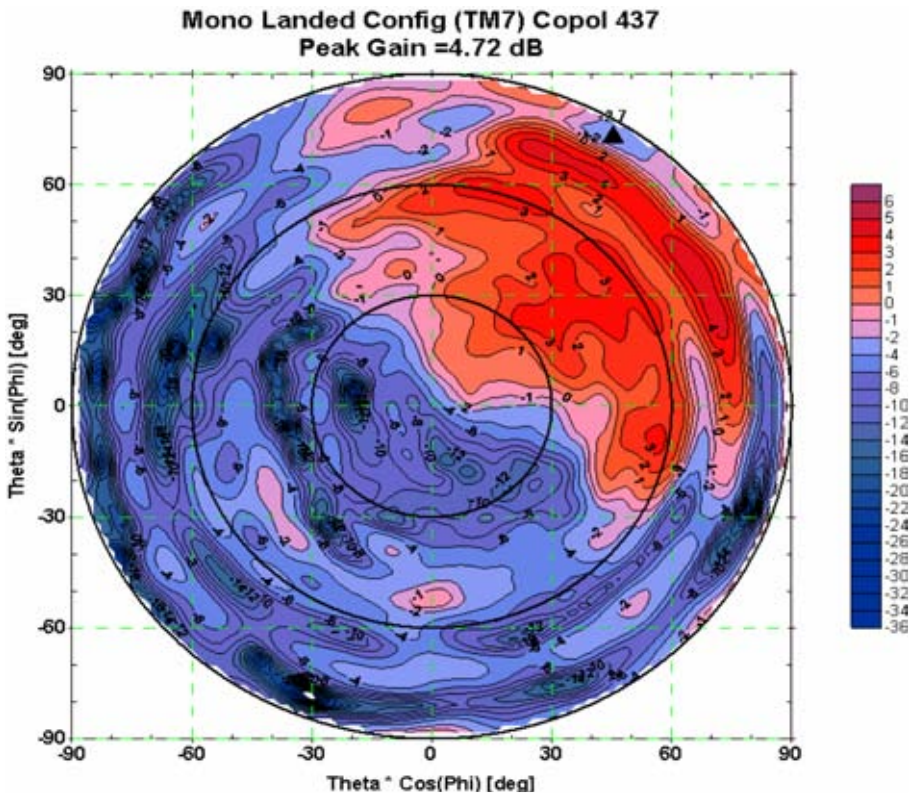

Figure 2-32 UHF monopole receive antenna pattern (Lander mockup, 437.1 MHz).

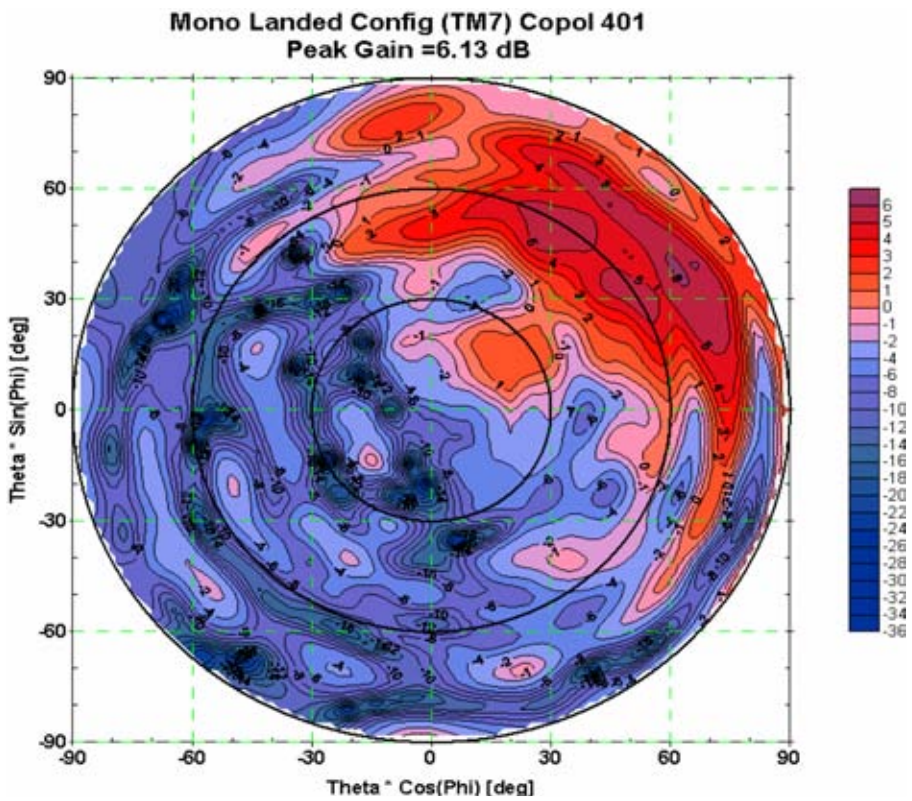

Figure 2-33 UHF monopole transmit antenna pattern (Lander mockup, 401.6 MHz).

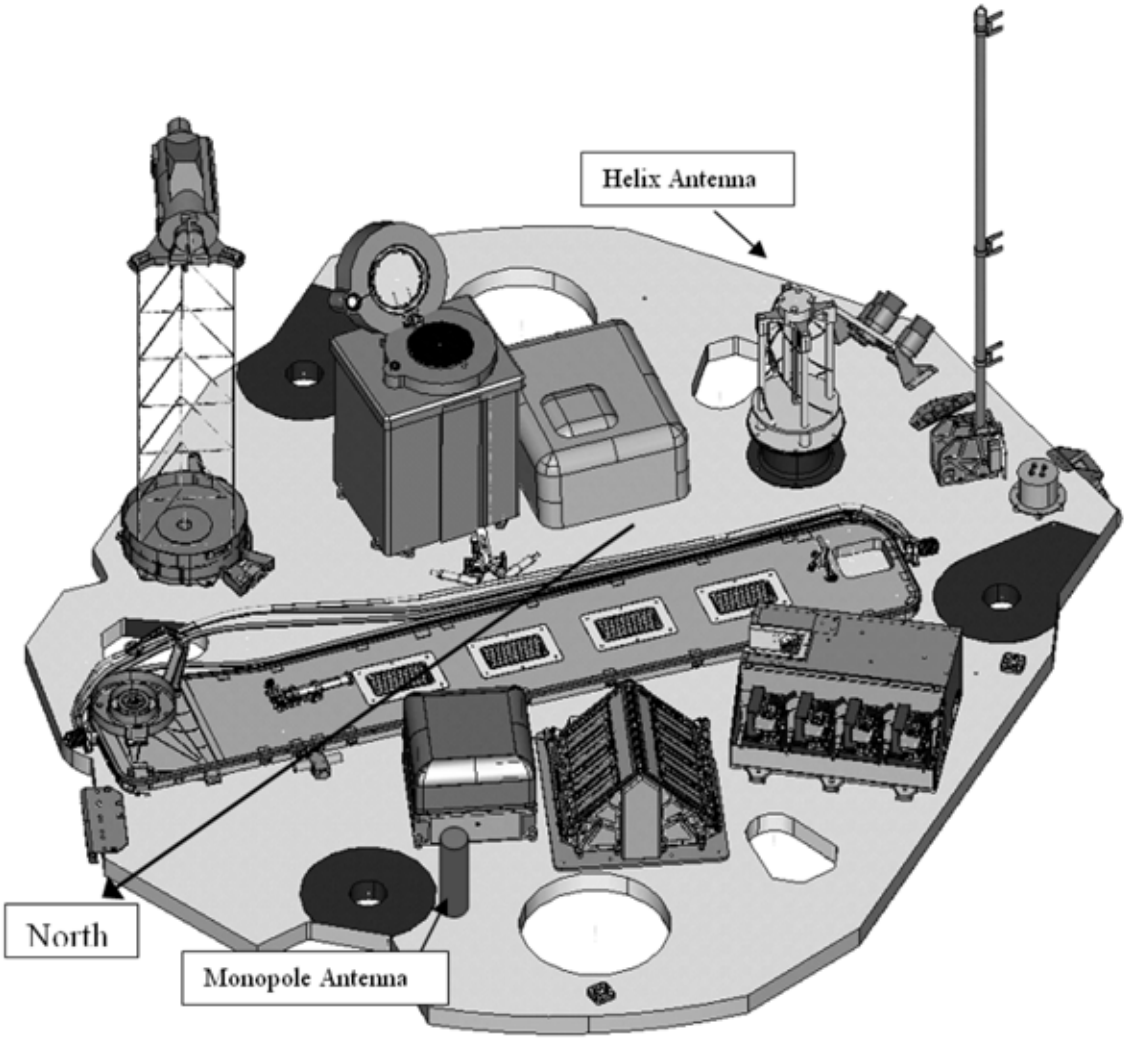

Figure 2-34 Phoenix UHF antennas among other deck objects.

One of the problems the MER operations team continues to deal with is to predict return data volume with precision, primarily because of the uncertainties in the UHF antenna gain patterns for both the orbiter and the landers.

For Phoenix, with a wavelength of about 29 in. (74 cm) in the 400-MHz band, several deck objects lay well within a wavelength distance, and the helix pattern was expected to be greatly distorted, potentially causing a similar prediction precision problem. The extent of the distortion had to be quantified to validate the planned operational strategy for communications, to investigate the necessity for a second (redundant) antenna, and to provide measurement data for comparison to pattern predictions, which could be used to investigate the patterns after the deck configuration was finalized.

Figure 2-35 (left) shows the lander mockup, with the helix antenna and the monopole antenna, as deployed for surface operations.

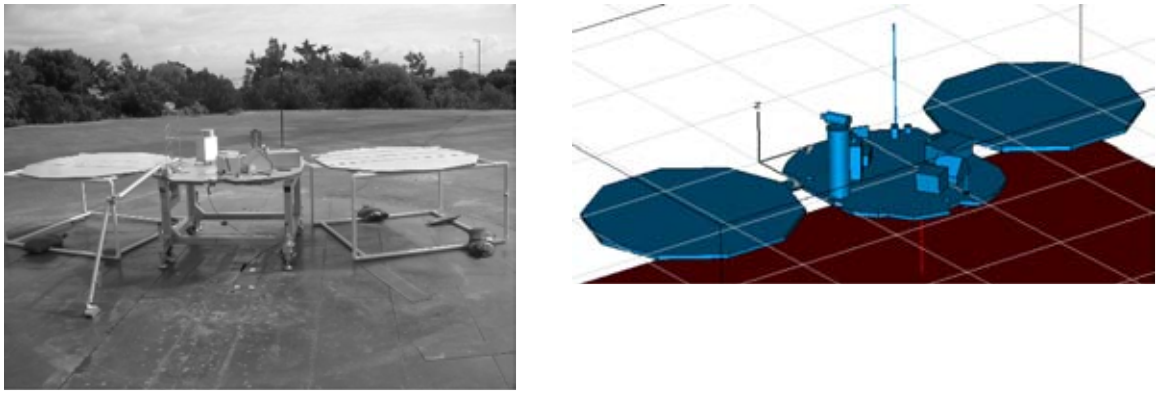

Figure 2-35 (Left) Phoenix Lander mockup; (Right) Phoenix model with ground effect.

At the right in the same figure is the analysis model for antenna patterns. Only the top surfaces were modeled. Many of the objects (Figure 2-34) are rather complicated, and in the interests of limiting cost due to excessive modeling the analysis models might be considered crude. Nevertheless the predictions (with their inherent modeling errors) matched the measured data (with its inherent measurement errors) well enough to have confidence that on average we had a good model for Phoenix-to-orbiter link calculations.

The measured data (such as that shown in Figure 2-31 for the helix and in Figure 2-32 and Figure 2-33 for the monopole) was used to make real-time engineering decisions at the system level, and it also permitted the validation of two antenna analysis packages, which were used for the Phoenix mission and can be used for the next Mars rover mission, Mars Sciences Laboratory (MSL). Measured data from this campaign, and analysis results from the prediction packages, also can be used to construct data volume prediction tools for use by the operations teams on the Phoenix and MSL surface missions.

2.5.3 UHF Coaxial Transfer Switches

The UHF system had one double pole double throw (DPDT) coaxial transfer switch and one single pole double throw (SPDT) coaxial transfer switch. The DPDT switch was the same model as in the X-band system. The switches were made by Sector Microwave. Table 2-13 shows the RF characteristics of the switches.

Table 2-13 RF characteristics of the coaxial transfer switches.

Parameter	DPDT switch value	SPDT switch value	Typical value (DPDT)
Insertion loss	0.2 dB maximum	0.4 dB maximum	0.1 dB
Isolation	60 dB minimum	60 dB minimum	105 dB
Return loss	–17.7 dB maximum		–33 dB
Switching time		100 ms maximum	

2.6 Landing Radar

The landing radar included a broadbeam altimeter and velocimeter function and was of Mars Polar Lander and Mars Exploration Rover (MER) heritage.

2.6.1 Radar Design

The radar, provided by Honeywell, was derived from a production altimeter. Relative to the previous projects, this radar was modified for operation at a lower minimum altitude and to provide a high resolution Doppler mode, including additional capability to measure the Doppler spectra of the return echoes. The Phoenix radar, designated FM3, was a new build for Phoenix. The pulse repetition frequency was decreased to reduce range ambiguity. The antenna and antenna switch designs were new [29].

The antennas are mounted to the bottom of the lander as shown in Figure 2-36. The antennas, paired for receive and transmit, formed four separate beams: one nadir-pointed beam (altitude and velocity) and three side beams (velocity only).

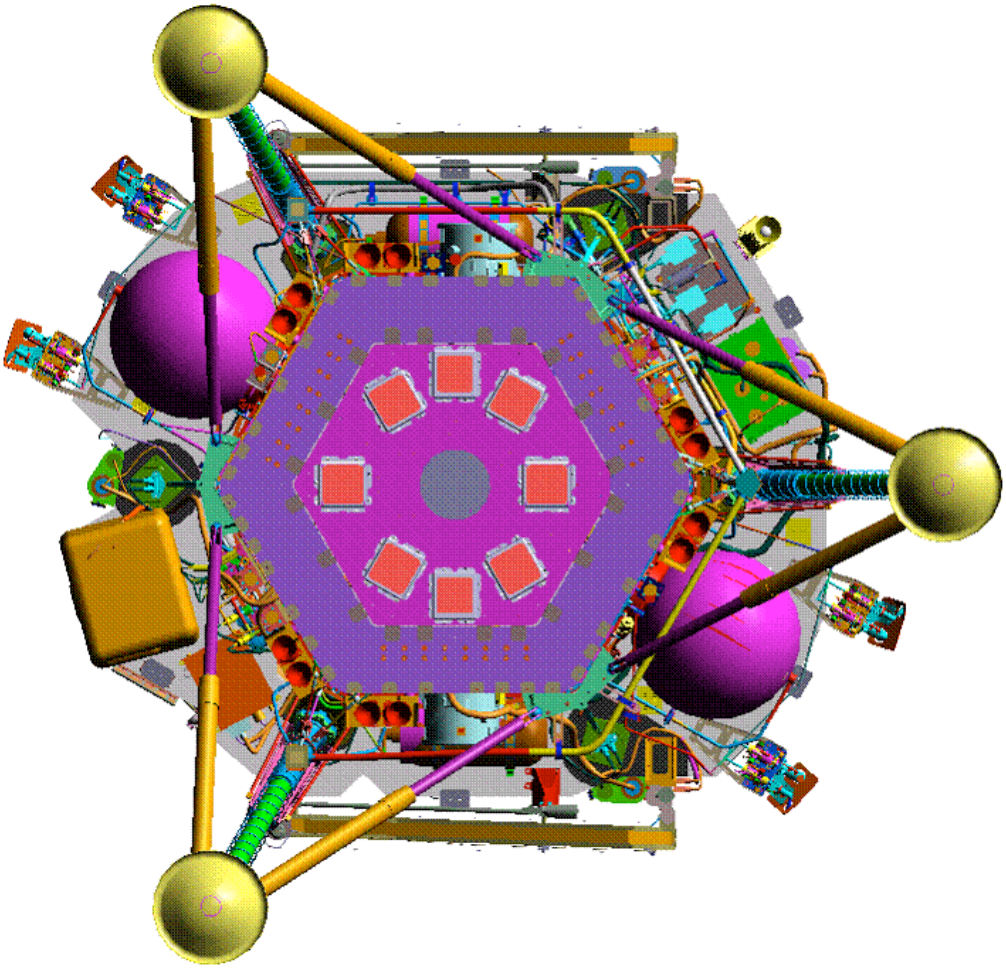

Figure 2-36 Looking up at the radar patch antennas from below the lander.

The three side beams were electronically steered 30 deg off-nadir and equally spaced around the lander in azimuth.

Each beam consisted of a separate transmit and receive antenna and was activated sequentially during radar operation. Using separate antennas for transmit and receive eliminated the need for a high-speed switch to alternate between transmit/receive events and allowed the radar to detect echoes much earlier in time when the lander was lower in altitude.

Figure 2-37 includes photographs of the antennas (top) and the radar electronics (bottom).

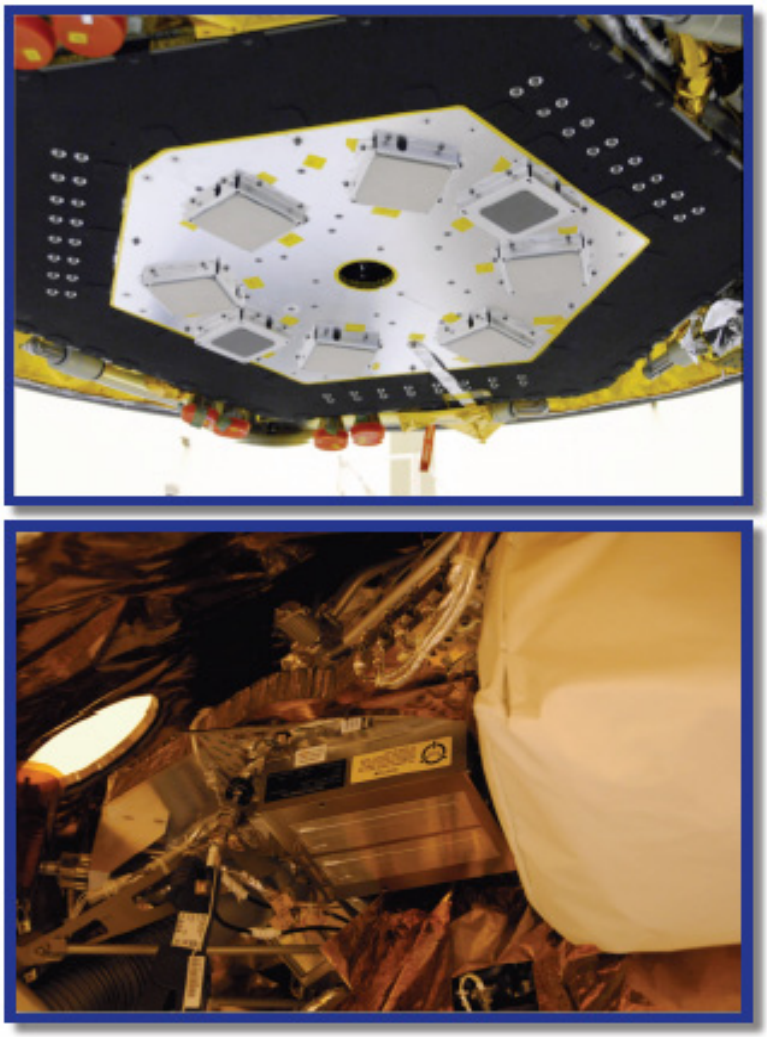

Figure 2-37 Landing radar antenna (top) and electronics (bottom).

The radar signal was a 4.3-GHz bi-phase modulated pulse, with a 100-ms measurement cycle. The pulse width and modulation characteristics of the radar varied over the operational altitude to match the desired signal strength and accuracy. Table 2-14 lists the characteristics of the Phoenix radar.

Table 2-14 Landing radar characteristics.

Parameter	Value	Notes
Transmit power	1 watt peak	Duty cycle < 1%
Antenna gain	11 dBi	
Antenna beamwidth	53 deg by 48 deg	
Pulse repetition frequency	14 kHz to 400 kHz	
Doppler sample rate	6 kHz or 3.24 kHz	
Operating modes	Standby, built-in test, altitude, altitude & velocity	
Warm-up time	1 minute	From power-on
Data and commanding interface	1553 bus	

During each measurement cycle, the radar made an altitude measurement from the nadir-pointed antenna beam. If commanded by the spacecraft, the radar would also make a range-gated Doppler measurement from one of the four antenna beams based on flight software command. At the end of the 100-ms cycle, the radar provided the altitude, a fast Fourier transform (FFT) of the spectrum, and validity flags to the spacecraft.

The Phoenix radar included two Doppler sampling periods, the shorter one used on Mars Polar Lander (MPL) and a longer one added for Phoenix. The longer sampling period provided finer velocity resolution toward the end of the descent when the vehicle was traveling slower. The pulse repletion rate was reduced from the MPL design for range ambiguity protection. The radar could measure the altitude and velocity over a range from 0 m to 2438 m (0 to 8,000 ft) above the ground; Doppler measurements were made over altitudes from 15 m to 1700 m (49 to 5,600 ft).

2.6.2 Radar Performance

Performance requirements included altitude measurements accurate to 5 percent and beam-velocity measurements accurate to 2 percent of the velocity along the beam direction. The radar consistently performed as specified – or better [30]. The radar worked well in the environment that it was tuned for (flat terrain, near-vertical descent). The radar contributed to a three-sigma vertical touchdown velocity of between 1.4 and 3.4 m/s, and a three-sigma horizontal touchdown velocity of 1.4 m/s maximum.

Table 2-15 summarizes radar statistics: number of measurements, first-measurement altitude, and altitude difference from navigation solution at the first measurement.

Table 2-15 Landing radar performance.

Parameter	Value	Notes
Measurements made	239 (altitude only mode) 434 (altitude & velocity mode)	Total: 673
Altitude at first measurement	2356 m (7730 ft)	Best estimate
Delta from navigation solution at first acquisition	1300 m (4300 ft)	“That’s why there was a radar” [29]

Figure 2-38 is a profile of the radar-reported altitude versus the time from landing (which is expressed as a SCLK or spacecraft clock number) compared with the profile generated from inertial measurement unit (IMU) data. Figure 2-39 shows the velocity profile compared with the IMU data.

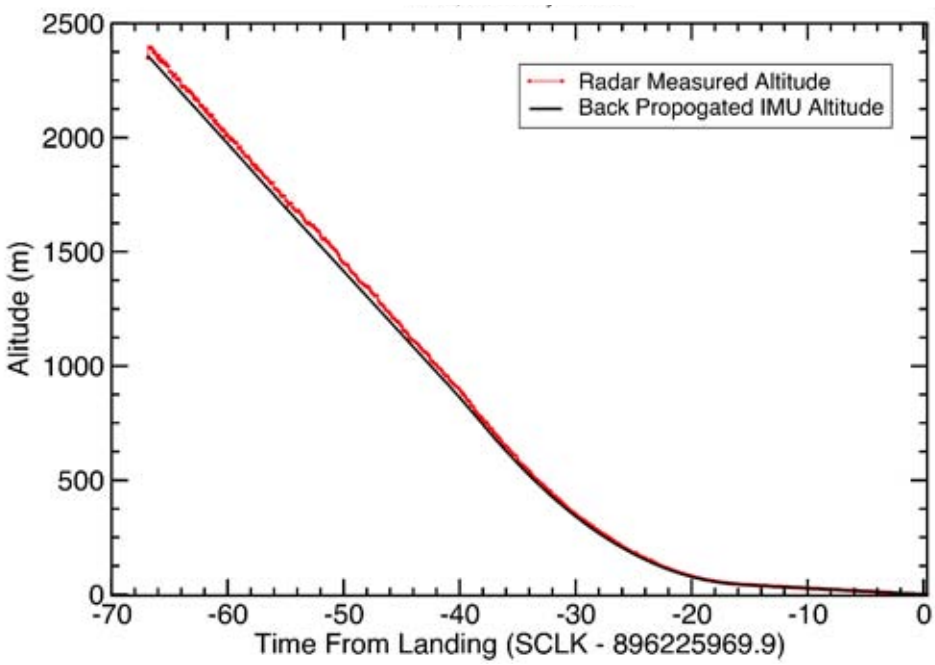

Figure 2-38 Radar versus IMU estimated altitude versus time.

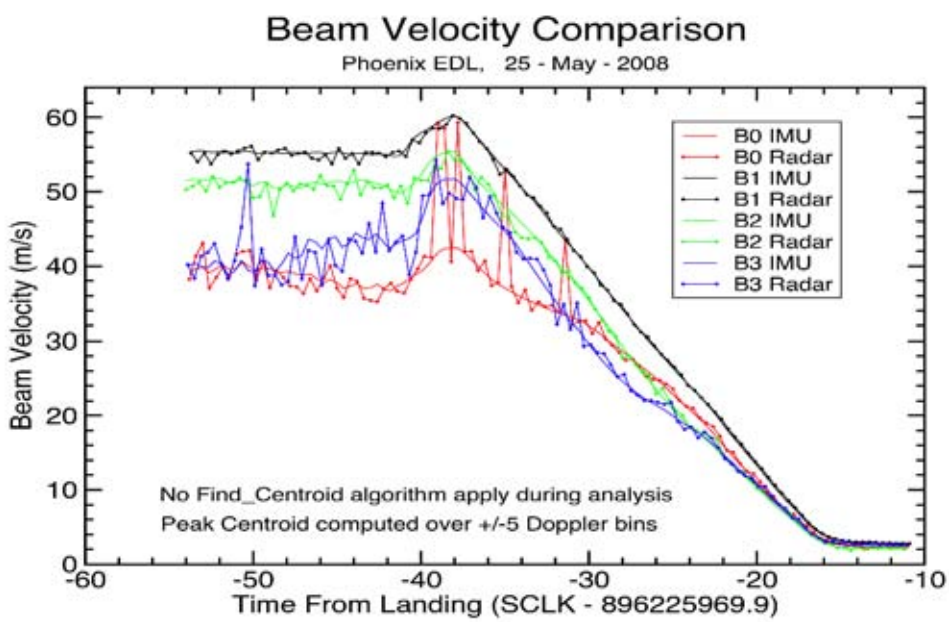

Figure 2-39 Velocity comparison between radar beams and IMU.

2.7 Telecom Hardware Mass and Power Summary

2.7.1 X-Band Mass

Table 2-16 summarizes the mass of the X-band components (used during cruise only), the UHF components, and the landing radar.

Table 2-16 X-band mass.

Component	Per unit (kg)	Total (kg)
X-band		14.7
SDST (2 units)	2.65	
SSPA (2 units)	1.35	
Microwave components		
X-band diplexer	0.36	
Bandpass filter	0.28	
Notch filter	0.13	
RF transfer switch	0.42	
Waveguide, adaptor, support	0.59	
Cables and connectors	1.12	
LGA and cabling	0.3	
MGA and cabling	3.5	
UHF		6.5
UHF helix antenna	1.1	
UHF antenna	1.2	
UHF transceiver (2 units)	1.85	
UHF microwave		
UHF diplexer	0.36	
UHF coaxial transfer switch	0.07	
UHF bandpass filter	0.06	
Radar and electronics	5.0	5.0

2.7.2 Telecom-Related Spacecraft Power Consumption

Table 2-17 summarizes the power consumed by the active units (SDST if powered, SSPA if transmitting, UHF transceiver when active, and the landing radar when operating).

Table 2-17 Spacecraft power for SDST, SSPA, UHF transceiver, and landing radar.

Component	Bus power (W)	Condition
SDST	11.5	Receive only
	13.9	Receive & transmit
SSPA	65.0	Transmitting
UHF transceiver	6.1	Receive only
	52.2	Receive & transmit
Landing radar	22.7	Standby
	25.4	Nominal operating

3 Ground Systems

3.1 X-Band Operations: The Deep Space Network

The Deep Space Network (DSN) was used in its conventional manner during the Phoenix cruise mission, at X-band, to

- transmit an uplink carrier and receive a downlink carrier for 2-way Doppler
- transmit commands on the uplink
- receive engineering telemetry on the downlink
- transmit uplink ranging modulation and receive downlink turn-around ranging
- receive ΔDOR tones on a 1-way downlink carrier

Figure 3-1 and Figure 3-2 show a 34-m antenna under construction and completed at Madrid, Spain [31].

Figure 3-1 34-m DSN antenna under construction at Madrid, Spain.

Figure 3-2 Completed 34-m antenna at Madrid, Spain.

The signal processing center (SPC) at each Deep Space Control Center (DSCC) site (Madrid, Spain; Canberra, Australia; or Goldstone, California, USA) serves the site's 70-m antenna and the several 34-m stations at one central location. Station operators at the SPC communicate with DSN control in Pasadena, California and with each mission's control center during tracking support of that mission. To minimize downlink noise and uplink RF power loss, the downlink low noise amplifier and the uplink transmitter are at the individual antenna site.

The Phoenix mission primarily used single (non-arrayed) 34-m stations [32] for most purposes. The Phoenix uplink and downlink were always at X-band, so no use was made of the DSN capabilities at S-band or Ka-band.

3.2 EDL Operations

The Green Bank observatory was used to receive the UHF as a direct to Earth (DTE) transmission during EDL (Figure 3-3).

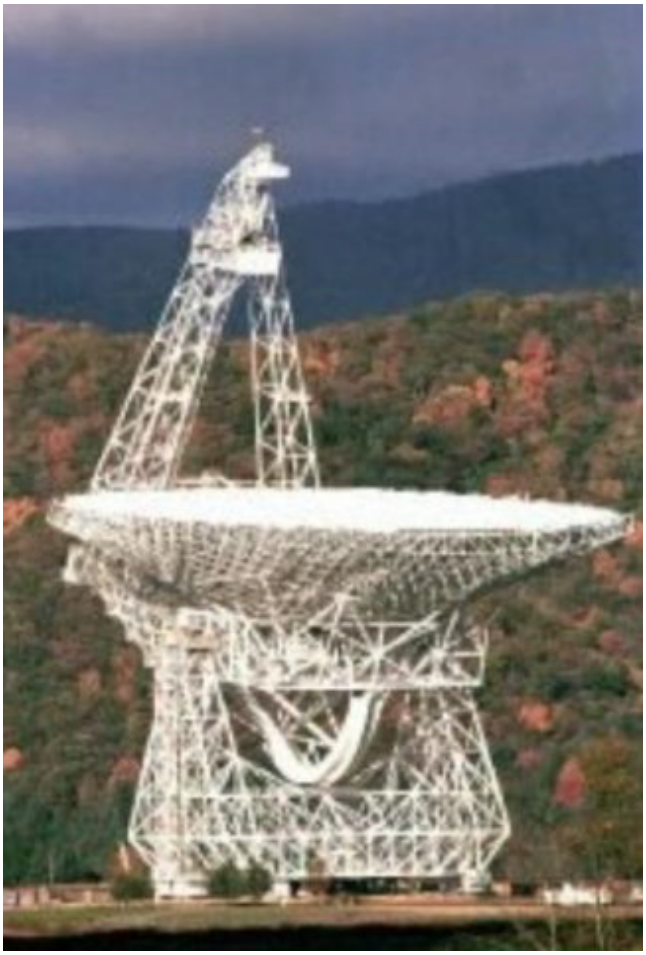

The Robert C. Byrd Green Bank Telescope (GBT) is the world's largest fully steerable radio telescope [33].

The GBT is described as a 100-m telescope, but the actual dimensions of the surface are 100 by 110 m. [34]. The overall structure of the GBT is a wheel-and-track design that allows the telescope to view the entire sky above 5 deg elevation. The track, 64 m (210 ft) in diameter, is level to within a few thousandths of an inch in order to provide precise pointing of the structure.

Unlike conventional telescopes, which have a series of supports in the middle of the surface, the aperture is unblocked so that incoming radiation meets the surface directly. This increases the useful area of the telescope and eliminates reflection and diffraction that ordinarily complicate a telescope's pattern of response. To accommodate this, an off-axis feed arm cradles the dish, projecting upward at one edge, and the telescope surface is asymmetrical.

In the Phoenix EDL link design, the GBT's gain to noise temperature (G/T) was estimated as 32.5 dB based on a system noise temperature of 70 K. After circuit losses, the received total power (Pt) was -164 dBm at entry minus 120 s, just when the unmodulated carrier (called "CW" for continuous carrier) switched to 8 kbps (Figure 2-10). This link budget was confirmed by tests performed at Green Bank in December 2007, using the UHF from the Opportunity rover (MER-B). The test confirmed a carrier-to-noise ratio within 2 dB of prediction [35]. Based on this link evaluation:

- Initial CW and modulated carrier phases would be easily detectable at Green Bank from CSS to about Entry + 180 s (~E+180), when Earth passes close to the Phoenix antenna null
- Probable plasma blackout period (~ E + 80 to 120 s).
- Just before parachute deployment, Green Bank would pick up the signal again.

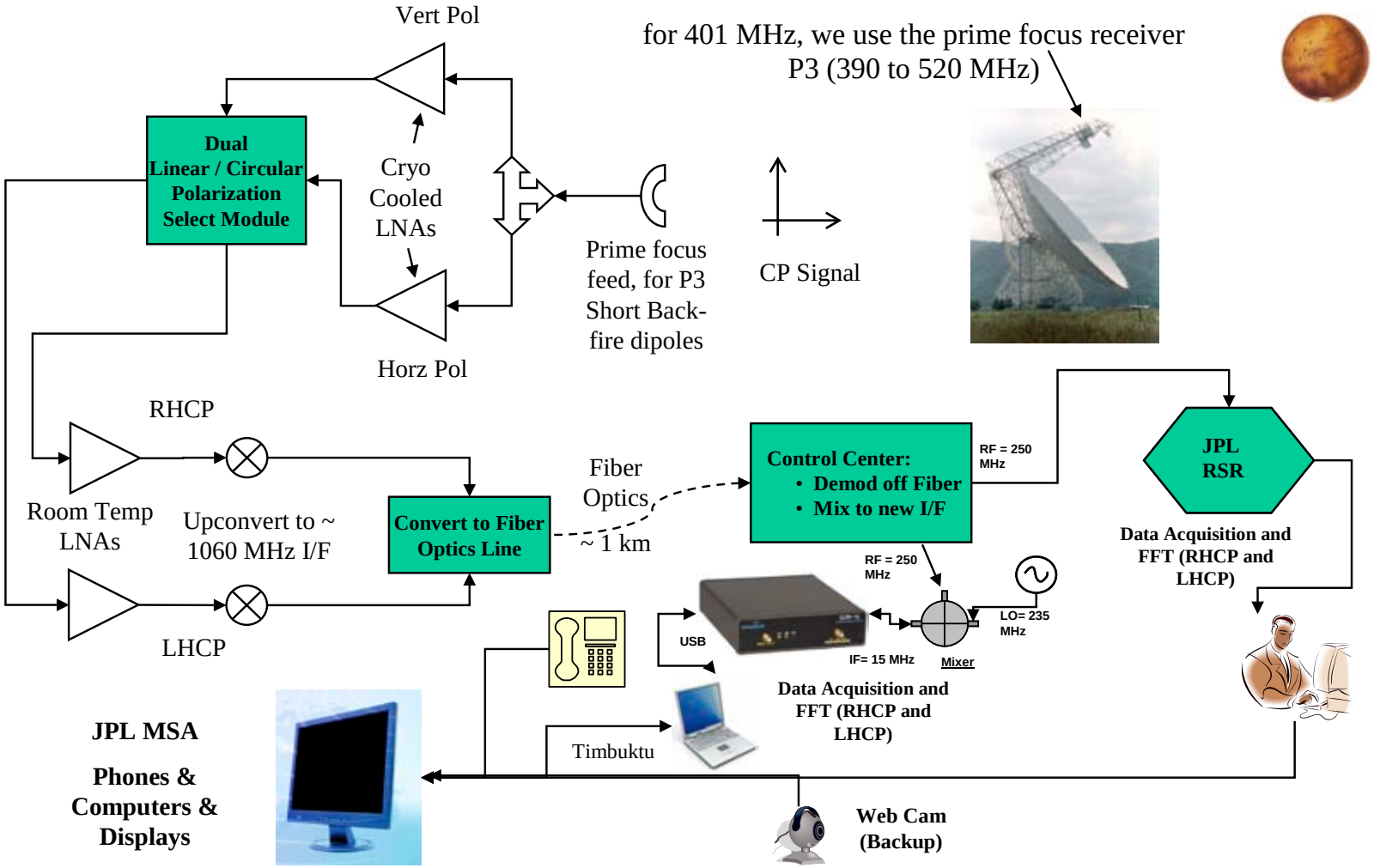

Figure 3-3 Block diagram of Green Bank UHF receiving setup for Phoenix EDL.

4 Telecom Subsystem Link Performance

4.1 X-Band Performance during Cruise through Separation

This section, from Ref. [36]

- compares measured versus predicted performance
- compares original downlink data rate plans with what was accomplished

4.1.1 Initial Acquisition

The LGAs played a crucial role in providing almost the earliest possible initial acquisition after launch despite the stations' being about 80 deg from LGA boresight. Because of the nearly hemispherical field of view of these antennas, lock on the 2100-bps telemetry signal was established by the DSN only 10 s after the exciter was powered on. This provided the flight team the earliest possible health and status of the spacecraft.

Because the DSN stations were concerned with saturating the ground receiver with excessive downink signal power from the spacecraft, the Goldstone DSN receivers (first in view after launch) were configured for a left hand circularly polarized signal. This deliberate polarization mismatch reduced the signal strength at the receiver by approximately 20 dB. For all subsequent tracking passes, the stations were configured for a right-hand polarized downlink signal.

Several hours after initial acquisition, the navigators delivered updated pointing coordinates due to a 1 sigma launch trajectory which improved the signal strength by close to 20 dB.

Figure 4-1 shows initial acquisition measured downlink signal level and after the mission provided actual trajectory data for a station antenna pointing update[3]. The measurement of carrier power is provided as a channel in the station monitor data stream.

[3] Analysis of AGC (Pc) changes, as compared with total power (Pt) changes is affected by modulation when the downlink is strong. The cause is similar to how the SDST cla_agc (telemetered measure of Pc) is affected by modulation on or modulation off while wb_agc (Pt) is not.

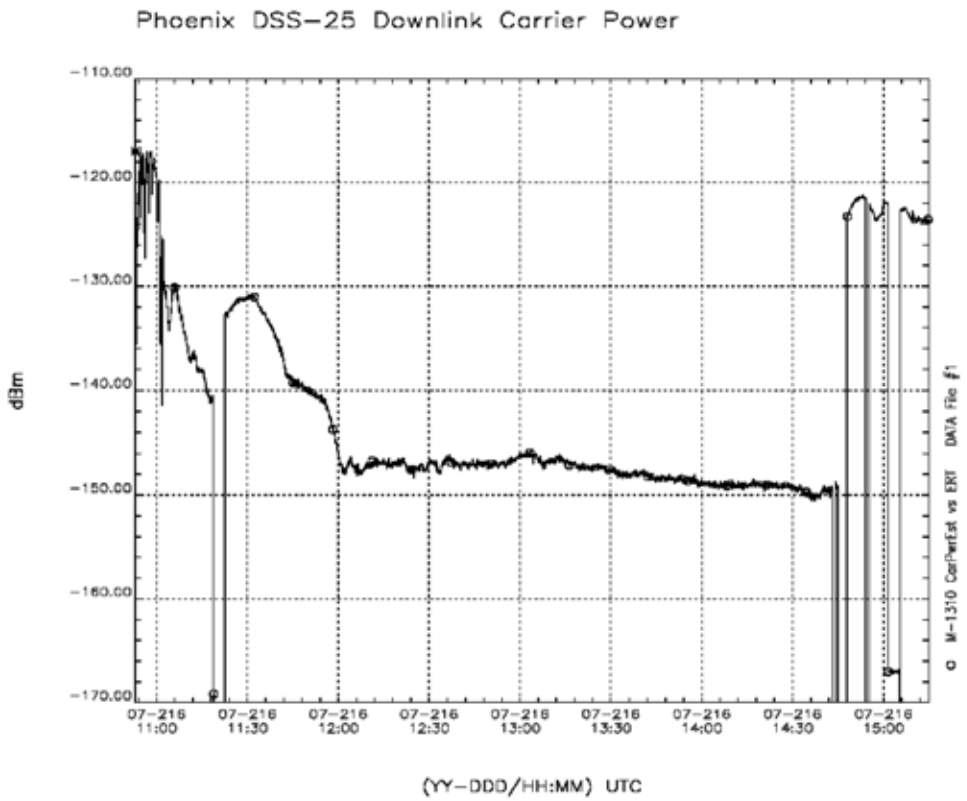

Figure 4-1 Downlink carrier power at 34-m station during initial acquisition.

4.1.2 Early Cruise

The cruise low-gain antennas were used for uplink and downlink from initial acquisition until the switch to the medium gain antenna which occurred as planned on Jan 8, 2008. Because of the large deadbands and Earth off-point angles required to balance telecom, thermal and power requirements, the low gain antennas proved to be ideal for early cruise and trajectory correction maneuvers. Figure 4-2 shows the planned antenna off-point angles (including attitude control deadbanding) during the cruise mission.

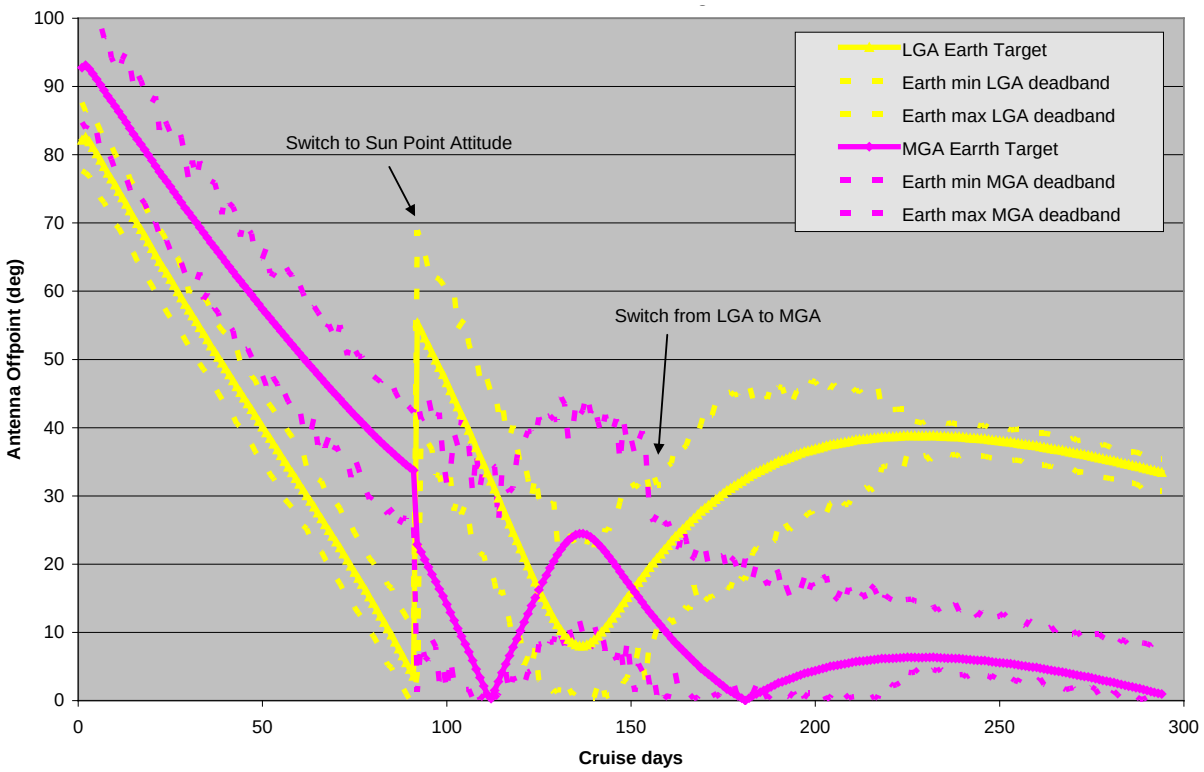

Figure 4-2 LGA and MGA antenna offpoint angles during cruise.

The telecom forecaster predictor (TFP) tool adapted for Phoenix includes spacecraft and station X-band link models.

Based on the measured performance from the LGAs, the antenna pattern measurements proved to have been extremely accurate for use in the TFP models.

Figure 4-3 is an example of a comparison between the measured and predicted downlink signal strength through the transmit LGA. This pass was on August 18, 2007 (doy 2007-230/231). The thinner curve is the predicted signal level, and the thicker curve is the measured value. The figure shows excellent correlation, almost always within 3 dB, given the sizeable deadbands that existed.

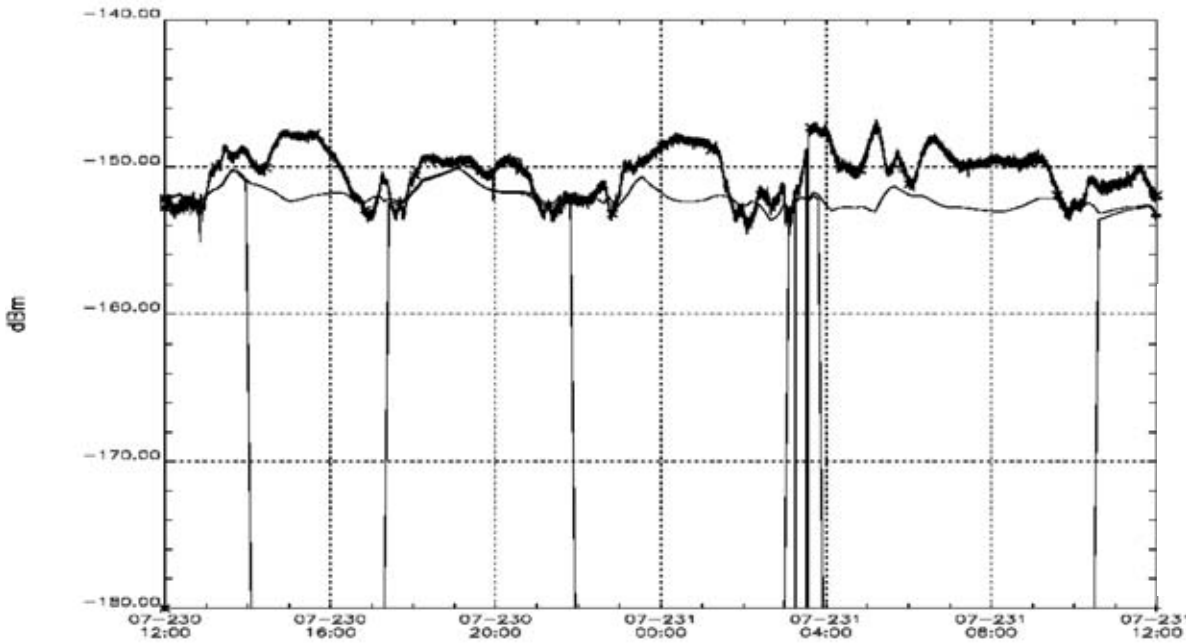

Figure 4-3 Example of measured 34-m carrier signal level compared with TFP predictions.

4.1.3 Trajectory Correction Maneuvers

Two-way Doppler was required during TCMs[4] which could only be guaranteed under pointing constraints defined by the telecom link analysis. Although communication could not be guaranteed beyond 90 deg off the LGA boresight, the mission decided to try to acquire as much two-way Doppler data as possible during the TCMs late in the cruise mission. Because the off-point angles were in excess of 135 deg from boresight, loss of signal was a certainty, and the goal was to maintain a two-way link for as long as possible to collect Doppler data.

In order to achieve this goal, the flight team telecom analyst ("telecom") recommended tracking the downlink signal for as long as possible and also leaving the DSN uplink signal on throughout the entire TCM in lieu of re-sweeping the uplink frequency which could at best be achieved in 95 s. For both TCM-3 and TCM-5, the Doppler imparted by the burn and the best lock frequency versus SDST temperature predicts proved the uplink signal frequency would remain within the carrier loop bandwidth of the SDST (± 1.3 kHz) during the burn. Prior to each TCM, an SDST best lock frequency update request was made to the DSN to decrease uplink frequency by approximately 0.5 kHz to track predicted best-lock frequency (BLF) drop due to SDST temperature change during the TCM. In both cases, the frequency "snap back" method worked perfectly and provided two-way Doppler data out to 120 deg off LGA boresight.

[4] The Phoenix mission did not have a requirement to provide telemetry during TCMs. However, during TCM-1 and TCM-2, the LGA offpoint angles were favorable, and the Earth range was small enough to support telemetry during the burn. For TCM-3 and TCM-5, only carrier lock (for the 2-way Doppler) could be achieved due to the large off-point angle and Earth range.

Figure 4-4 shows how the LGA offpoint angle varied during TCM-5 over the course of the turn to burn attitude, the burn, and the turn back to cruise attitude. Figure 4-5 shows the measured and predicted signal level at a 70-m station (DSS-43) during the TCM. The black curve is the prediction, and the blue curve the measurement.

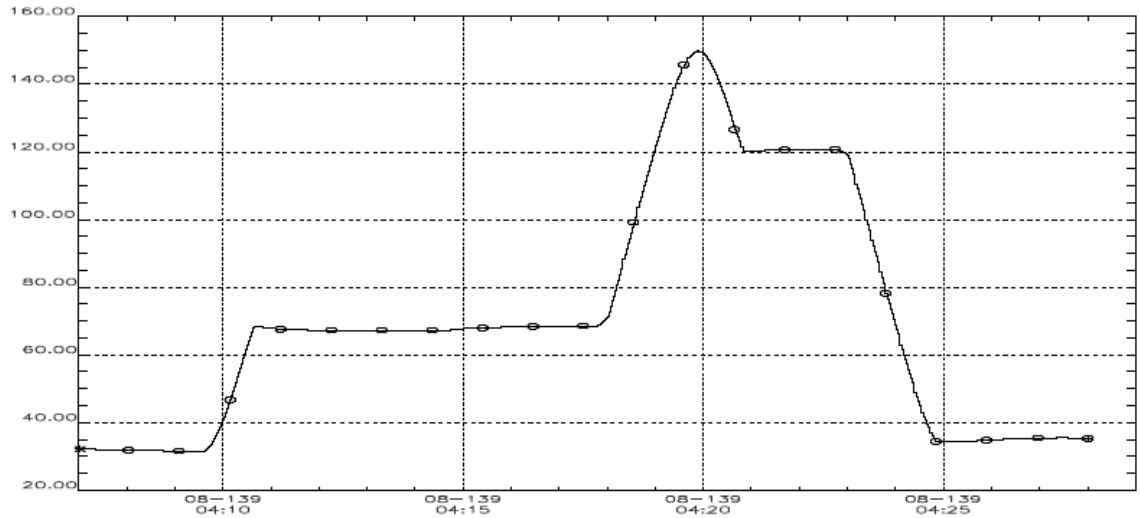

Figure 4-4 LGA offpoint angle during TCM-5 (turn, burn, turn back to cruise).

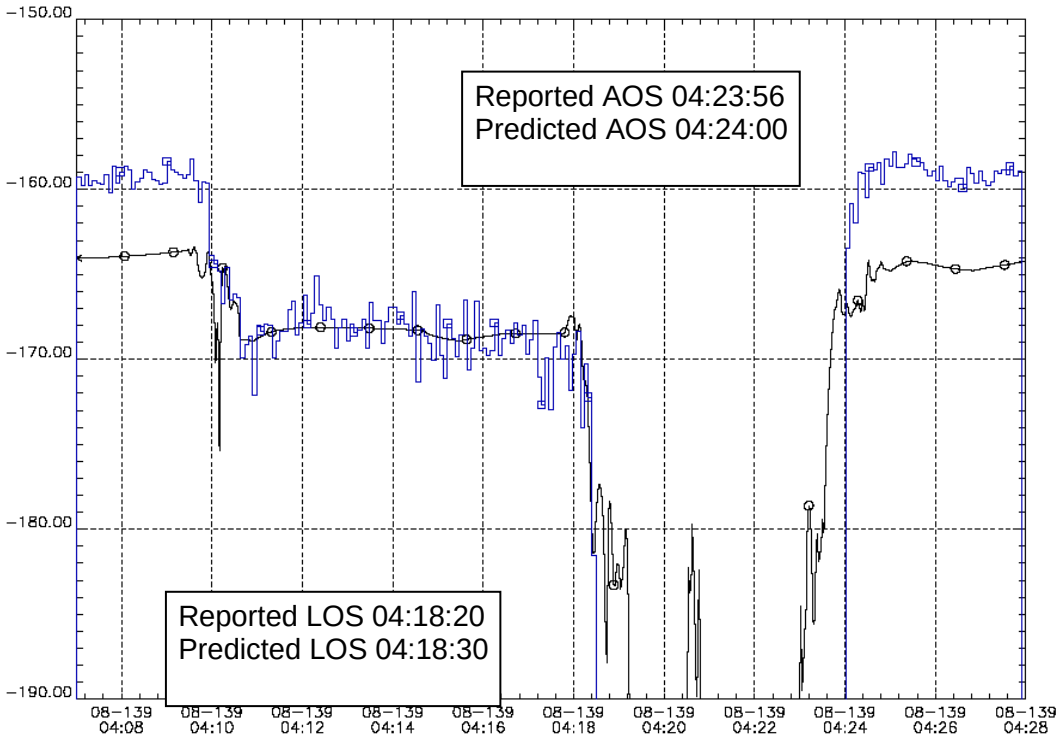

Figure 4-5 Measured versus predicted downlink carrier at 70-m station during TCM-5.

4.1.4 Cruise Data Rates

The minimum required operational downlink rate was 40 bps. However, performing payload and flight system checkouts at this rate was not practical due to the large volume of engineering data that had to be returned. For this reason, the mission was keenly interested in the supportable downlink rate over the course of the cruise.

Figure 4-6 shows comparisons between the predicted and actual downlink rates during the cruise mission. In order to provide 2100 bps at important times, the mission scheduled the 70-m stations that could provide that rate.

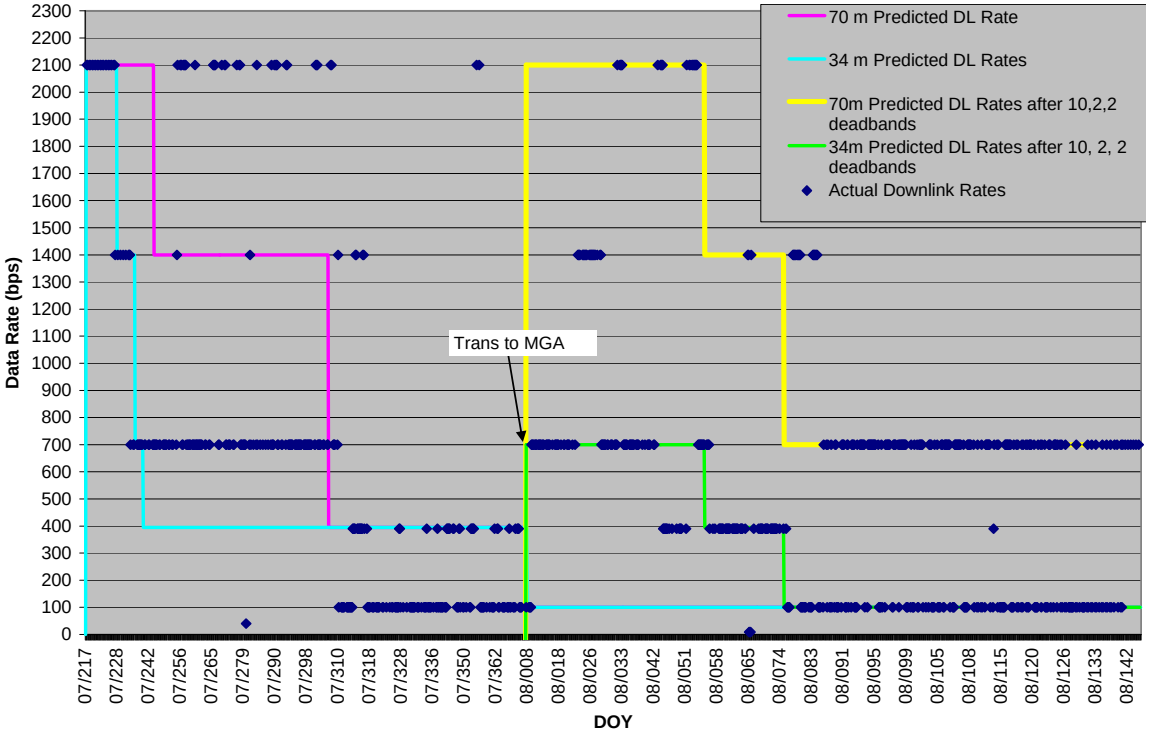

Figure 4-6 Predicted supportable data rates and actually used rates during cruise.

The original telecom predicts assumed the baseline attitude control deadbands, which greatly impacted the telecom performance. Based on these results, the mission made a decision to reduce and maintain deadbands of 10 deg in the X axis, 2 deg in the Y axis, and 2 deg in the Z axis. Telecom reassessed the data rate capability for this more stringent pointing, and 700 bps downlink rate was implemented throughout much of late cruise. Without the tighter deadbands and 70-m DSN coverage, the downlink could not have achieved higher than 100 bps downlink rate for the last 5 months of the cruise mission. This rate was not sufficient for monitoring the spacecraft during critical events.

4.2 UHF Performance during EDL and Surface Mission

4.2.1 EDL (UHF)

The Phoenix spacecraft arrived at Mars on May 25, 2008, targeted to a landing site at 68 deg northern latitude. Three active orbiters (Odyssey, MRO, and Mars Express (MEX)) were utilized to capture information during the Phoenix EDL. This section is summarized from [25].

Figure 4-7 depicts the arrival geometry, showing the orbits of the Odyssey, Mars Express, and MRO spacecraft. Due to the high latitude of the selected landing site and the high inclination of each of the orbiters, it was possible to adjust the true anomaly of each orbiter to allow all three to be in view of Phoenix during EDL.

Figure 1-7 shows the EDL profile of activities. Upon separating from the cruise stage 7 minutes prior to atmospheric entry, the Phoenix spacecraft began transmitting a UHF carrier signal through the wraparound antenna on the backshell of the entry vehicle. Two minutes prior to entry, Phoenix began modulating telemetry information on the UHF carrier at a rate of 8 kbps. This continued throughout the hypersonic entry phase, during which it was predicted that a short blackout period might be experienced due to the buildup of plasma around the entry vehicle. A little less than 4 minutes after entry, a parachute was deployed. At this point the lander increased its data rate to 32 kbps for the remainder of the descent. The data rate increase was primarily driven by a desire to reduce the latency between generation of onboard telemetry data and transmission of the telemetry. At an altitude of roughly 700 m, Phoenix throttled up its descent engines and completed a powered descent to the surface, landing roughly 7 min after entry.

The Phoenix relay support represented the first operational use of the MRO Electra UHF relay payload. Electra's software-defined radio architecture allowed post-launch implementation of a filtering strategy that mitigated electromagnetic interference (EMI) from several of the MRO science instruments, enabling MRO relay operations to be carried out without having to power off the relevant instruments**.**

During this entire period, the MRO spacecraft acquired a high-fidelity open-loop recording of the Phoenix UHF signal, using its multi-bit sampling to allow full recovery of the telemetry stream via post-processing on the ground [37]. This strategy provided the most robust approach to acquiring EDL telemetry. However, MRO is not configured to allow downlinking of data products from its Electra radio in real time.

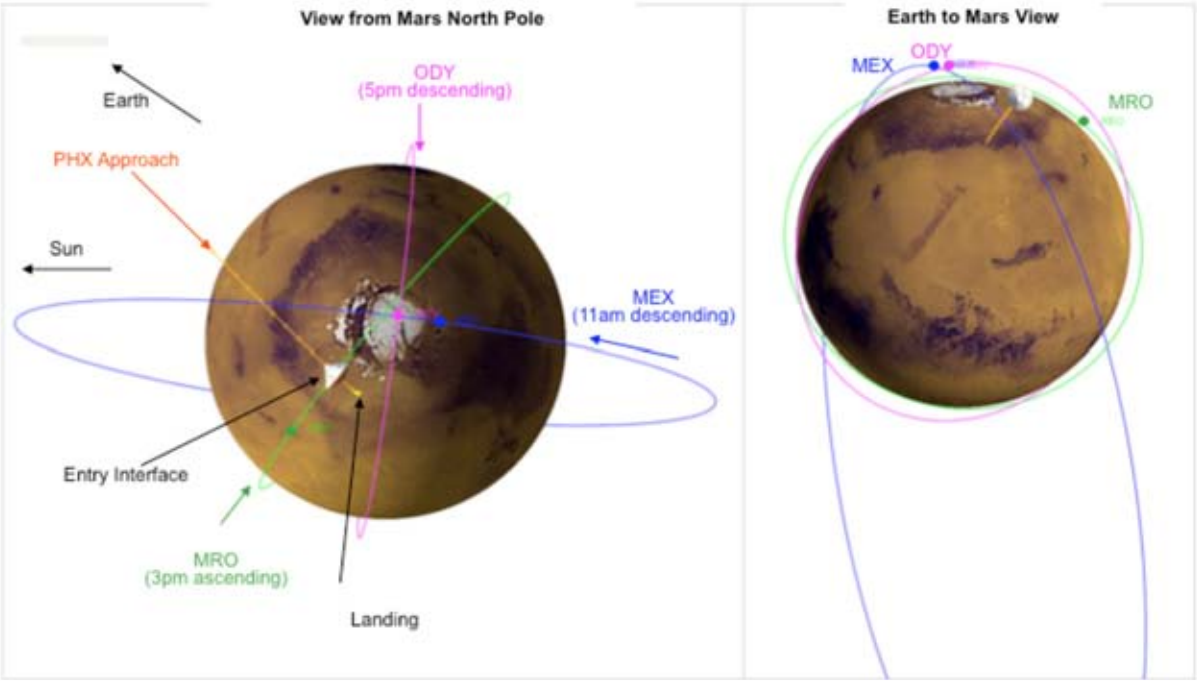

Figure 4-7 Phoenix arrival geometry.

By contrast, the Odyssey spacecraft was configured to provide real-time visibility into the Phoenix EDL. With support from the 70-m antenna at NASA's Goldstone Deep Space Communications Complex, Odyssey was able to maintain a downlink data rate to Earth of 124 kbps during EDL, sufficient to allow "bent-pipe" transmission of the Odyssey CE-505 transceiver relay data products, including both the recorded open-loop (canister mode) data prior to Phoenix parachute deployment and the 32-kbps demodulated Phoenix telemetry stream acquired after parachute deployment.

To provide the real-time status of the spacecraft before parachute deployment, ground software was configured to process the Odyssey/CE-505 canister mode open-loop samples (received from Odyssey at 85 kbps) and generate a spectrogram of Phoenix carrier amplitude and frequency.

After parachute deployment, the Odyssey link provided direct visibility of the 32-kbps Phoenix telemetry stream. The Mars Express Melacom payload was configured to acquire a 1-bit open loop recording of the Phoenix signal throughout EDL.

4.2.1.1 Phoenix EDL Communications "Firsts"

The design and implementation of EDL communications for the 2007 Phoenix Lander distinguished itself in a number of ways from previous Mars missions.

First, Phoenix EDL was observed by a total of four independent assets, three relay orbiters and one terrestrial ground station, providing unprecedented insight into this critical phase. Both, the Odyssey link and the DTE link allowed the mission control teams and the public to witness the EDL events unfold as they occurred; only delayed by the one-way light time. For the initial part of EDL, Odyssey sampled and downlinked spectral data from which Doppler information was extracted. After parachute

deployment, the orbiter locked onto and relayed Phoenix's 32-kbps signal, the highest data rate used during EDL for any of NASA's Mars missions to date.

Furthermore, the EDL communications implementation employed, for the first time, a sample and recording scheme onboard the orbiters instead of acquiring the signal directly. In the case of MRO, the open-loop recording allowed for the successful extraction of Phoenix telemetry on the ground. Moreover, because of the unprecedented high data rate, the amount of data collected in the later, more critical, parts of EDL allowed for detailed insight into the events unfolding during terminal descent.

The implementation approach also offered the opportunity for international participation. The European Space Agency’s (ESA's) MEX orbiter was used as an additional venue to observe the EDL events by recording spectral data for the entire duration of EDL. The flawless EDL planning, execution, and event observation is a testament to the successful collaboration among all the organizations.

Finally, the carefully crafted orbital choreography of the relay orbiters in support of EDL communications directly contributed to one of the most dramatic images in recent planetary exploration. MRO successfully captured the Phoenix spacecraft as it was descending beneath its parachute against the backdrop of Heimdal crater (Figure 4-8).

Figure 4-8 MRO Image of Phoenix descending beneath its parachute.

4.2.1.2 MEX

MEX was configured to acquire a canister mode recording of the Phoenix signal, providing monitoring of the carrier and spectrum. The MEX data was transmitted to Earth via the Mars Express lander communications (melacom) system immediately following EDL. Doing this required an exception to MEX operational rules constraining the duration before which the X-Band transmitter can be powered on safely after eclipse

exit). The spectrogram of the recorded signal (Figure 4-9) was available to JPL within about 1.5 hours.

In the spectrogram, the bright red line starting around 7 kHz after 345 s is the tone emitted from PHX during EDL. The PHX signal appears at about 345 s because Melacom was programmed to start recording 5min 45sec before the predicted AOS. Melacom never lost the RF signal during EDL. The possible “black out” period when Phoenix entered the atmosphere was not observed. The small irregularity on the signal line at 810 s shows a short stop in the Doppler shift and confirmed the opening of the parachute. The two green lines in the spectrogram show the corridor in which the frequency was expected. The 3-kHz offset from the actual had also been observed during the previous MEX-MER test campaign and is possibly caused by an inaccurate knowledge of the Melacom reference oscillator frequency due to oscillator aging.

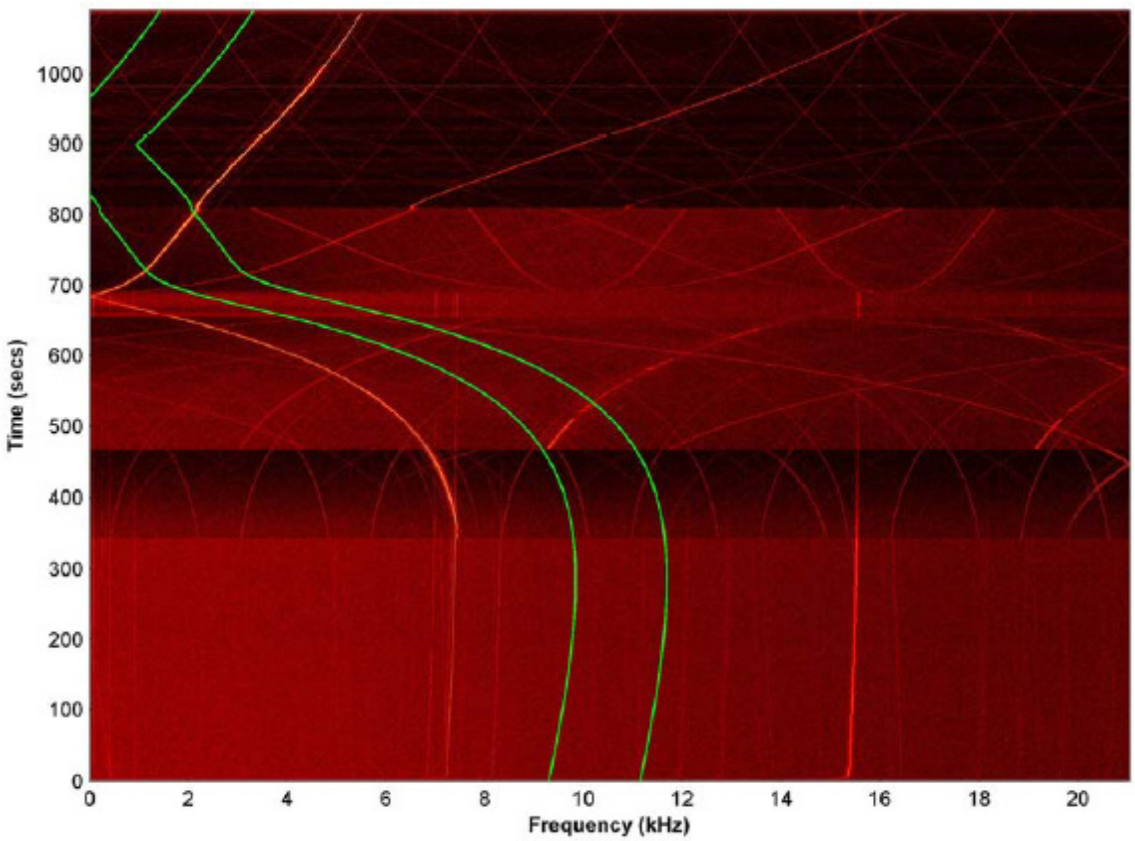

Figure 4-9 MEX Melacom recorded open loop RF spectrum during Phoenix EDL.

4.2.1.3 UHF DTE to Green Bank

In addition to the orbiters, the 100-m Green Bank Telescope in West Virginia was configured to receive the Phoenix UHF transmission during EDL. The received signal was far too weak to enable extraction of the Phoenix telemetry, but it was sufficient to allow real-time detection and monitoring of the Phoenix UHF carrier signal throughout EDL. A radio science open-loop receiver was operated in a predict-driven mode

compensating for Doppler; thus, dynamic activity was not expected to degrade the link. According to preflight link analysis, the expected SNR of this link during the period around peak heating was very weak at or near the threshold level (1 to 2 dB).

An outage in the signal strength data was observed at Green Bank during the predicted blackout period (between roughly 64 s to 120 s) [38]. This outage, discussed in more detail in the next section, can be attributed to the very low SNR of the received signal at Green Bank. The assessment of performance at Green Bank was based in part on the knowledge of the attenuation levels that were measured and predicted for the three links from the lander to the orbiting spacecraft.

Figure 4-10 and Figure 4-11 show the predicted Doppler frequency shift and the predicted received signal level (carrier-to-noise ratio) at Green Bank during EDL [39].

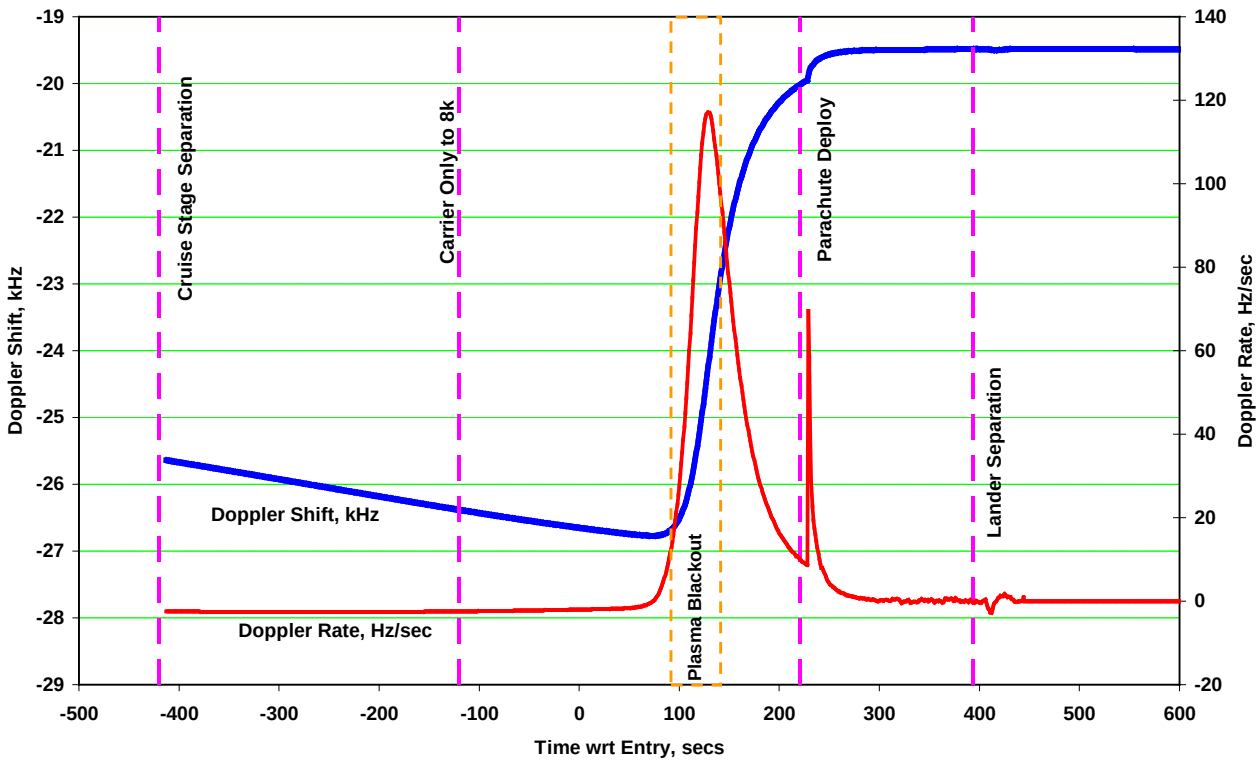

Figure 4-10 Phoenix to Green Bank predicted Doppler.

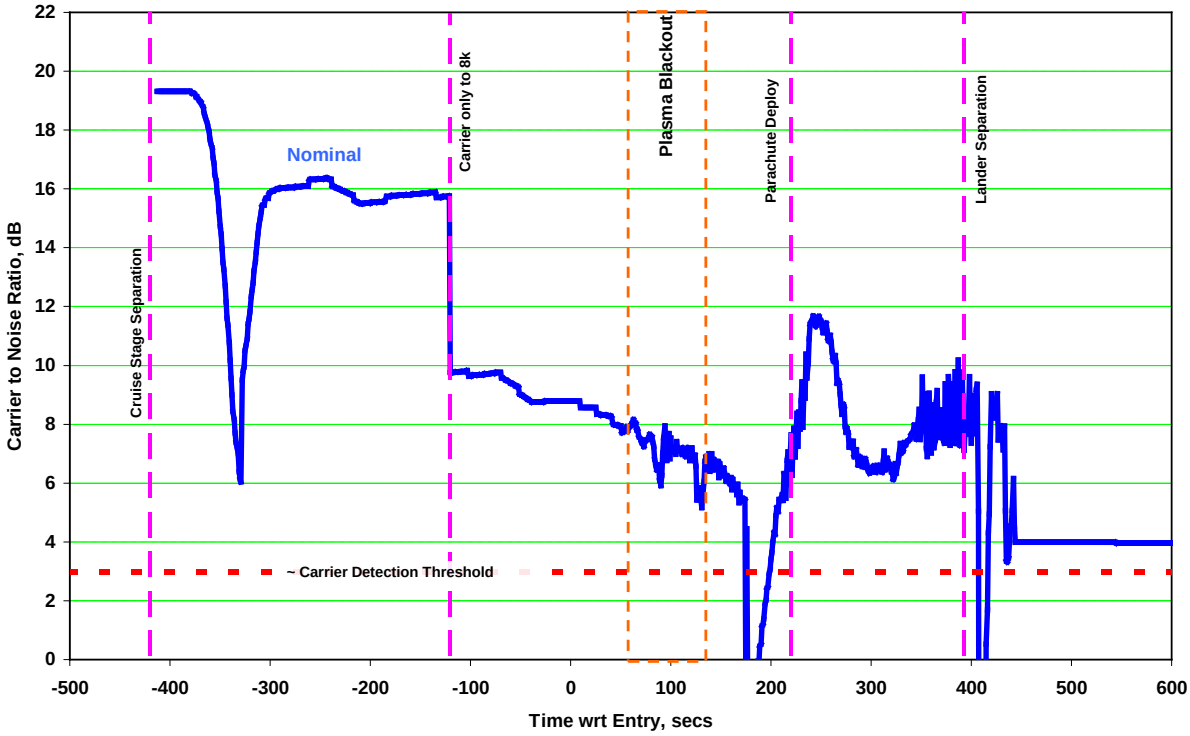

Figure 4-11 Phoenix to Green Bank predicted carrier to noise ratio.

4.2.1.4 "Brownout" to Orbiters Near the Time of Maximum Heating

This descriptive summary is from [38]. During planetary atmospheric entry at hypersonic velocities, a spacecraft is enveloped by a sheath of ionized particles as a result of the dissociation and subsequent ionization of the atmospheric gases (for Mars, 97 percent CO_2 and 3 percent N_2 by mass in the free stream, the region where atmospheric pressure, temperature, and relative velocity not yet affected by the passage of the Phoenix through it) as they are heated and compressed by the shock or heated within the adjacent boundary layer. When the electron number density traversing the signal path gets sufficiently high, communications can become disrupted. The degradation takes the form of added attenuation or even total signal loss (blackout) at the receiver, caused by reflection or absorption of signal energy at the link frequency.

Previous studies of Mars entry blackout suggested that there was a greater potential for a communications blackout during peak heating at the 401-MHz Phoenix return-link frequency. Preflight predictions of an expected blackout of the link suggested a 1 ± 1 min outage period centered around the time of peak heating. The outage period was thus predicted to range from no outage to a maximum of 2 min, assuming conservative uncertainties believed to be the case during early preflight analysis. These bounds assumed most-favorable and worst-case assumptions of the entry parameters.

In actuality, Phoenix entered the Martian atmosphere on May 25, 2008, and did not suffer a signal outage to any of the three orbiter relay links during the period around peak heating. During postflight analysis, a close inspection of the received signal data revealed significant fades (brownout) that coincided with high levels of electrons that enveloped

the vehicle during the period around peak heating, as predicted by the aerothermodynamic entry analysis.

Figure 4-12 shows the cone angle, theta, from Phoenix to MRO, Odyssey, and MEX. The wraparound UHF antenna used for communications during the EDL phase, which includes atmospheric entry, was shown in Figure 2-30 with theta in the horizontal axis.

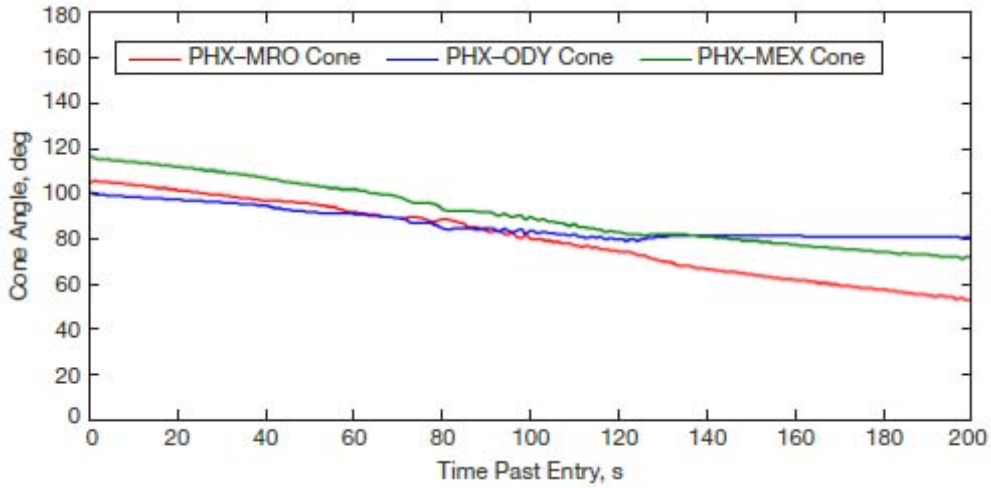

Figure 4-12 Cone angle (theta) from Phoenix to each of three orbiters during EDL.

The MRO signal levels presented in Figure 4-13 were estimated from processing of the in-phase (I) and quadrature (Q) samples of the carrier that were recorded onboard MRO at a 150-kHz rate and telemetered to Earth on the 8.4-GHz (X-band) DTE link. The processing of the samples involved performing fast Fourier transforms (FFTs) at 1-Hz bin resolution. Similar processing techniques were applied for the Phoenix-to-Odyssey and Phoenix-to-MEX data sets.

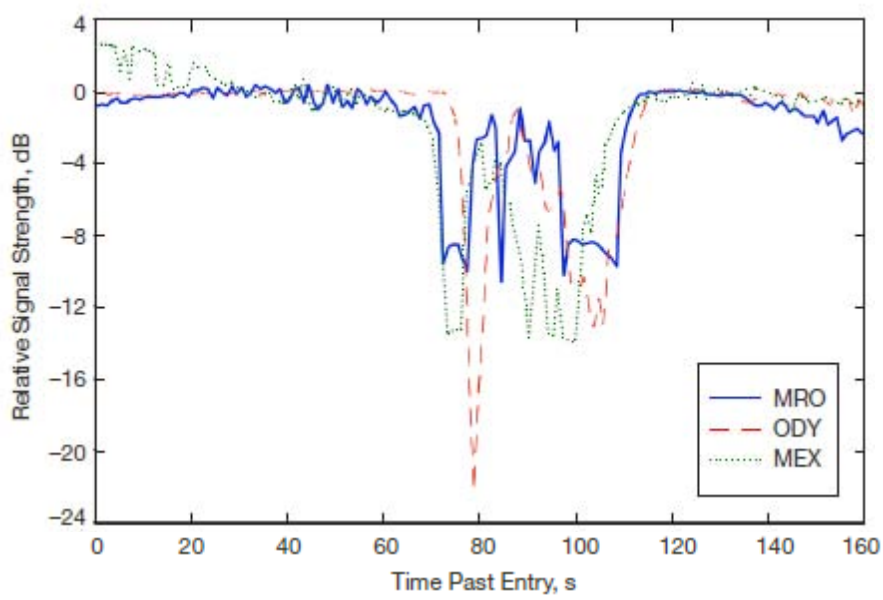

Figure 4-13 Relative signal strengths for Phoenix-to-orbiter links.

The complex nature of the variations seen between 70 and 110 seconds in Figure 4-13 may be due to a combination of the signal path traversing different regions of electron number density as the antenna aspect angle changes, changes in electron number density itself due to turbulence about the vehicle, as well as possibly a small amount of unmodeled response of the activated automatic gain control (AGC) circuitry in the MRO Electra radio to received signal level changes.

4.2.2 Surface (UHF Relay)

After landing, Phoenix began a surface mission that had a planned duration of 90 Martian days (sols). In fact, Phoenix operations continued well beyond 90 sols before the lander succumbed to the shorter days and reduced power as Martian winter approached. On sol 152, the lander's fault protection software triggered a safe mode, and over the next several sols the lander experienced a number of low-energy faults. The last UHF contact occurred on sol 157 [21].

As summarized from [25], the nominal surface relay plan incorporated operational support from Odyssey and MRO, with ESA's Mars Express available as a backup relay asset in the event that the NASA orbiters became unavailable for any reason. The Phoenix mission placed the following requirements on the relay communications network:

- Deliver 1 Mb of command data over the forward link to Phoenix during the Martian morning (between 02:00 and 07:00 local mean solar time, LMST).
- Acquire 30 Mb of telemetry data over the return link from Phoenix during the Martian afternoon/evening (between 12:00 and 19:00 LMST).
- Acquire an aggregate data volume of 60 Mb of telemetry data over the return link from Phoenix, based on two or more passes each sol.

Table 4-1 shows pass durations, intervals between passes, and number of potential passes per day for overflights of Phoenix by each of the three Mars orbiters based on potential landing sites at three different latitudes: 65 deg, 70 deg and 72 deg N. The actual landing site landing latitude was 68 deg N.

Table 4-1 UHF pass statistics for MRO, Odyssey, and Mars Express.

Event	Phoenix-to-MRO			Phoenix-to-ODY			Phoenix-to-MEX		
	65N	70N	72N	65N	70N	72N	65N	70N	72N
Pass duration (minutes)	8.11	8.07	7.85	10.73	10.70	11.00	28.23	25.39	24.37
Pass revisit time (hours)	4.23	4.17	3.48	3.51	2.49	2.27	4.32	7.19	6.76
Total daily visibility (hours)	0.57	0.75	0.86	1.15	1.60	1.78	1.27	1.33	1.35
Passes per day	4.2	5.6	6.6	6.5	9.0	9.8	2.7	3.1	3.3

Figure 4-14shows the use of both strategic and tactical planning for surface operations, similar to the approach being used with the Mars rovers. Strategic plans were planned in two-week chunks, while tactical plans were for individuals sols.

Figure 4-15 shows the daily operations cycle, with the sol beginning with an early morning relay contact to deliver commands to the lander for the upcoming sol's activities.

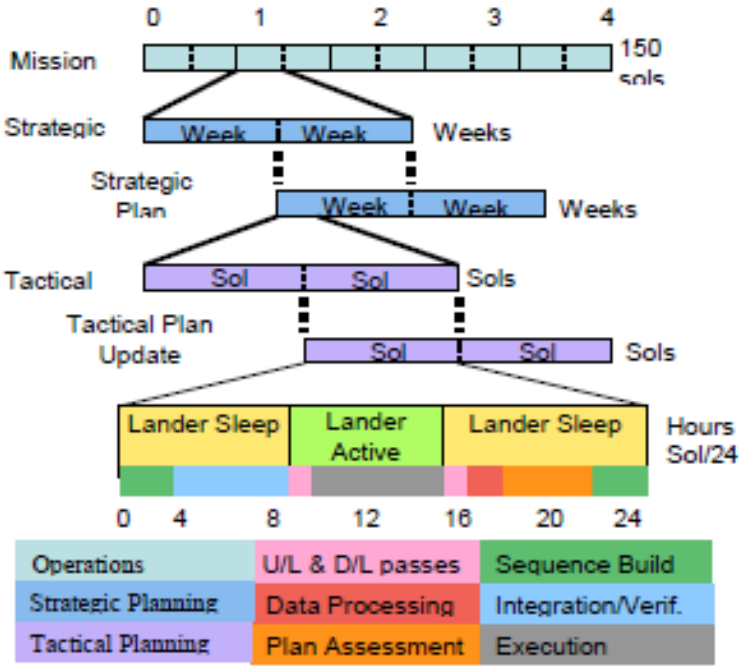

Figure 4-14 Phoenix surface operations concept.

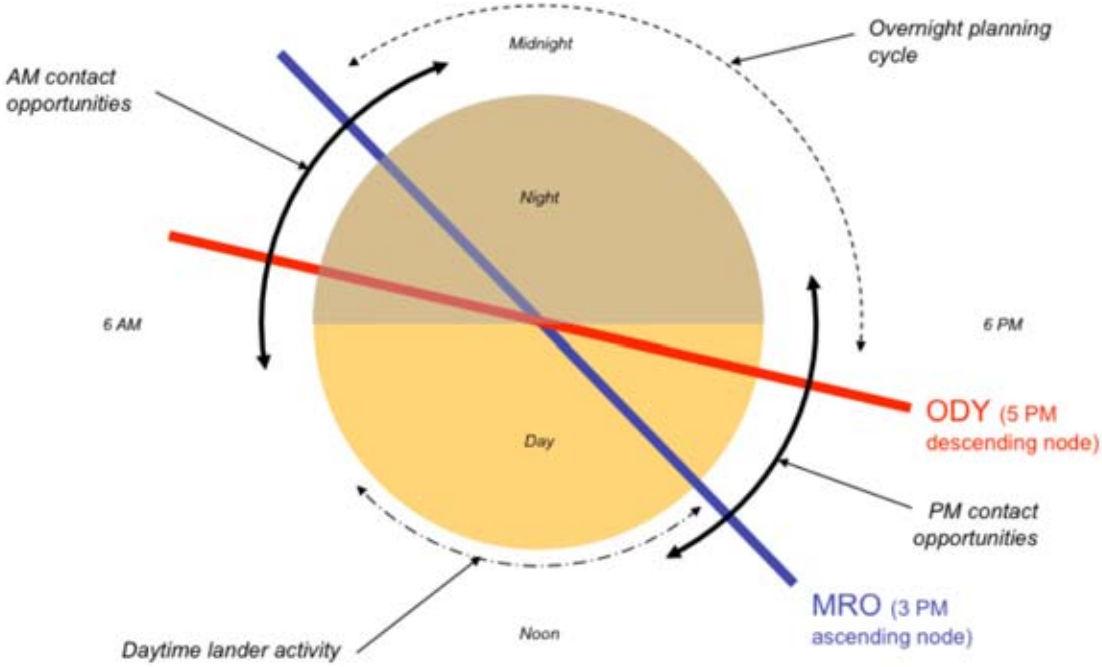

Figure 4-15 Overview of daily operations cycle with Odyssey and MRO relays.

Lander science activities were typically conducted in the middle of the day, with the high solar elevation providing maximum power and offering the best illumination of the science workspace. In the afternoon and early evening, science and engineering measurements gathered during the sol were returned.

During the Martian night, data from the prior sol was used to establish the science strategy and, ultimately, the detailed command sequences for the next sol. Because of this, it was critical that the end-to-end latencies for forward and return-link data delivery were minimized, with the following goals.

- Forward link: assuming the availability of DSN coverage for the given orbiter, Phoenix should deliver command products destined for the lander to the Odyssey or MRO ground data system as late as 2 hr prior to the relay pass during which those products would be transmitted.
- Return link: assuming DSN coverage, any Phoenix telemetry received on the return link during an Odyssey or MRO relay pass should be returned to Earth and delivered to the Phoenix ground data system within 1 hr, not including any additional delay due to occultation of the orbiter downlink by Mars.

During actual operations, latencies well below these were routinely achieved.

The helix and monopole UHF antenna combination worked well to cover Orbiter over-flight geometry. The tactical selection of antenna increased data return. The monopole significantly outperformed the helix antenna for low elevation (< 20-deg) passes particularly in the "northwest" region of the lander. The omni-directional circularly polarized pattern of the helix antenna more consistently matched the data volume predicts and outperformed the monopole for the high elevation over-flights. The combination of the surface effect on the monopole pattern and the variability of the polarization loss, made the predicted data volumes much less reliable. Consequently, the helix ended up being the workhorse on the surface. If the lander had experienced a failed antenna or a failed coaxial switch, the second antenna would have been critical to maintaining the mission. Data volume predicts were adjusted based on trend data with some success, but fine tuning volume for passes just above threshold was not possible.

4.2.2.1 Odyssey Return-Link Performance

This section compares a set of Phoenix lander return-link actual data volumes through Odyssey against predicted data volumes for the overflights. The comparisons are for overflights that occurred between July 8 and August 7, 2008. The predicted data volume for each overflight is based on one of four criteria: mean predicted link performance ("0-dB margin"), and performance that is 1- to 3-dB worse than mean ("1-dB margin", "2-dB margin", and "3 dB margin"). The 0-dB case predicts the largest return-link volume, and the 3 dB case predicts the smallest.

Table 4-2 summarizes the comparisons. In the top section of the table, two comparisons are made for each prediction criterion: first, the percentage of Odyssey overflights in which the actual data volume was less than predicted, and second, the percentage of overflights in which actual data volume was more than 10 percent less than predicted. The right column shows the results: for the most optimistic ("0-dB margin") prediction, 27.45 percent of the Odyssey overflights returned less than the predicted volume and 7.84 percent returned an amount more than 10 percent below predicted.. The remaining pairs of rows show comparable statistics for the other margin criteria (1 dB, 2 dB, and 3 dB).

The bottom section of the table provides other statistics, including the percentage of overflights within 10 percent of the predicted volume – or greater - and the average

percentage that the data volume was over the predicted volume. For example, with a 2-dB margin policy, column 2 of the bottom section shows that the 2-dB margin policy resulted in 98 percent of the overflights returning data volumes no lower than 10 percent below the predicted volume. Column 3 shows the 2-dB policy produced predicts such that the data volume returned was an average of 17.8 percent greater than predicted.

The statistics in this table were produced after-the-fact, with the actual return-link data volume known for each sol. Though these statistics were developed too late to affect Phoenix UHF link planning, they provide a starting point or a sanity check for planning surface relay communications criteria for other Mars missions.

For current (MER) or future (MSL) surface missions, such statistics would be a starting point for configuring and predicting data volumes for future groups of sols. The objective, for a group of sols, would be to tweak the predictions to bring the predicted and actual data volumes closer together without increasing too much the risk of the actual volume being much lower than predicted on any given sol.

Since the end of the Phoenix mission, MER has updated the prediction program GTP so that configuration options (such as the margin policy and the orbiter roll angle) are maintained in a table under configuration control by telecom, but with trade-off options (such as rover orientation (yaw, pitch, roll), orbiter selection (Odyssey or MRO), and minimum elevation angle at the rover that can be entered by the planner. The trade-off predictions can be made for future or previous passes. The latter would be chosen for comparison with actual return-link volume. In the MER update, the predictions are shown as individual curves and tabulations for each available data rate, margin policy, and elevation angle criterion. Sets of data similar to these tables have resulted in updates of the margin criteria and elevation angle criteria for rover passes with MRO.

Table 4-2 UHF data volume (DV) comparison with predictions (30-day period with Odyssey).

Margin applied to model (dB)	Two Types of Deficiencies Analyzed	Percentage of Total Overflights with Data Volumes below Predicts (%)
0	Actual DV is below predict	27.45
0	Actual DV is more than 10% below predict	7.84
1	Actual DV is below predict	19.61
1	Actual DV is more than 10% below predict	3.92
2	Actual DV is below predict	9.80
2	Actual DV is more than 10% below predict	1.96
3	Actual DV is below predict	1.96
3	Actual DV is more than 10% below predict	0.00

Margin applied to model (dB)	Percentage of Overflights with Data Volumes better than 10% below Predicts (%)	Average Actual Data Volume over Predict (%)	Standard Deviation of Actual Data Volume over Predict (%)
0	92.16	7.48	16.98
1	96.08	11.66	17.15
2	98.04	17.83	17.71
3	100.00	27.84	19.46

4.2.2.2 MRO Return-Link Performance

The MRO predicts were less conservative than the Odyssey predicts. The MRO data volume trend data proved that on average, the predictions were extremely accurate, but the variability from pass to pass was significant.

Table 4-3 summarizes the average data volume delta between the predicted return volume and the data volume reported by the MRO scorecard in both a percentage and volume in megabits. With a 10-deg horizon mask applied, the telecom model was predicting on average within a quarter of a percent of the actual data volume returned. Unfortunately, during 25 percent of the overflights, the return data volume reported by the scorecard was more than 10 percent below the prediction.

Table 4-3 Comparison of Phoenix-MRO return link predicted and actual data volumes.

10 deg mask		
Average Data Volume Delta (%)	Average Data Volume Delta (Mbits)	Percentage of passes more than 10% below predict
-0.22%	0.26195	25.00%
15 deg mask		
Average Data Volume Delta (%)	Average Data Volume Delta (Mbits)	Percentage of passes more than 10% below predict
13.13%	6.8385	3.75%

Figure 4-16 displays the variability in return data volume versus prediction through MRO for a 60 sol period over the mission.

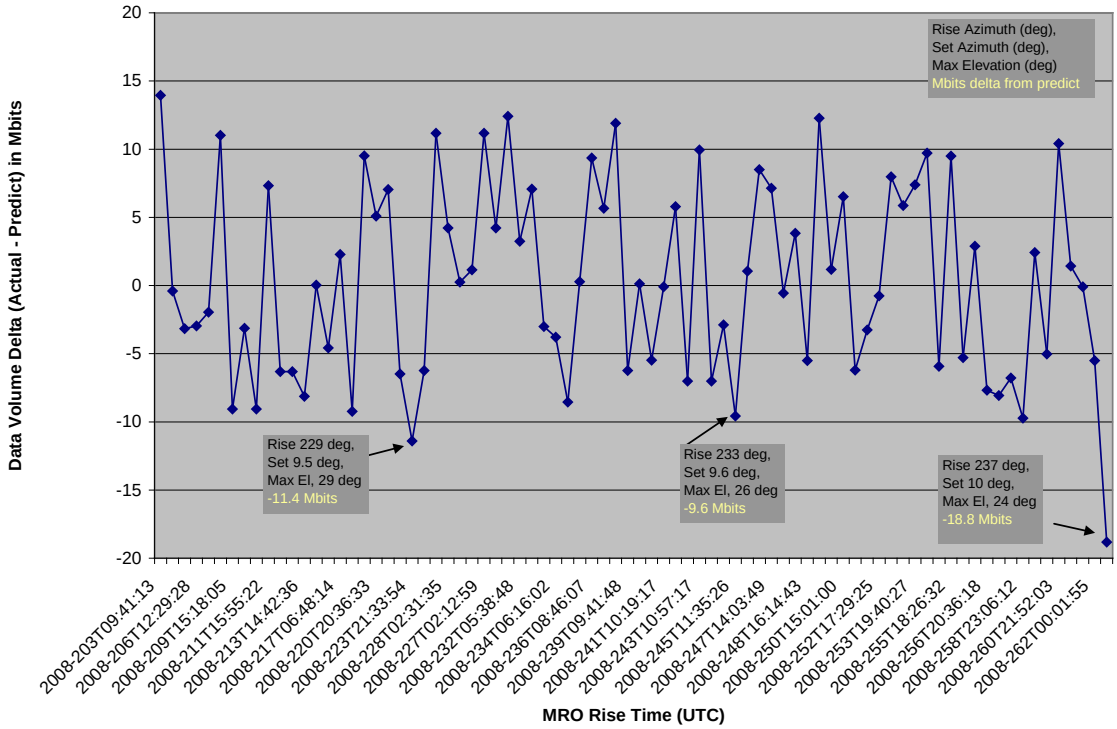

Figure 4-16 Phoenix-MRO return-link data volume residual (actual minus predicted).

The telecom model could have been – but was not – adjusted with more conservative MRO receiver threshold assumptions. The Phoenix science team was presented with this actual versus predicted data which assumed a 2-dB margin policy. They opted to leave the model alone and proceed to plan to a 10-deg horizon mask. The logic behind the decision was that the Odyssey telecom model was conservative enough to guarantee the planned data volume would be returned, so it was not necessary to apply the same conservatism to MRO. The scientists decided if they were depending on a critical

volume of data through MRO, they would still use the existing 2-dB margin criterion, but they would plan a 15-deg minimum elevation in lieu of the standard 10-deg mask.

4.2.2.3 Sol by Sol Return-Link Performance (Both Orbiters)

The mission requirement was to forward link 1 Mb per sol in a single overflight between 2 AM and 9 AM Mars local solar time and return 60 Mb per sol total transmitting 30 Mb of data in a single overflight between 12 PM and 7 PM local solar time. These volumes included transmission and encoding overhead (but not Proximity-1 protocol overhead).

Figure 4-17 shows the sol-by-sol data return (Odyssey values in blue and MRO in red). Compare these with the requirement of 60 Mb per sol. Only when the Phoenix spacecraft was in safe mode was this requirement not met.

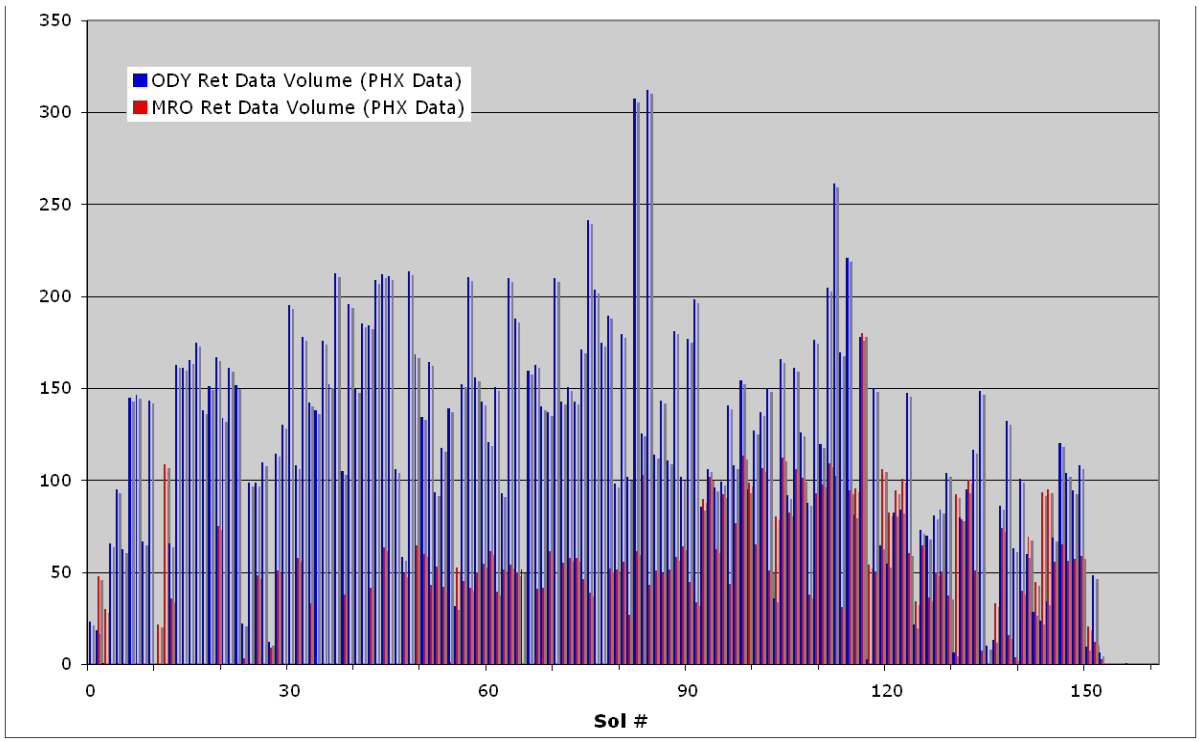

Figure 4-17 Return-link data volume per sol compared with 60 Mb requirement.

Although the commanding requirement was only 1 Mb per sol, once the UHF link capability was characterized, the uplink bundles regularly totaled between 1 and 2 Mb without issue. The Odyssey AM passes were increased to 32 kbps forward-link rate, which gave the science team an average 12 Mb forward-link capability, which rarely needed to be fully utilized.

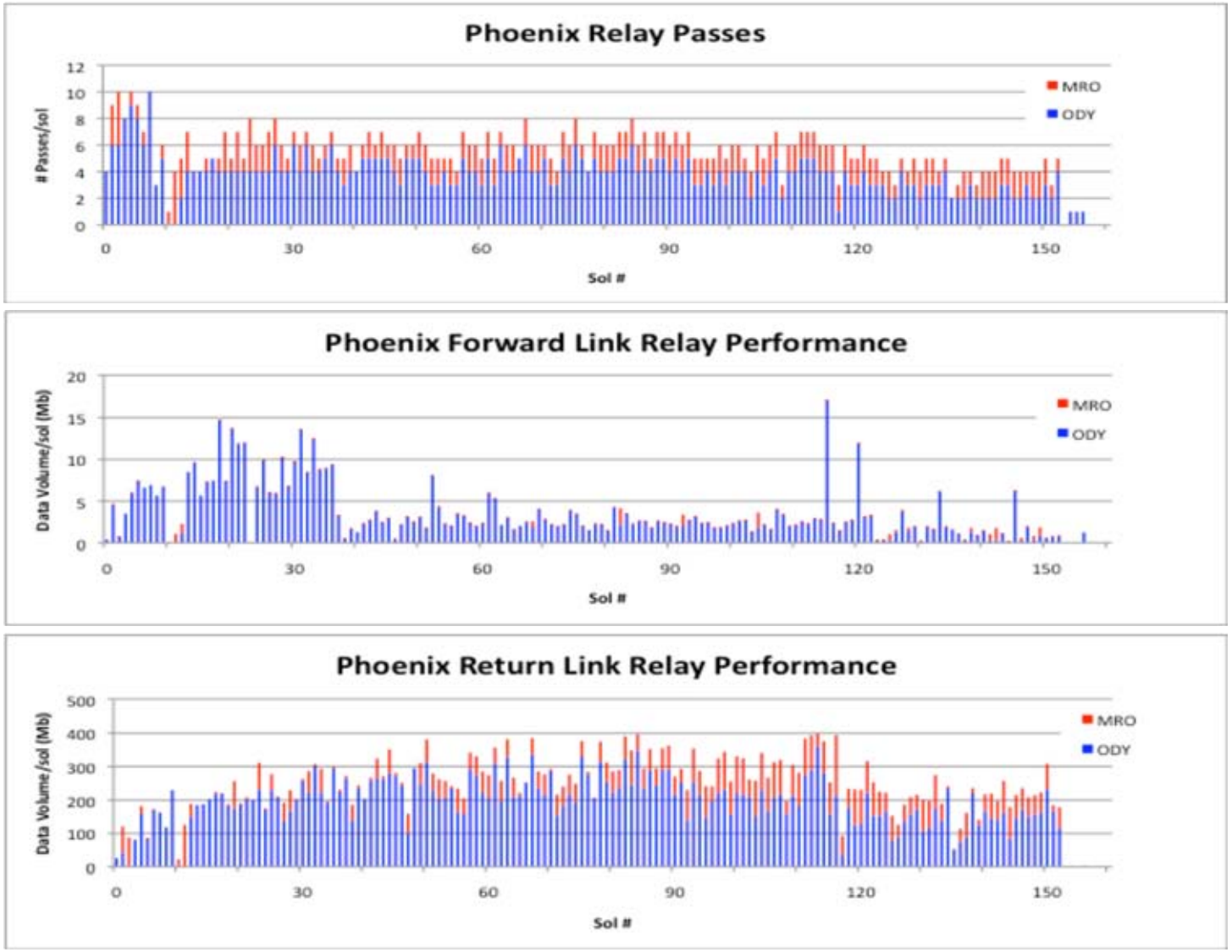

Figure 4-18 Relay metrics: (top) number of passes per sol, (center) forward-link performance, (bottom) return-link performance.

Figure 4-18 from Ref. [25] provides three sets of relay metrics for the two orbiters shown together. From top to bottom, these are the number of relay passes per sol, forward-link data volume, and return-link data volume. Over the 157-sol landed mission duration, Odyssey and MRO supported 860 relay passes for an average of more than 5 passes per sol. Odyssey provided the majority (71 percent) of the relay contacts. Phoenix limited its use of MRO to no more than two passes per sol, given that MRO was still in the midst of its primary science mission at this time.

A total of 574 Mb of command data was delivered to Phoenix. The vast majority (97 percent) of the command traffic was handled by Odyssey. On the return link, Phoenix returned more than 38 Gb of data via Odyssey and MRO over the duration of the surface mission. This is an average of 242 Mb/sol, more than four times the 60 Mb per sol requirement.

4.2.2.4 Mars Express

The availability of MEX for backup or contingency relay support provided important risk mitigation, given the UHF-only nature of the PHX mission. Because of its elliptical orbit, Mars-Express could provide complementary contact opportunities with Phoenix to MRO and Odyssey. Figure 4-19 shows the overflight durations for 0-deg and 10-deg minimum elevation angles to MEX from Phoenix [37].

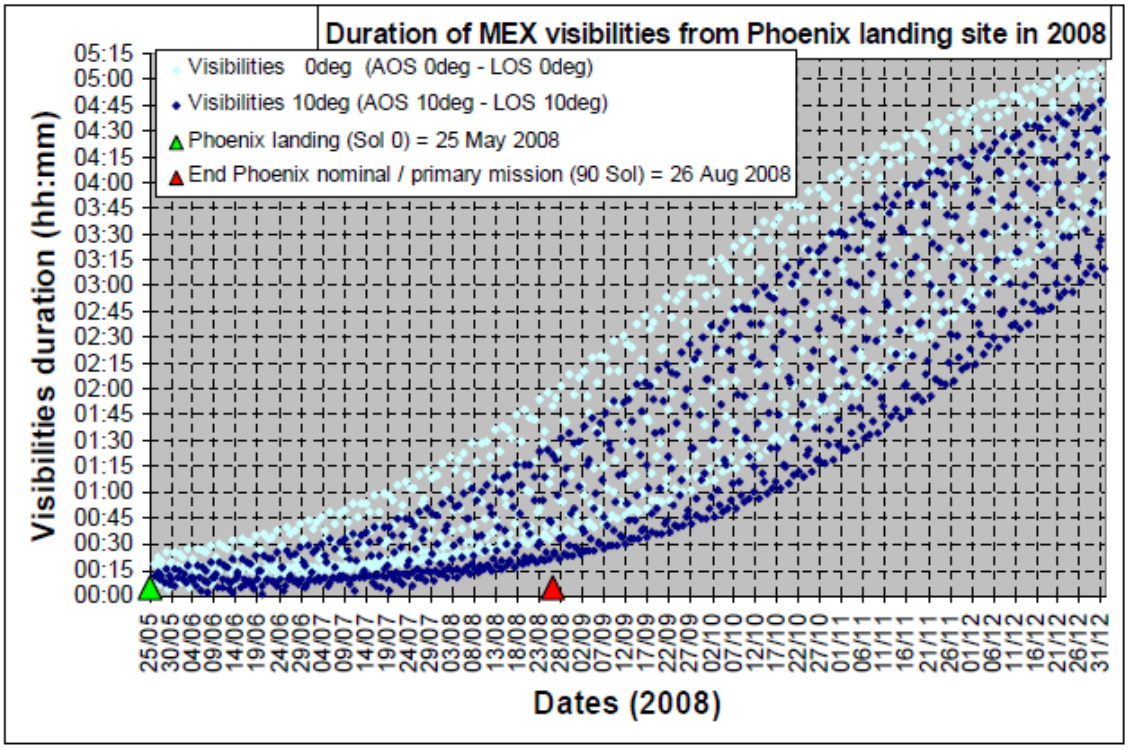

Figure 4-19 Overflight durations between MEX orbiter and Phoenix.

Mars Express was not used routinely to support Phoenix during the surface mission. However, MEX did receive the 1-way link during a portion of EDL. A demonstration pass with MEX was successfully conducted on the third sol of surface operations. This

pass verified Mars Express's capability to provide relay support to Phoenix. The pass was configured for an 8-kbps forward-link rate and a 32-kbps return-link rate. Several other MEX demonstration passes were conducted during the mission.

The Mars Express project proposed to Phoenix 15 contact opportunities during over-flights in the critical first week on the Martian surface. MEX was configured to be available to provide relay support assuming a nominal landing or open-loop recording if needed. To invoke any of these booked passes, even at short notice, the Phoenix project would only need to provide each time, a direct operations request (DOR) file to the MEX project in time for uplink to the MEX spacecraft. This would also demonstrate Mars Express relay capability for Phoenix, which might become useful if one of the NASA orbiters were to become unavailable. For any of these passes Mars Express would reuse a special lander pointing tested in 2008 with the rover Opportunity, which directs the Melacom antenna to bore-sight within 35 deg towards the landing site in order to optimize the RF link budget between lander and orbiter.

After the successful landing, 3 of those 15 passes were updated in two "RTN Link only" and one "FWD&RTN Link" pass to demonstrate MEX lander relay capabilities. For this the Phoenix team sent an updated DOR to MEX mission control via a data interface and notified the MEX flight control team. This DOR was uplinked to Mars Express according to procedure during the next ground station pass. A subsequent confirmation e-mail notified the PHX team of the successful update. Table 4-4 summarizes these overflights.

Table 4-4 Summary of Phoenix-MEX passes on doy 2008-149, -151, -152.

DOY	PHX SOL	Forward-link rate	Return-link rate,	Return-link volume, Mb	Notes
2008-149	3	32 kbps	8	29.96	Continuous above 10 deg elev
2008-151	5	none	32	14.48	Dip in AGC at high elev (Phoenix antenna pattern?)
2008-152	6	none	128	62.04	Strongest AGC at MEX of the three overflights

Figure 4-20 shows the link geometry for the Phoenix-MEX return link on doy 2008-152, and Figure 4-21 shows the resulting return-link performance at 128 kbps [40].

4.2.2.5 Determining Lander Position with Doppler

Observations of the Doppler shift on the UHF relay link also demonstrated the power of this radio metric observable to quickly provide high-accuracy in situ positioning for Mars relay users; Doppler data from just a handful of UHF overflights provided nearly three orders of magnitude improvement in the lander position knowledge relative to a solution based on pre-entry DSN tracking and inertial measurements during EDL.

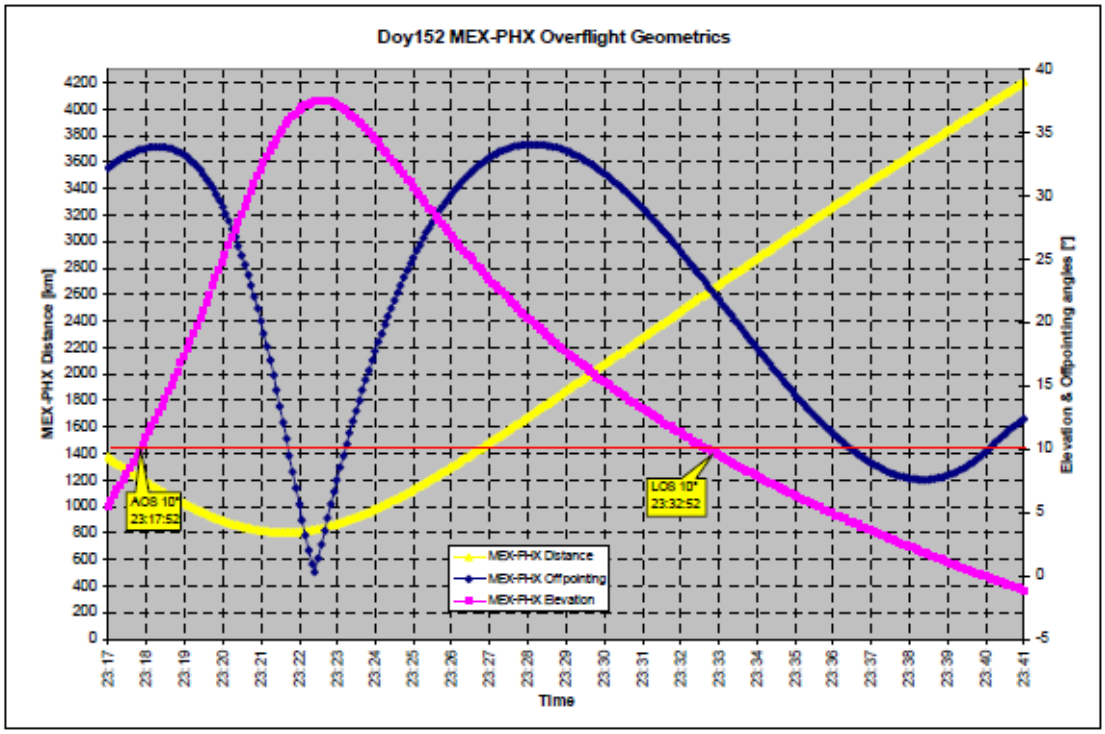

Figure 4-20 Phoenix-MEX distance, elevation angle, and off-boresight angle on doy 152.

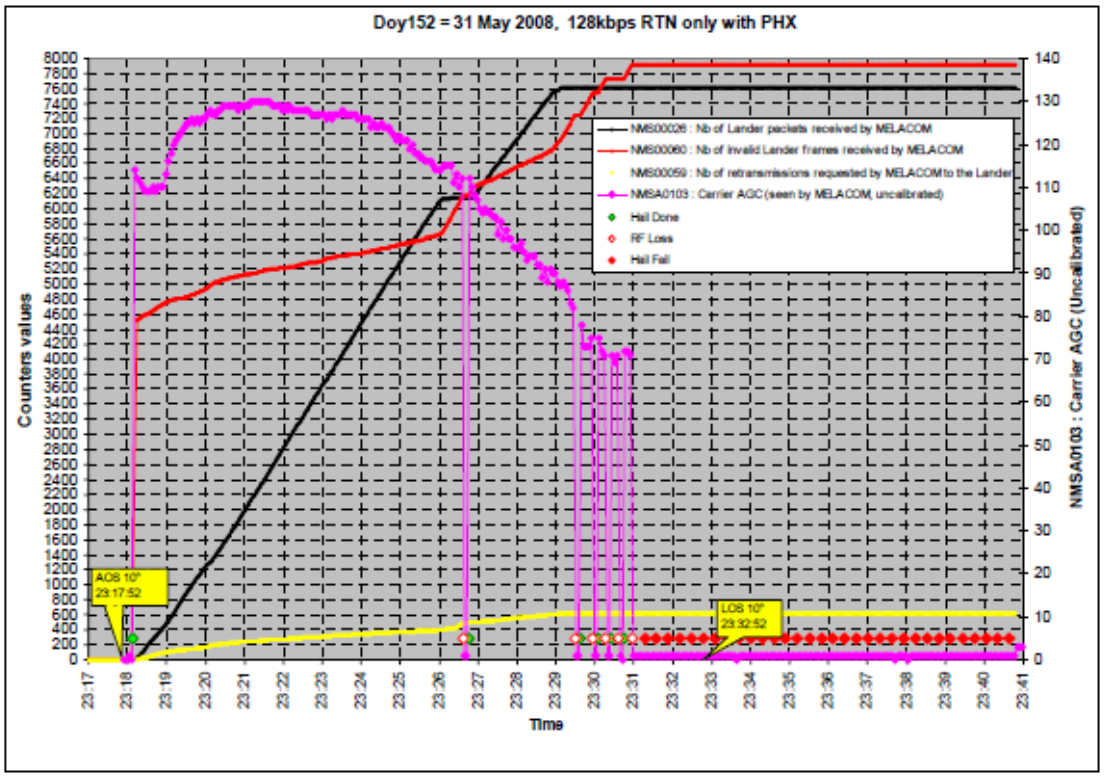

Figure 4-21 Phoenix-MEX return-link performance on doy 152.

5 Flight Operations

Data flow was described in Ref. [13] for forward and return links of Mars surface vehicles such as the Mars Science Laboratory and the Phoenix Lander with the NASA orbiters (Odyssey and MRO). This section describes the data flow with the Mars Express orbiter.

5.1 Phoenix-MEX Mission Operations System

This section is summarized from [40]

5.1.1 Overflight Planning and Forward-Link Concept

The interface concept shown in the Figure 5-1 flow diagram was mainly driven by the need for the MEX 3-month planning cycle to be combined with the Phoenix 3-day cycle.

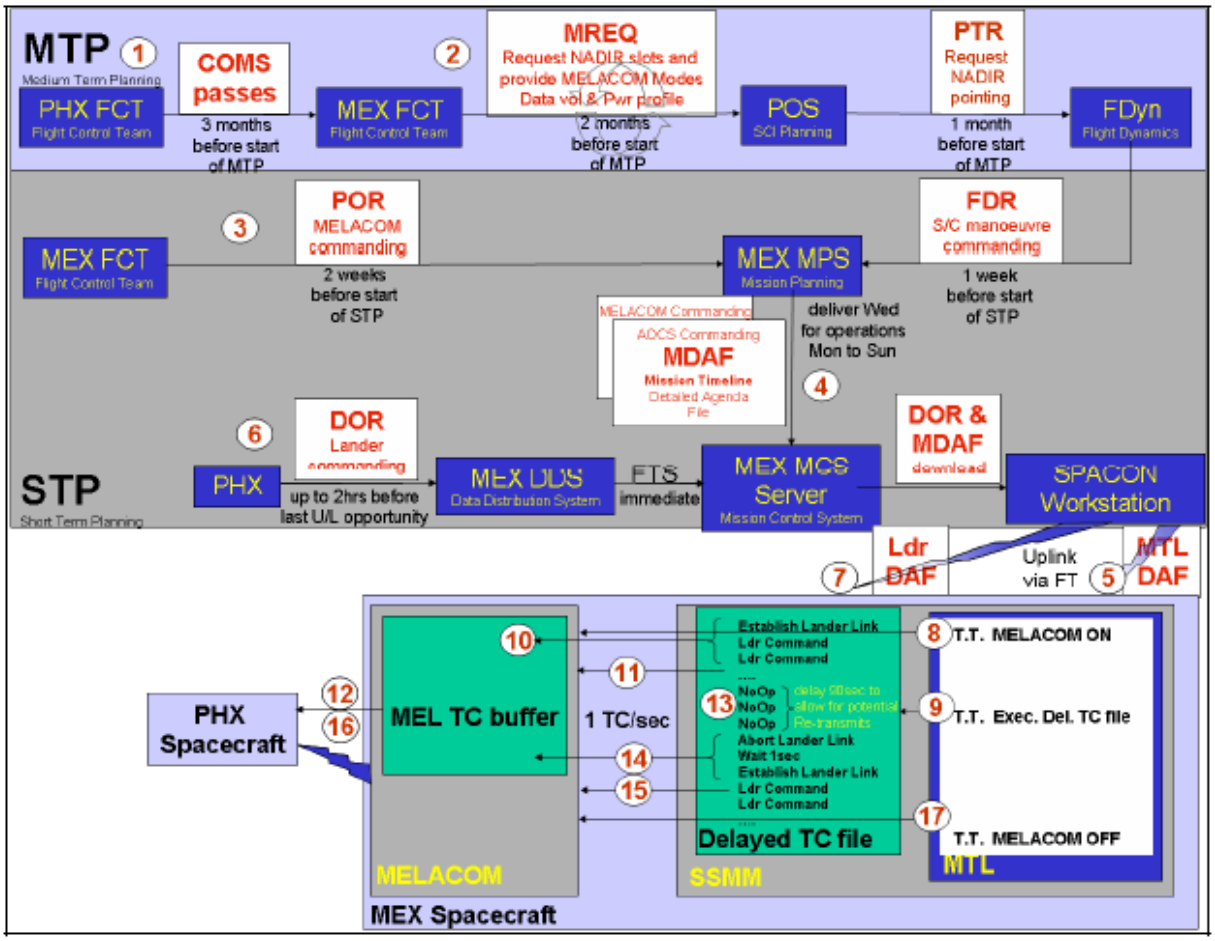

Figure 5-1 MEX-to-Phoenix overflight planning and forward-link concept.

Details of each of the numbered steps in the diagram are in Ref. [40]. In the following sentences, the numbers correspond to those in the figure. In greatly condensed form, the activities began 3 months before the overflight with Phoenix providing a selection of

overflight windows, including start/end times, during which MEX might be asked to support (1). Two months before the overflight, the European Space Operations Centre (ESOC) determined MEX pointing angles to support the link (2). Parameters were made the final two weeks before (3), and ESOC generated command files 1 week before (4). No later than 2 hours before the last uplink opportunity, Phoenix deposited a DOR command file (6). The MEX operator uploaded the file (7). At the start time for the overflight, the Melacom was switched on from the mission timeline (8) and the DOR command was triggered (9). The Melacom established the RF link with the lander (11), and cycles, each consisting of "abort RF Link & wait 1sec", "establish RF Link", "filling MEL TC buffer", "wait for potential re-transmits" occur (13–16). At the window end, Melacom was switched off, automatically aborting the RF link to the lander (17).

5.1.2 Telemetry

Figure 5-2 is a flow diagram of the Phoenix telemetry processing systems, with components located at ESOC, JPL, and onboard the Phoenix and MEX spacecraft.

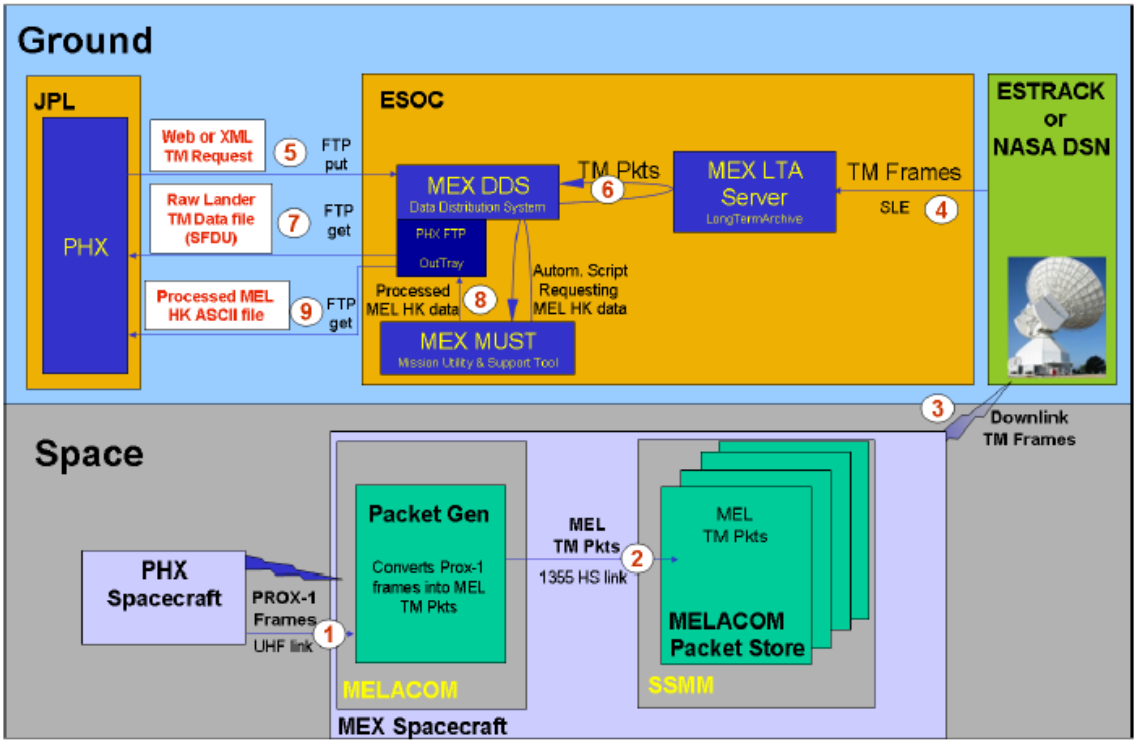

Figure 5-2 Phoenix-MEX telemetry interfaces. (Note: The circled numbers are procedure steps in Ref. [40].)

Return-Link-Only pass: While an RF Link was established between Melacom and a lander, the incoming Prox-1 frames, containing lander telemetry were wrapped into Melacom telemetry packets. Depending on the size of the received Prox-1 frames, Melacom packed one or several lander frames into one telemetry (TM) packet and added a Pkt Header with a dedicated (lander specific) application identification (APID) and generation timestamp.

Canister pass: When Melacom was configured to record an open-loop RF spectrum, the system sampled the received RF frequency at a certain rate and generated the Melacom telemetry packet with the lander specific APID and time stamped the packet.

In both cases, the telemetry was stored on MEX until the next scheduled station pass. At the time of downlinking, the recorded Melacom telemetry packets (TM Pkts) were wrapped into VC1 transfer frames and were downlinked to a ground station which could be either ESA or NASA DSN.

The TM frames received on Earth were routed to the ESOC MEX control system for storage. To retrieve the lander data, the Phoenix project sent a telemetry retrieval request either via web or extensible markup language (XML) interface to the MEX data distribution system (DDS). The DDS fetched the data and placed it on a server. The Phoenix project then performed an “FTP get” session. The data was delivered in raw binary format and included the DDS header, the Melacom TM Pkt header (CCSDS), as well as the Prox-1 frame header.

5.2 Surface Ground Operations

The remaining parts of “Flight Operations” are summarized from [41] and [36].

Since Phoenix operated as a stationary lander, the relative orbiter geometry, relay opportunity timing, and link performance could be predicted for the rest of the mission after the final touchdown orientation was known. Assumptions about post-landed azimuthal orientation were eased by a Phoenix requirement to control its touchdown azimuth to within a few degrees. Dynamics of landing may induce a pirouette effect, perturbing the azimuth up to an estimated ±15 deg. The remainder of the final lander orientation was constrained by landing site selection and expected landing system performance. The exact timing of overflights was set no later than about 8 weeks ahead of Phoenix Entry Descent and Landing (EDL). In order to provide optimized communications coverage for the critical EDL events, both Odyssey and MRO adjusted their in-plane mean-anomaly such that they were both in the vicinity of the Phoenix landing site at the time of EDL. As such, the time of the overflights for the rest of the mission was set by this initial epoch.

5.3 Tactical Operations

Since all Phoenix spacecraft communications depended on an intermediary, any problems with the intermediary also become the Phoenix operations team’s problems. These ranged from anomalies on the relay spacecraft, to support by the DSN, and even included personnel scheduling issues on the relay orbiters’ operations teams. The Phoenix communications and fault protection approaches were made as insensitive as possible to any of these problems. The Phoenix strategic planning was designed to avoid causing an anomaly on Phoenix if one or several orbiter overflights did not transfer data. Phoenix employed two operational mitigations: (a) configure on-board fault protection to declare an “uplink loss” fault due to lack of successful relay only after several sols have elapsed, and (b) maintain "run-out" science sequences on the lander to be executed during these few sols of no ground contact.

In addition to the mission requiring the lander to be self-supporting for a short duration without ground interaction, the operations team also planned for diversity in relay orbiter

coverage, not placing all the relay responsibility on a given orbiter. If a relay anomaly prevented its support of lander communications, the next alternate orbiter pass would allow for short-term or long-term adjustment of the lander communications strategy if needed.

5.4 X-Band Telecom Constraints

A common practice for configuration of spacecraft during fault protection responses is to place the communications system in a known, safe, and robust uplink and downlink state. To achieve robustness usually involves using a communications configuration with the highest link margins, and therefore lowest data rates, to provide the best chance of successful receipt of commands and return of data. Further, to reduce the effect of spacecraft attitude variations or error, the most robust configurations typically utilize antennas with lower gain and wider beam-widths.

5.5 UHF Telecom Constraints

The following factors led to the decision to make the Phoenix surface mission dependent on UHF relay only. On the Martian surface, the data return requirements could not be demonstrated to be met with the X-band system alone, thus creating reliance on single-string hardware in an otherwise block-redundant and single-fault tolerant architecture. With the demonstrated performance of the UHF relay link between the MERs and Odyssey, the addition of the MRO to the orbiting relays, and a viable UHF-EDL communications strategy, an all-relay hardware design approach could be justified. Additional benefits included a significant mass savings on a lander design that was beginning to be pushed to its limits, as well as a significant reduction in spacecraft implementation complexity. The Phoenix telecom system consisted of one antenna for EDL and two antennas for surface communications cross-strapped to block-redundant transceivers and spacecraft electronics.

5.6 Surface Relay Link Strategy and Operations

While high-data-rate fault communications may often be achievable, there are situations were the operations team may prefer a lower communications rate, usually for one of two reasons: (1) if the spacecraft is experiencing an anomaly related to the communications subsystem itself, the lower data rates may be necessary to achieve a robust link, or (2) lower data rates may allow for more frequent opportunities to interact with the spacecraft routinely, taking advantage of the lower-elevation, lower-margin overflights.

In order to achieve a change in relay data rate, it is the orbiters that must be commanded to change their state, not the lander. In an anomaly, the configuration change will have to be accomplished after the ground detects a fault (seen in the received lander data) or suspects a fault may have occurred (by lack of communications from the lander), and must be achieved within the turn-around-times that are possible with the latencies in operations decision processes, DSN passes with the orbiters, and upcoming relay opportunities with the lander.

5.6.1 Transceiver Prox-1 Frame Duplication Workarounds

Due to the CE-505 radio's proximity-1 frame duplication idiosyncrasy (Section 2), a 5-minute and an 8-minute forward-link delay were applied to the 8-kbps and 128-kbps return rate passes with Odyssey, respectively. Prior to these forward-link delays being implemented in the on-board blocks, spacer files were used at the beginning of each of our command products to consume forward-link time during the low SNR portion of the pass. The frame duplication idiosyncrasy also affected the return link, so packet gaps were an issue at the beginning of the passes with Odyssey. Small packets were particularly vulnerable to being dropped during low signal-to-noise ration portions of the link. Delaying a data priority table (DPT) change on the downlink until a healthy SNR is established was a possibility but not implemented in order to maximize data return. Instead, the packet IDs that were being lost regularly were re-transmitted in the middle of the pass as part of the UHF block in order to reduce the overall quantity of re-transmits.

The 32-kbps forward-link rate was less vulnerable to the frame duplication idiosyncrasy and added significant margins on the forward-link volume capability. One disadvantage of a 32-kbps forward-link rate is that it cannot be changed tactically. Only the return rate can be changed tactically, so when Phoenix entered safemode, the mission opted to leave previously sequenced passes at the higher 32 kbps or 128 kbps rate combination and then simply implement all of contingency overflights, which were sequenced at 8 kbps/8 kbps.

5.6.2 Fill-Data Workarounds

Fill bits created wasteful buffer over-write issues on Odyssey and increased downlink latency of Orbiter engineering telemetry which slowed down Telecom assessment. Management of the Odyssey buffer over-write issues was tedious and led to wasted throughput. Phoenix UHF transceiver power on and off times had to be reduced in order to reduced the quantity of data being transmitted to Odyssey.

If fill bits could be discarded instead of packetized and treated equally to critical data, buffer over-write issues would not have existed. The overflights that occurred during the Mars morning ("AM" LMST) were utilized for uplinking the science activities for the day, and since the spacecraft had generally just awakened, the AM overflights were returning a significant amount of fill bits. In addition to the fill bits consuming Odyssey buffer space, they delayed the return of MER data and Odyssey engineering and science data. Future programs should consider discarding fill bits instead of packetizing and downlinking them along with critical data.

Figure 5-3 displays the quantity of fill data transmitted through Odyssey (blue) and MRO (red) throughout the mission.

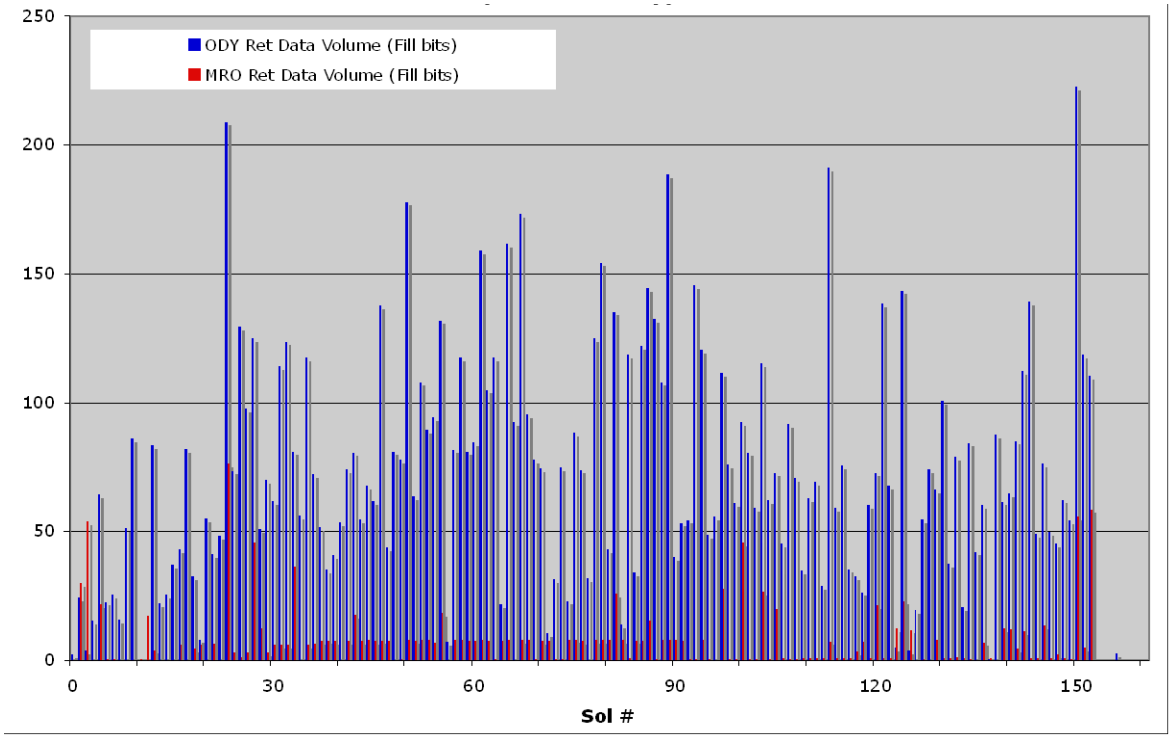

Figure 5-3 Megabits of fill data returned sol by sol during the mission.

5.6.3 Data Throughput Workarounds

MRO became a reliable relay asset, but early in the mission, the relays were not dependable enough to ensure critical data return. Modification to the on-board MRO blocks to delay the hail start until the return signal strength was above threshold considerably improved the consistency of the successful links. The data rates of 8 kbps/128 kbps and 8 kbps/32 kbps were the preferred data rates for MRO due to self locking issues when using 8 kbps/8 kbps.

From a Phoenix perspective, the "remote no more data" (rnmd) forward-link completion data word was the only proximity-1 compatibility issue with MRO. Because a frame transmitted by MRO at the end of the forward-link session was being interpreted as an acknowledgement by the Phoenix CE-505 UHF transceiver, Phoenix would transmit the next frame in the sequence regardless of whether MRO confirmed receipt of the last frame. During low signal-to-noise ratio portions of the pass, the "rnmd" frame would periodically place the radios out of sync, which would prevent the remainder of the over-flight from being successful. The MRO Electra software update eliminated the rnmd frame, which theoretically eliminated the "out of sync" frame condition.

6 Lessons Learned

Most of these lessons learned were developed by Lockheed Martin from Phoenix spacecraft ATLO and flight operations experience [36]. The ones on the landing radar lessons are from [29].

6.1 Spacecraft Design and Hardware

SDST

Standardize on a basic transponder design, which is then improved through discrete Group Buys, each supporting several projects. This conserves test time and minimizes cost for each new project in development.

Low-gain X-band antennas and UHF antennas

Consider defining the antenna performance requirements inclusive of the spacecraft structure, so antenna performance measured after integration with a mockup structure becomes the acceptance criteria. This lesson was made apparent in the amount of testing and analysis expended on the X-band low-gain and UHF wraparound antennas. Helix and monopole full-spacecraft mockup RF pattern test results were critical for accurate UHF return-link data volume predicts.

Retest of possibly reworked “inherited” antennas is critical when a complete documentation trail is not available.

Flight build processes should be applied to all hardware regardless of design complexity. The UHF Monopole design was perceived as extremely robust and mechanically simplistic, and it was not built with the same level of diligence as more complex hardware. Consequently, both time and budget were spent exonerating the hardware.

Microwave components

One issue with the inherited Phoenix cruise stage passive microwave components was a flake in the interior silver plating of one of the waveguide pieces. An MRO in-flight wave transfer switch (WTS) failure implicated foreign object damage (FOD). An extensive inspection and test program was required before the components could be accepted for Phoenix flight.

Coaxial switches

Phoenix assessed inherited Mars01 single pole double throw (SPDT) and double pole double throw (DPDT) coaxial switches. They were deemed to have too many problems and residual uncertainties, so new switches were procured. The newly procured transfer switches were redesigned with larger packaging, which eliminated blind assembly. The gap distances were increased and verified during the final assembly process. The Phoenix coax switches experienced no issues during testing, cruise, or surface missions.

Interference to UHF transceiver

EMI/EMC testing in ATLO only produced cursory results for payload interference. Such tests should be run with flight-like sequences.

Landing radar design

Eliminate the Barker code applied to the transmit pulse (Honeywell has removed it from their production HG9550 radar altimeter). Pre-launch radar testing showed Doppler spectra containing multiple peaks rather than the single peak assumed by the radar processing algorithm. The unwanted peaks came from pulse-compression side lobes in the vicinity of nadir.

Lower the pulse repetition frequency in all range steps to make ambiguous returns impossible over the altitude of operations. On Phoenix, range steps 1 through 3 used a frequency greater than 400 kHz.

Use a better antenna beam for velocity measurement. Electronically steering 30 deg off boresight with a 3 × 3 array is at the edge of feasibility.

6.2 Operations

SDST

Determine or confirm functional performance of the current project's SDST through testing and learn idiosyncrasies from previous projects' flight team experiences.

WTS

Phoenix elected to switch antennas for the downlink by powering one SSPA or the other rather than using the WTS, similar to the decision the EPOXI[5] project made with regard to powering its TWTAs rather than using its WTS. This approach was deemed a lower risk of X-band failure in the face of the WTS failure that MRO experienced. The Phoenix and EPOXI approaches could be deemed as correct, as no failures or degradation occurred.

UHF transceiver

In-flight characterization is ultimately required to fully understand RF interaction between the UHF radios (at both ends of the relay link) and the other subsystems and science payload (at both ends of the relay link).

The Proximity-1 Frame Duplication behavior in "reliable mode" affected forward and return-link reliability during low signal-to-noise (SNR) ratio portions of the pass. Although the mitigation recommended to uplink each command load twice to reduce the risk of corruption was implemented, Phoenix experienced lost commands until the signal strength was healthy enough to support a link without re-transmits.

If radio behaviors are tested early in the program, fault protection software can be used to place radios in compatible modes during safemode operations. These behaviors can be incorporated in the safemode block design which should consider orbiter configurations during safemode.

[5] EPOXI is Extrasolar Planet Observation and Characterization (EPOCh) and Deep Impact Extended Investigation (DIXI). It is a continuation of the Deep Impact mission with new targets.

Landing radar operations

Re-examine the margin in the IMU propagation error at low altitudes. The radar was required to work all the way to the surface, forcing several non-optimum design trades. However, the radar was not used below 30 m.

Effort had been expended to prevent the radar from seeing the heat shield. In hindsight, the radar should have been intentionally turned on during its warm-up to see the heat shield release and to collect data on the separation rate.

Surface operations

Telecom (and systems) invented portions of the surface operations process during operational readiness tests (ORTs). They also uncovered real operational issues with relay communications as a result of surface ORT experience after launch.

Operational planning latencies differed significantly between landers and orbiters. The Phoenix lander used a 3-day planning cycle while the Mars Express used a 90-day cycle. Lander commanding products were available to the orbiter control center with only short notice; often without a second chance for uplink (in case the planned ground-station pass failed). To accommodate these differences, an orbiter system with a high degree of autonomy (automatic DOR checking, automatic housekeeping [HK] data retrieval) is recommended.

Lander operations used various forms of lander site local solar time and sol numbers for planning, while orbiter operations were mainly scheduled in UTC spacecraft event times and DOY. To avoid any confusion between the orbiter team and the lander team, the teams must agree upon a common reference time for all scheduled activities.

MEX Melacom data for Phoenix was labeled with one APID, whether canister mode or lander telemetry. Because the two data sets were processed differently at the Phoenix control center, it is advised to use two different APIDs for the two types of data.

The data recovery mechanisms for when telemetry had been lost on the downlink for MEX was a manual, offline process. It was not suited for the much shorter latencies required for lander operations. For future missions it is recommended to implement some kind of file-transfer mechanism on the downlink (orbiter to ground) or an automated data recovery mechanism so that missing parts can be automatically re-transmitted.

7 Abbreviations and Acronyms

1553	(MIL-STD-1553) a standard for digital communications published by the United States Department of Defense
AGC	automatic gain control
Alt	altitude
AOS	acquisition of signal
APID	application identification
ASM	attached synchronization marker
ASCII	American Standard Code for Information Interchange
ATLO	assembly, test, and launch operations
AU	astronomical unit
Aux osc	auxiliary oscillator
Az	azimuth
BLF	best-lock frequency
BP	bandpass
bps	bits per second
BVR	Block V receiver
BW	bandwidth
BWG	beam waveguide
C3	acceleration
CCD	charge-coupled device
CCSDS	Consultative Committee on Space Data Systems
C&DH	command and data handling
CDU	command detector unit
CE	Cincinnati Electronics
CLGA	cruise low-gain antenna
cla_agc	carrier lock accumulator automatic gain control
Clk	clock
cm	centimeter
CMD	Command
CP	coupler
CP	cross polarized
CRC	cyclic redundancy code
CSS	cruise stage separation

CTS	coaxial transfer switch
CV	constant velocity
CW	Continuous wave (carrier only)
DAC	digital to analog converter
dB	decibel
dBi	decibels referenced to isotropic gain
dBic	decibels referenced to isotropic gain (circular polarization)
dBm	decibels referenced to milliwatts
DC	direct current
DDS	data disposition/distribution system
DESCANSO	Deep Space Communications and Navigation Systems Center of Excellence
delta-V	change in velocity
DL	downlink
D/L	downlink
DLA	declination of launch azimuth
DOR	direct operations request
ΔDOR	delta differential one-way ranging
doy	day of year
DPDT	double pole double throw
DPM	digital processing module
DPT	data priority table
DPT	downlink priority table
DSN	Deep Space Network
DSS	Deep Space Station
DTE	direct to Earth
DTM	
DTT	digital tracking and telemetry
DV	data volume
DX	diplexer
E	entry
EDL	entry, descent, and landing
EDU	engineering development unit
El	elevation
EIRP	effective isotropic radiated power
EMI	electromagnetic interference

EPOXI	Extrasolar Planet Observation and Characterization (EPOCh) and Deep Impact Extended Investigation (DIXI)
ESA	European Space Agency
ESOC	European Space Operations Centre
ESTRACK	European Space Tracking
f1	fundamental frequency of the SDST
FCT	Flight Control Team
FDR	flight dynamics request
FFT	fast Fourier transform
FOD	foreign object damage (or debris)
FSK	frequency shift key
FSW	flight software
ft	foot
FTP	file transfer protocol
FTS	fixed time step safemode
FWD	forward
Gb	gigabit
GBT	Green Bank Telescope, West Virginia
GEM	graphite epoxy motor
GHz	gigahertz
GNC	guidance navigation and control
GND	ground
G/T	gain to noise temperature
GTP	generalized telecom predictor program
H	hypersonic or hypersonic event (events 1 through n)
HEF	high efficiency
HK	housekeeping
HSJ	heat shield jettison
Hyper	hypersonic or hypersonic event (events 1 through n)
Hz	hertz
I	in phase
ID	identification
I/F	intermediate frequency
IMU	inertial measurement unit

in.	inch
ISO	isolator
I/Q	in phase/quadrature
JPL	Jet Propulsion Laboratory
Ka-band	radio frequencies from to 26.5 to 40 GHz
kbps	kilobits per second
kHz	kilohertz
km	kilometer
km/s	kilometers per second
kbps	kilobits per second
kW	kilowatt
lbf	pound force
LCP	left circular polarization
LED	light emitting diode
LGA	low gain antenna
LHCP	left-hand circular polarization
LIDAR	light detection and ranging
LMA	
LMST	local mean solar time
LNA	low noise amplifier
LO	local oscillator
LOS	loss of signal
LTA	long term archive
m	meter
MARDI	Mars descent imager
Mb	megabit
Mbit	megabit
MCS	Mission Control System
MDAF	mission detailed agenda file
MECA	microscopy, electrochemistry, and conductivity analyzer
MECO	main engine cut off
MEL	Melacom
Melacom	Mars Express Lander Communications
MER	Mars Exploration Rover

MER-A	Spirit Mars Exploration Rover
MER-B	Opportunity Mars Exploration Rover
MET	meteorological station
MEX	Mars Express orbiter
MGA	medium gain antenna
MGS	Mars Global Surveyor
MHz	megahertz
MIRA	Mars Express instrument resource analyzer
mm	millimeter
MOLA	Mars Orbiter Laser Altimeter
MPL	Mars Polar Lander
MREQ	MIRA instrument request file
MRO	Mars Reconnaissance Orbiter
ms	millisecond
m/s	meters per second
MSL	Mars Science Laboratory
MSP	Mars Surveyor Program
MSP'01	Mars Surveyor Program 2001
MTP	medium term plan (4-week cycle)
MUST	mission utility and support
N	newton
N/A	not applicable
NASA	National Aeronautics and Space Administration
NF	notch filter
nm	nanometer
nmi	nautical mile (1.85200 kilometer)
NRZ-L	non return to zero level
OD	orbit determination
ODY	Odyssey
ORT	operational readiness test
PC	power converter
PCM	pulse code modulation
Pc/No	ratio of carrier power to noise spectral density
PD	parachute deploy
PD	power divider

PDU	protocol data unit
PEB	payload electronics box
PF	proto flight
PF-1	protoflight unit 1
pH	acidity/alkalinity
PHX	Phoenix
PM	phase modulation
POR	payload operations request
Pr/No	ranging power to noise spectral density ratio
PRF	pulse repetition frequency
Prox-1	Proximity 1
Pt	received total power
P&T	pressure and temperature
Pt/No	total power to noise spectral density ratio
PTR	pointing request
PWR	power
Q	quadrature
RAC	robotic arm camera
RCP	right circular polarization
rcvr_spe	receiver static phase error
RF	radio frequency
RHCP	right-hand circular polarization
RLA	right ascension of launch azimuth
Rnmd	remote no more data
RP	rocket propellant or refined petroleum (kerosene)
RS	Reed Solomon
RSR	radio science recorder
RTN	return
Rx	receive
S-band	radio frequencies from 2 to 4 GHz
SDST	small deep space transponder
SECO	sustainer engine cut off
SEP	Sun–Earth-probe angle
Sep	separation
SFDU	standard formatted data unit

SIRTF	Space infrared telescope facility (Spitzer)
SLE	space link extension services
SN	serial number
SNR	signal-to-noise ratio
SPC	Signal Processing Center
SPDT	single pole double throw
SRM	solid rocket motor
S/S	subsystem
SSI	surface stereo imager
SSPA	solid-state power amplifier
STE	system test equipment
Subcar	subcarrier
Sw	switch
SYM	symbol
TCM	trajectory correction maneuver
TD	touchdown
TECO	third stage engine cut off
TEGA	thermal and evolved gas analyzer
TIP	target interface point
TLM	telemetry
TM	telemetry
TM Pkt	telemetry packet
TMU	telemetry modulation unit
Trans	transceiver
Trans	transfer
TTE	turn to entry attitude
TVAC	thermal vacuum chamber
TWTA	traveling wave tube amplifier
Tx	transmit
UHF	ultrahigh frequency (300 to 3000 MHz)
U/L	uplink
ULDL	uplink downlink
UTC	Universal Time Coordinates
UV	ultraviolet

VCXO	voltage controlled crystal oscillator
Vel	velocity
VGA	variable gain amplifier
VI	inertial velocity
ΔVLBI	delta very long baseline interferometry
W	watt
wb_agc	wideband automatic gain control
WTS	wave transfer switch
X-band	radio frequencies from 7 to 12.5 GHz
Xfer	transfer
XML	extensible markup language

8 References

[1] "Photo galley, the spacecraft," Phoenix Mars Mission website, University of Arizona, Tucson, accessed July 28, 2010. http://phoenix.lpl.arizona.edu/images.php?gID=140&cID=1

[2] "Phoenix Lander Self Portrait on Mars, Vertical Projection," JPL Phoenix Mission website, Jet Propulsion Laboratory, Pasadena, California, December 15, 2008. http://www.jpl.nasa.gov/news/phoenix/images.php?fileID=16734

[3] *Phoenix Launch, Mission to the Martian Polar North*, Press K, Jet Propulsion Laboratory, Pasadena, California, August 2007, http://www.jpl.nasa.gov/news/press_kits/phoenix-launch-presskit.pdf

[4] *Phoenix Landing, Mission to the Martian Polar North*, Landing Press Kit, Jet Propulsion Laboratory, Pasadena, California, May 2008, http://www.jpl.nasa.gov/news/press_kits/phoenix-landing.pdf

[5] "Arctic Expedition Prepared Researchers for Mars Project, Jet Propulsion Laboratory (JPL)," News & Features (web page), Jet Propulsion Laboratory, Pasadena, California, February 5, 2009. http://www.jpl.nasa.gov/news/features.cfm?feature=2017

[6] "Phoenix Mars Lander Is Silent, New Image Shows Damage," *Phoenix Mars Mission* (website), University of Arizona, Tucson, May 24, 2010. http://phoenix.lpl.arizona.edu/05_25_10_pr.php

[7] Mars Phoenix Lander, *NASA Facts* (web page), Jet Propulsion Laboratory, Pasadena, California, February 2, 2008. http://www.jpl.nasa.gov/news/fact_sheets/mars-phoenix.pdf

[8] *Phoenix Mars Lander*, "Mission Overview" (web page) , Jet Propulsion Laboratory, Pasadena, California, continually updated (accessed July 28, 2010. http://www.jpl.nasa.gov/news/phoenix/missions.php

[9] *Phoenix Analyst's Notebook Users* Guide, website, PDS Geosciences Node, Washington University in St. Louis, Missouri. http://an.rsl.wustl.edu/phx/help/index.html?acronyms.htm (Click on Phoenix Mission and then Landing Site.)

[10] *Phoenix Analyst's Notebook Users Guide*, PDS Geosciences Node, Washington University in St. Louis, http://an.rsl.wustl.edu/phx/help/index.html?acronyms.htm

[11] K. Fujii, *Phoenix Project Mission Plan*, JPL D-27254 (Internal document), Jet Propulsion Laboratory, Pasadena, California, November 2, 2005.

[12] E. Bailey, P. Desai, R. Kornfeld, S. Shaffer, M. Schoenenberger, D. Skulsky, *Phoenix EDL Reconstruction*, D-66509 (internal document), Jet Propulsion Laboratory, Pasadena, California, October 7, 2008.

[13] A. Makovsky, P. Ilott, and J. Taylor, *Mars Science Laboratory Telecommunications System Design*, Descanso Design & Performance Summary series, Article 14, Jet Propulsion Laboratory, Pasadena, California, November 2009. http://descanso.jpl.nasa.gov/DPSummary/summary.cfm?force_external=1 (Go to Article 14.)

[14] *NASA's Phoenix Mars Lander Working With Sticky Soil*, July 28, 2008, http://www.jpl.nasa.gov/news/phoenix/release.php?ArticleID=1808

[15] *Phoenix Mars Mission, Uncovering the Mysteries of the Martian Arctic*, University of Arizona, Tucson, Arizona, November 2005. http://phoenix.lpl.arizona.edu/pdf/fact_sheet.pdf

[16] *Phoenix Landing, Mission to the Martian Polar North*, Landing Press Kit, Jet Propulsion Laboratory, Pasadena, California, May 2008, http://www.jpl.nasa.gov/news/press_kits/phoenix-landing.pdf

[17] *Frequency and Channel Assignments*, Module 201, Rev. A, September 19, 2008, *DSN Telecommunications Link Design Handbook*, JPL D-19379, Rev. E (also referred to as 810-005), Jet Propulsion Laboratory, Pasadena, California, issued January 15, 2001, http://eis.jpl.nasa.gov/deepspace/dsndocs/810-005/

[18] *Proximity-1 Space Link Protocol—Physical Layer*, Recommended Standard CCSDS 211.1-B-2 (Blue Book), Consultative Committee for Space Data Systems Secretariat, National Aeronautics and Space Administration, Washington, District of Columbia, March 2006. http://public.ccsds.org/publications/archive/211x1b3ec1.pdf

[19] *Phoenix Telecom Design Control Document*, JPL D-12345 (internal document), Jet Propulsion Laboratory, Pasadena, California, July 6, 2006.

[20] *UHF Transceiver Model C/TT-505 Theory of Operation / User's Manua*l, Rev. 1.2, D-66597 (internal document), Jet Propulsion Laboratory, Pasadena, California, (also CMCEC Document # 648855, CMC Electronic Cincinnati, Mason, Ohio), May 4, 2001.

[21] *Phoenix Mars Lander*, "News and Features," (web site), Jet Propulsion Laboratory, Pasadena, California, continually updated (accessed July 28, 2010). http://www.jpl.nasa.gov/news/phoenix/news.php

[22] *Group Buy II SDST Inheritance Review* (Kepler and Phoenix), D-66508 (internal document, Jet Propulsion Laboratory, Pasadena, California (General Dynamics GDC4S), March 3, 2005.

[23] J. Taylor, *Dawn Telecommunications*, DESCANSO Design and Performance Summary Series, Jet Propulsion Laboratory, Pasadena, California, August 2009. http://descanso.jpl.nasa.gov/DPSummary/summary.cfm?force_external=1 (Go to Article 13.)

[24] W. Boger, D. Burgess, R. Honda, C. Nuckolls, "X-Band, 17 Watt, Solid-State Power Amplifier for Space Applications," *IEEE MTT-S International Microwave Symposium Digest*, vol. 3, pp. 1379–1382, 2005.

[25] C. D. Edwards, Jr., K. N. Bruvold, J. K. Erickson, R. E. Gladden, J. R. Guinn, P. A. Holt, B. Jai, M. D. Johnston, R. P. Kornfeld, T. J. Martin-Mur, G. W. McSmith, R. C. Thomas, P. Varghese, G. Signori, P. Schtnitz, "Telecommunications Relay Support of the Mars Phoenix Lander Mission," *2010 IEEE Aerospace Conference* (Big Sky, Montana), March 6–10, 2010.

[26] P. Ilott and B. Arnold, *Phoenix EDL UHF Relay Communications Status* , D-66511 (internal document), Jet Propulsion Laboratory, Pasadena, California, February 9, 2005.

[27] *Proximity-1 Space Link Protocol—Data Link Layer*, Recommended Standard CCSDS 211.0-B-4 (Blue Book), Consultative Committee for Space Data Systems Secretariat, National Aeronautics and Space Administration, Washington, District of Columbia, July 2006. http://public.ccsds.org/publications/archive/211x0b4.pdf

[28] P. Ilott, J. Harrel, B. Arnold, N. Bliznyuk, R. Nielsen, D. Dawson, and J. McGee, *UHF Relay Antenna Measurements on Phoenix Mars Lander Mockup*, Jet Propulsion Laboratory, Pasadena, California, October 22, 2006 http://trs-new.jpl.nasa.gov/dspace/bitstream/2014/40721/1/06-1936.pdf

[29] S. Shaffer, C. Chen, E. Belz, E. Bailey, D Shafter, *Phoenix Radar EDL Reconstruction Results*, D-66513 (internal document), Jet Propulsion Laboratory, Pasadena, California, September 9, 2008.

[30] E. D. Skulsky, S. Shaffer, E. Bailey, C. Chen, B. Cichy, and D. Shafter, "Under the Radar: Trials and Tribulations of Landing on Mars," *31st Annual Guidance, Navigation, and Control Conference*, American Astronautical Society, Rocky Mountain Section, February 2008.

[31] *Deep Space Network*, website, Jet Propulsion Laboratory, Pasadena, California, continually updated (accessed July 28, 2010). http://deepspace.jpl.nasa.gov/dsn/

[32] *DSN Telecommunications Link Design Handbook*, D-19379 (also referred to as 810-005), Rev. E, Jet Propulsion Laboratory, Pasadena, California, continuously updated, http://eis.jpl.nasa.gov/deepspace/dsndocs/810-005/ (Go to Space Link Interface; reference Modules 101, 103, and 104.)

[33] *Green Bank Observatory Photo Gallery*, web page, National Radio Astronomy Observatory, Green Bank, West Virginia, accessed July 28, 2010. http://www.nasa.wvu.edu/Gallery/GreenBankObservatory/gbt.html

[34] *National Radio Astronomy Observatory*, web page, National Radio Astronomy Observatory, Green Bank, West Virginia, accessed July 28, 2010. http://www.gb.nrao.edu/GBT/

[35] P. Ilott, L. Craig, and S. Butman, *PHX EDL UHF DTE Link Update*, D-66510 (internal document), Jet Propulsion Laboratory, Pasadena, California, May 6, 2008.

[36] G. Signori, *Phoenix Mars Lander Telecommunications Development and Operational Lessons Learned*, D-66512 (internal document), Jet Propulsion

Laboratory, Pasadena California, (Deep Space Communication Systems for JPL), December 4, 2008.

[37] O. Reboud, J. Schulster, T. Ormston, A Moorhouse, P. Schmitz, B. W. Arnold, C. D. Edwards, P. Ilot, B. B. Jones, M. S. Keuneke, R. P. Kornfeld, and D. Fortune, *An Interplanetary and Interagency Network – Lander Communications at Mars*, SpaceOps 2008 Conference, AIAA 2008-3536, American Institute of Aeronautics and Astronautics, 2008.

[38] D. Morabito, R. Kornfeld, K. Bruvold, "The Mars Phoenix Communications Brownout during Entry into the Martian Atmosphere," *Interplanetary Network Progress Report 42-179*, Jet Propulsion Laboratory, Pasadena, California, pp. 1–20, November 15, 2009. http://ipnpr.jpl.nasa.gov/progress_report/42-179/179A.pdf

[39] P. Ilott and B. Arnold, *Phoenix-to-Green Bank UHF DTE Signal Evaluation* (preliminary), D-66507 (internal document), Jet Propulsion Laboratory, Pasadena, California, May 25, 2008.

[40] P. Schmitz, *MEX-PHX EDL and On-surface Support Final Report*, MEX-ESC-TN-5171, European Space Agency, Darmstadt, Germany, October 2008. (Also archived as JPL D-66514, internal document, Jet Propulsion Laboratory, Pasadena, California).

[41] C. A. Lewicki, J. Krajewski, P. Ilott, and J. Dates, "Phoenix Mars Scout UHF Relay-Only Operations, *AIAA 9th International Conference on Spacecraft Operations (SpaceOps)* (Rome, Italy, June 19–24, 2006), American Institute of Aeronautics and Astronautics (also on NASA Technical Reports Server), 2006.